CHARACTERIZATION OF MULTIPLE LOG-PERIODIC ARRAY ANTENNAS FOR SURVEILLANCE SYSTEMS USING A NOVEL ARRAY-FACTOR

By

OKOYE, ARINZE CHRISTIAN (B. Eng. (FUTO), M. Eng. (FUTO))

(20144942048)

A DISSERTATION SUBMITTED TO THE POSTGRADUATE SCHOOL,

FEDERAL UNIVERSITY OF TECHNOLOGY, OWERRI

IN PARTIAL FULFILLMENT OF THE REQUIREMENTS FOR THE AWARD OF DOCTOR OF PHILOSOPHY (Ph.D) DEGREE IN TELECOMMUNICATIONS ENGINEERING

IN THE DEPARTMENT OF ELECTRICAL/ELECTRONIC ENGINEERING, SCHOOL OF ELECTRICAL SYSTEM AND ENGINEERING TECHNOLOGY (SESET)

NOVEMBER, 2023

CERTIFICATION

This is to certify that this work titled "Characterization of Multiple Log-Periodic Array Antennas for Surveillance Systems Using a Novel Array-Factor," was carried out by **Okoye, Arinze Christian** (M. Eng) with registration number (**20144942048**) in partial fulfillment of the requirements for the award of Doctor of Philosophy (Ph.D) degree in Electrical/Electronic Engineering (Telecommunication Engineering option).

ENGR. PROF. M. C. NDINECHI — 12/2/24
(Principal Supervisor) **DATE**

ENGR. DR. C. C. MBAOCHA — 12/2/24
(Co-Supervisor) **DATE**

ENGR. DR. C. K. AGUBOR — 12/2/24
(Co-Supervisor) **DATE**

ENGR DR. N. CHUKWUCHEKWA — 14/2/24
(Head of Department) **DATE**

ENGR. PROF. M. C. NDINECHI — 14/2/24
(Dean, S.E.S.E.T) **DATE**

PROF. B. O. ESONU — **DATE**
(Dean, Postgraduate School)

DATE

(External Examiner)

DEDICATION

I dedicate this project to the holy family of Jesus, Mary and Joseph.

ACKNOWLEDGEMENTS

I acknowledge all the people that contributed in many ways to the success of the project reported in this dissertation.

I am most grateful to my main Supervisor and Dean of School of Electrical Systems Engineering and Technology, Engr. Prof. M. C. Ndinechi. Also to the co-supervisors Engr. Dr. C. C. Mbaocha and Engr. Dr. C. K. Agubor for accepting to supervise this work. All your advice and constructive criticisms are highly appreciated.

My thanks go to the able Head of Department, Engr. Dr. N. Chukwuchekwa for the excellent way he pilots the affairs of the department.

In a special way, I thank all the lecturers that taught me in Electrical/Electronic Engineering Department, FUTO. Engr. Prof. Chukwudebe, Engr. Prof. Okafor, Engr. Prof. F.K. Opara, Engr. Prof. Mrs. G. N. Ezeh, Engr. Prof. I. E. Achumba, Engr. Prof. D.O. Dike, Engr. Prof. L. Uzoechi, Engr. Prof. F.I. Izuegbunam, Engr. Dr. C. C. Mbaocha, Engr. Dr. N. Chukwuchekwa, Engr. Prof. O. J. Onojo, Engr. Dr. C. K. Agubor and Engr. Dr. O. C. Nosiri.

I thank the Dean of Postgraduate School, Prof. B. O. Esonu for all his sacrifices in fine-tuning this project. May God bless you and all your staff members.

My thanks also go to my parents, Late Mr. Emmanuel Okoye and Mrs. Eucharia Okoye for their prayers and encouragement. My warmest regards and big thank you to Chinwendu my wife; Chinemerem and Ifechukwu my children; my siblings, my colleagues in the classroom, and so many other people too numerous to mention that contributed in various ways to the success of this work. A big thank you to you all.

TABLE OF CONTENTS

List of Tables

List of Figures

ABSTRACT

This research endeavors to comprehensively characterize Multiple Log-Periodic Array (MLPA) antennas, specifically in the context of surveillance systems, using a novel array factor. This array factor streamlines the numerical characterization of MLPA antennas, regardless of the number of elements involved. The study employs a rigorous analytical approach, incorporating the Magnetic Vector Potential (MVP) model and pattern multiplication approach through a top-down methodology. The MVP model was chosen for its auxiliary function, which greatly simplifies the analytical processes. In practical terms, experimental Multiple Log Periodic Array antennas were designed and evaluated for this study. The parameters of these antennas were numerically assessed in the far field using the newly developed Array Factor. MatLab R2010a software played a pivotal role in simulating various parameters of the Multiple Log-Periodic Array antennas, including Array Antenna patterns, Electric/Magnetic fields, Average Poynting Vector, Radiation Intensity, Radiated Power, Directivity, and Directive Gain. The results demonstrated that the array antennas had a Directivity/Gain of 15.68dB or 45.68dBm, at the operating frequency range of 1.350GHz to 2.690GHz. The collective array patterns generated by the MLPA antennas were in line with expectations, relying on the corresponding field of single element. Multiple Log-Periodic Array antennas expanded the function of Single Log-Periodic Array (SLPA) antennas by significantly enhancing radiation gain and signal coverage. Thus, the novel Array Factor accelerates the process of characterizing array antenna parameters, thereby alleviating the bottleneck in computing antenna losses. This marks a significant advancement in the field of antenna technology.

Keywords:

Array Antennas, Array Factor, Log Periodic Antenna (LPA), Surveillance Systems, Electromagnetic waves, Magnetic Vector Potential (MVP), Wire Antennas, Frequency Independent Antennas.

CHAPTER ONE

INTRODUCTION

1.1 Background Information

The current state of security challenges has obviously demonstrated that the nature of threats to global security has changed drastically. Global attacks, such as terrorism, cyber-attacks, and nuclear proliferation have triggered a new dimension of security situation. African countries are not left out of this security issue as the people of Africa and Nigeria in particular suffer at the hands of opportunistic, militant actors and terrorists in almost all the geopolitical regions of the country. The activities of these groups include February 10, 2016 blow up of the Bonny Soku Gas Line which carries natural gas to the Nigeria Liquified Natural Gas plant and an independent power plant at Gbaran, and also an attack on the 48-inch export pipeline at the Forcados export terminal (This Day, 2016).

The techniques of these attacks include coordinated armed attacks, assassinations, kidnapping, rocket attacks, use of improvised explosive devices (IEDs), bombings and arson; and use of military uniforms and vehicles as a ploy to approach the intended targets. These attacks, among others, have no doubt had a distressing effect on the country's oil revenue projection in the 2021 financial budget. There is hardly a day that passes in this country without one hearing the news of the citizens being kidnapped, murdered, and properties worth millions of naira being destroyed. In the latest research conducted by Intersociety which cut across all the distressing Christian areas of the country; the report states thus, "The number of defenseless Christians killed in Nigeria from Jan to April 2021 is 1,470; …" (International Christian Concern, 2021).

History shows that numerous security threats could never have developed into a fully-fledged problem, had they been identified and tackled at an earlier stage. This current security challenges call for urgent and tactical means of control. It predisposes the military as well as the entire country to difficult situation – hence, the need to monitor communications over a very wide frequency range. This requires sophisticated and high sensitive wide band surveillance systems for monitoring the activities of people within areas of interest. Thus, one of the measures to actualize this is through the use of Wide Area Surveillance Systems (WASS) – operated by multiple array antennas.

Surveillance involves the monitoring of the behavior, activities, or other changing information, usually of people in order to influence, manage, direct, investigate or protect them. This comprises of observation from a distance by means of electronic equipment, or interception of electronically transmitted information. WASS provides continuous views of extensive areas.

The Modern surveillance systems operate within High Frequency (HF), Very High Frequency (VHF) and Ultra High Frequency (UHF) bands, and Multiple or Stacked Log-Periodic Array Antennas perform extremely well within these frequency bands.

Antenna can be defined as any piece of material that has the capability to transmit or receive electromagnetic waves. Antennas could be mounted outdoors, indoors, or built within devices that possess transmitting or receiving systems. There are three (3) main forms of antenna namely: Wire antennas, Slot antennas, and Aperture antennas. These choices of antennas are deployed at various communication systems depending on their individual characteristics and nature of the environment they are to operate. However, the most widely used type of these

antenna classes is the wire antenna. Wire antenna is the simplest, the cheapest as well as the most flexible form of antenna. It can easily be made in various shapes to realize unique antenna characteristics which include: dipole, loop, helical, and array antennas.

An array antenna entails the combination of more than one antenna of similar or dissimilar elements. Two main forms of array antennas are: equal amplitude array antennas and Log-Periodic Array antennas. When the array of antennas is made of similar elements with dimensions (length of elements and spacing) that vary with a constant, τ, the array antenna is tagged Log Periodic Array (LPA) Antennas. They are utilized in applications where a large frequency band is required to be transmitted/received such as in broadcasting stations, Satellite Mobile Vehicles (SMVs), Radio Detection and Ranging (RADAR) technologies. Numerous advantages are derived from LPAs that account for its usage in signal transmission/detection. These benefits include wide bandwidth, and low Voltage Standing Wave Ratio (VSWR). Though LPA antennas have obvious shortcomings which include large size, however, application of a correct mix can drastically reduce/minimize the challenges to the barest minimum that will be suitable for design. This will go a long way to optimize the gain and VSWR of the LPA used in practical wireless applications.

LPA antennas provide solutions for Communication, Navigation and Identification (CNI) searching, detection and jamming of all communications signals from HF to UHF, monitoring applications, surveillance applications, signal intelligence applications, electronic warfare applications, among others (Zhang et al., 2019). LPA antennas possess broad band design feature and high power handling capacity. It ensures clear communication for ground, sea, and ground-to-air applications in this era of information warfare (Yu-Jiun, & Chieh-Ping,

2010). Categories of the available LPA antennas for surveillance applications include: dual polarized log periodic antennas, cross polarized log periodic antennas, vertical polarized log periodic antennas, and horizontal polarized log periodic antennas (Bolli et al., 2020).

Whenever there are multiple LPA antennas either arranged in a series, parallel, circular or any other desired form, an array of LPA results. This is otherwise called Multiple Log Periodic Array (MLPA) antennas. In other words, this could be termed an array of arrays, since radiating elements constituting the LPAs are already an array. Parallel LPA antennas occur when MLPA antennas in the array pattern are all arranged in parallel. This kind of antenna arrangement has the advantage of simple configuration and wide signal coverage cum reception. To compute the Electric and Magnetic (E and H) fields generated by these array antennas, one requires an "Array Factor" (AF).

An array factor is a multiplier used for easy and speedy analysis of array antennas. It facilitates the computation of the Electric and Magnetic (E and H) fields, power transmitted/received/lost by array antennas among other parameters. In absence of the Array Factor, characterization of array antennas is a very challenging task especially when the number of radiating elements, *n*, in the array is equal or greater than 2 ($n \geq 2$). Thus, it is difficult to compute the parameters of Log Periodic Array (LPA) Antennas and even more difficult to compute that of MLPA antennas. This is owing to the fact that one has to calculate the parameters of the individual elements in the LPAs one after the other and then sum them together – even when the number of elements is up to twenty (20). Similar condition is applicable for calculating the parameters generated in MLPA antennas. With the availability of an Array-Factor, it is easier to compute all those needed parameters. For instance, one can

easily compute the total field generated by Multiple Log Periodic Array (MLPA) Antennas, simply by multiplying the field generated by the first radiating element in the MLPA antenna with the Array-Factor.

1.2 Problem Statement

The Multiple Log-Periodic Array (MLPA) antennas have no multiplier termed "Array-Factor" for easy computation/ characterization of its parameters. It has been difficult to formulate this array factor because MLPA antennas are antennas of complex geometry. Thus, MLPA antennas are very tedious to characterize in terms of their parametric behaviours. Recall, MLPA antennas constitute an array of LPA antennas with varying amplitudes and spacing. No Array-Factor has been formulated for such an array thereby making it very difficult determining the antennas parameters like the Power Loss (PL), the Radiated Power (RP), Radiation Resistance, Average Poynting Vector, and the Electro-Magnetic (EM) fields during signal radiation/reception. The Antenna engineer will have to, one after the other, analyze, calculate, and then sum the Power Loss on each and every radiating element that make up the antenna array before the total Power Loss by the MLPA antennas could be ascertained. This can be challenging and could become unfeasible as the number of LPA antennas in the array increases.

Consequently, antenna system designers find it very difficult forecasting the performance of MLPA antennas, as there is no available array factor. They spend a lot of money and time purchasing expensive softwares for carrying out drive test after costly prototype development and deployment. Thus, huge amount of money could be spent in applying corrective measures in redesigning such MLPA antennas for better performance.

Also, most of the surveillance systems deployed in monitoring activities are limited in their coverage area. This can be traced to the use of narrow band, non-directional antennas as well as single array antennas, instead of Multiple Array Antennas, in activity monitoring. Such antennas lack wide area coverage capacity.

1.3 Objectives of the Study

The main objective of this research work is to characterize Multiple Log-Periodic Array antennas for surveillance systems using a novel Array-Factor

The specific objectives include:

i. To derive array factor for the set of first dipole elements in MLPA antennas (array of equal dimensions) via pattern multiplication approach.
ii. To develop a novel array factor for MLPA antennas via pattern multiplication approach.
iii. To derive the Electromagnetic (EM) fields generated by the first radiating element in MLPA antennas using Magnetic Vector Potential model.
iv. To characterize the MLPA antenna parameters using the developed novel array factor.
v. To design and simulate MLPDA antennas of a sample band width using MatLab R2010a object oriented tools.

1.4 Justification of the Study

The need to evaluate the performance of Multiple Log-Periodic Array antennas– in order to ascertain the antenna parameters such as the power loss, is of utmost important to antenna system engineers. This evaluation, for a single antenna, does not pose much challenge. However, evaluating such for array of antennas becomes challenging and demanding; particularly for Log Periodic Array antennas as the radiating elements' amplitude and spacing change progressively. This is so, as the engineer will need to analyze, calculate and then sum, the power loss of each and every radiating element that make up the Multiple Log Periodic Array (MLPA) antennas prior to the determination of the total power loss by the MLPA antennas. However, the advent of the Array Factor resulted to rapid characterization of the antenna parameters, thereby minimizing the difficulties faced in computing antenna losses.

The novel Array Factor has an immense benefit to system designers in the design and development of efficient and cost effective array antennas. With the aid of this Array Factor, system designers could easily predict the total electromagnetic fields generated, power radiated, power received, power lost by MLPA antennas at the far field of the array antennas prior to costly prototype development and deployment. This saves the time for carrying out drive test and finance for the purchase of high cost softwares.

In organizations like communication companies, Array Factor assists in ensuring power economy. It facilitates the determination of system power loss via radiated power density. Thus, when the radiated power density is far less than the power input, the system engineer adjusts the level of the transmitted signal by checking for mismatch between the transmitter

and the Multiple LPA antennas. This enhances effective radiated power – by minimizing power loss, and thus ensures power economy.

More so, the emergence of wideband wireless communication systems necessitated the demand for high data rate antenna at mobile communication Industries, broadcasting stations, and Satellite Mobile Vehicles (SMVs). A good number of these communication systems operate within Very High Frequency (VHF) and Ultra High Frequency (UHF) bands, and Log-Periodic Array antennas do operate optimally within these bands.

1.5 Scope of the Study

This dissertation is limited to analysis on Multiple Log-Periodic Dipole Array (MLPDA) antennas.

The Log-Periodic Dipole Array (LPDA) antennas were assumed to possess similar structure, with equal spacing between the LPA antennas.

In the course of the analysis, negligible width was assumed for the antenna in order to lessen the complexity in the calculation of current flowing through the elements.

Then, the design antenna was simulated using MatLab R2010a object oriented programming tools.

The operating frequencies of the antenna were 1.35 GHz – 2.69GHz.

The design/scaling factor used for the design was 0.93.

The spacing factor that was used for the design was 0.17.

The operating bandwidth used was 2.0.

The boom length of the antenna was 1.56 ft

The number of elements considered for each of the LPA antenna was sixteen (16).

CHAPTER TWO

LITERATURE REVIEW

2.1 Antenna and Its Characteristics

Smith (2016) defined an antenna as a device designed to efficiently radiate and receive electromagnetic waves. Rohde and Schwar (2015) defined an antenna as a device for transforming Radio Frequency (RF) signal – travelling on a conductor – into an electromagnetic wave in free space. According to the authors, antennas exhibit a characteristic known as reciprocity, meaning that antennas maintain the same features despite whether it is acting as a transmitting or receiving antenna. The author explained that antenna have to be tuned to the same frequency band of its connected radio system so as not to impair the transmission and the reception.

Abdullahi and Ahmad (2018) defined antenna as a device that radiates and receives radio waves. The author revealed different mechanisms by which antennas radiate to include resonant antennas where there is a movement of charges as the energy changes between the electric field and the magnetic field – hence, the antenna causes the field lines to vibrate, releasing waves that propagate in free space away from the resonant antenna. The other mechanism is by having an impedance transition that causes the energy being propagated in a transmission line to be launched into free space. This method is witnessed in horn antenna.

In some systems, the functional behavior of the system is designed within the directional features of the antennas. Some antennas are used just for transmitting electromagnetic (EM) waves/signals in all directions or for point-to-point communication, which is realized

whenever there are disturbances to the electrical and magnetic fields. These EM waves propagate in free space in the z-direction as Transverse Electromagnetic waves, and their equations, according to (Dhande, 2009), is given by:

$$\frac{\partial^2 E_X}{\partial t^2} = \frac{1}{\mu_0 \xi_0}\frac{\partial^2 E_X}{\partial z^2}, E_X e^{j(wt \pm \beta z)} \quad (2.1)$$

$$\frac{\partial^2 H_y}{\partial t^2} = \frac{1}{\mu_0 \xi_0}\frac{\partial^2 H_y}{\partial z^2}, H_0 e^{j(wt \pm \beta z)} \quad (2.2)$$

$$f = \frac{w}{2\pi}, \lambda = \frac{1}{\sqrt{\sigma \mu_0}\varepsilon_0 f}, \beta = \frac{2\pi}{\lambda}, Z_0 = \frac{E_0}{H_0}, Z_0 = \sqrt{\frac{\mu_0}{\varepsilon_0}} \quad (2.3)$$

where,

E_x is Electric field in the x – direction.

H_y is Magnetic field in the y – direction.

ε_0 is permittivity of free space

μ_0 is permeability of free space

λ is the wavelength

Z_0 is intrinsic impedance

β is wave number

t is time

f is frequency

2.1.1 Antenna Characteristics:

The characteristics of an antenna comprise its operational properties or parameters. These characteristics include the antenna radiation pattern, radiation intensity, directivity and gain, polarization, nulls, bandwidth among others. Hence, the antenna characteristics are illustrated in Figure 2.1.

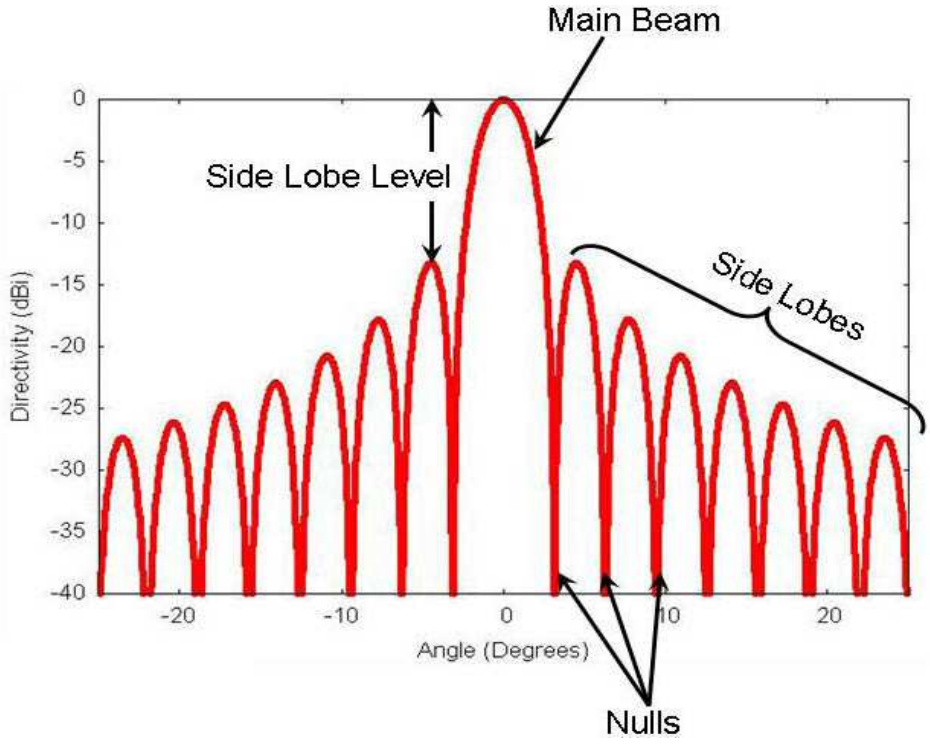

Figure 2.1: Antenna Characteristic behaviours (Typical Antenna Pattern, 2021)

The parameters used to describe antenna characteristic behaviours are discussed in under-listed subheadings:

i. Radiation Pattern – This is the mathematical function or a graphical expression of the antenna radiation properties as a function of space coordinates (Rodrigo, 2010; Srivastava, Pandey & Singh, 2014). Radiation Pattern is a plot of the variation of the power radiated by an antenna against the arrival angle as observed in the antenna's far

field. It indicates the manner the radiated power is distributed within space. Radiation pattern can either take the form of elevation or azimuth pattern. Radiation Pattern also indicates the comparative strength of the radiated field in various directions from the radiating antenna, at a steady distance.

According to (Rodriguez, 2011; Hasan & Al-Rizzo, 2020), the area of the pattern where most of the radiation is directed is termed the main lobe; the side lobes are found at the sides of the main lobe where the radiation is higher than the adjacent areas. It is energy radiated in directions other than the desired direction (main lobe); the side lobe directly opposite the main lobe is called the back lobe.

Dhande (2009) itemized the properties of antenna radiation patterns as follows:

a. Antenna radiation pattern is measured in the far field of the antenna at $r > \frac{2D^2}{\lambda}$, where D is the largest antenna dimension
b. The intensity of the field pattern varies inversely with distance
c. The radiated power density of the pattern varies inversely with square of distance
d. The shape of the radiation pattern is not dependent on distance

The graph of the magnitude of the magnetic or electric field as a function of the angular space produces the field pattern, while the plot of the square of the magnitude of the magnetic or electric field as a function of the angular space produces the power pattern (Balanis, 2005)

ii. Nulls – This is the area with minimal level of the effective radiated power. Null possesses a little directivity angle compared to the main beam. It assists in restraining interfering signals in a particular direction (Rohde & Schwar, 2015).

iii. Power Gain – This is the product of the inverse of input power and antenna output power. It is also the product of power gain in a particular direction and the inverse of power gain of a reference antenna in the same direction. Antenna gain in a given direction is the quantity of energy radiated in that direction when compared to the energy that will be radiated in the same direction by an isotropic antenna when driven by the same input power. An antenna gain of 3dB when compared to an isotropic antenna and the resonant half-wave dipole of different lengths are written as 3dBi and 3dBd respectively (Rohde & Schwar, 2015).

Different units for measuring Antenna gain include:

a. dBi (decibels relative to an isotropic radiator) is an antenna gain with respect to an isotropic radiator. It is written thus:

$$\text{G dBi} = 10 * \log\left(\frac{\text{G Numeric}}{\text{G isotropic}}\right) = 10 * \log(\text{G Numeric}) \quad (2.4)$$

b. dBd (decibels relative to a dipole) is used to explain the gain of an antenna with respect to a theoretical dipole. It is used when referring to the gain of omni-directional antennas of higher gain. In other words, gain in dBd is an expression of antenna gain beyond 2.2 dBi. Hence, an antenna with a gain of 3dBd also has a gain of 5.2dBi.

iv. Directive Gain,$D(\theta, \varphi)$ - This is defined as the ratio of antenna radiation intensity to that of a hypothetical isotropic radiator that radiates the same power. It is represented in equation (2.5):

$$D(\theta, \varphi) = \frac{4\pi U(\theta, \varphi)}{P_{rad}} \quad (2.5)$$

Where P_{rad} is the radiated power

v. Directivity, D_{max} – It is the ratio of the antenna's radiation intensity to the radiation intensity of isotropic source (Kraus, 1999). According to (Singh, Solanki & Solanki, 2014), directivity is a measure of the ability of the antenna to concentrate its power in a particular direction, while antenna gain is the ratio of the radiated power to input power. It is the capability of an antenna to concentrate its energy radiation in a desired direction during signal transmission or to receive energy better from a particular direction while receiving (Rohde & Schwar, 2015). The formular for directivity is written below as:

$$D_{max} = \frac{U}{U_0} = \frac{4\pi U_{max}}{P_{rad}} \quad (2.6)$$

Where; D_{max} is the Directivity (dimensionless), U_{max} is the maximum radiation intensity (W/ unit solid angle), U is the radiation intensity (W/unit solid angle), U_0 is the radiation intensity of isotropic source (W/unit solid angle)

vi. Polarization – This is the orientation of electromagnetic waves far from the source. It is described by (Rohde & Schwar, 2015) as "the ratio of the maximum directivity of an antenna to its directivity in the backward direction". The polarization of the transmitting antenna must be matched with that of the receiving antenna for optimum performance. Electromagnetic field polarization means the orientation of the electric field vector with respect to time. In vertical polarization, the E-field vector of EM wave is orthogonal to the earth. For horizontal polarization, the E-field of EM wave is parallel to the earth. Circularly polarized wave occurs when E and H field vectors of the EM wave are equal in magnitude, with phase difference of 90^0 (Gao, Zhang, Sun & Wu, 2019; Dhande, 2009). Polarization could be linear (such as vertical, horizontal, and oblique) or circular (such as Circular Right Hand, Circular Left Hand, Elliptical Right Hand, and Elliptical

Left Hand). This is the direction of oscillation of the electrical field vector. While mobile communication systems are vertically polarized, broadcast systems have horizontal polarization.

vii. Bandwidth – Beam width is that range of frequencies over which the antenna can operate effectively. It is the angular distance between the half power points. Directive gain has an inverse relationship with the beam width where most of the radiated power is not divided into side lobes. Rohde and Schwar (2015) defined bandwidth as the number of Hz for which an antenna will have a Standing Wave Ratio (SWR) less than 2:1. The authors also expressed bandwidth as percentage center frequency of the band written as:

$$BW = 100 * \frac{F_H - F_L}{F_C} \quad (2.7)$$

Where: F_H=highest frequency of the band, F_L=lowest frequency of the band, F_c=center frequency of the band

viii. Half power Beam Width (3-dB points) – This is the points in the horizontal and vertical axes of the radiation diagram where the transmitted power is half the amplitude of the main radiation direction (Smith, 2016). 3-dB beam width (Half Power beam width) is simply described as the angle between the points in the main lobe that are lower from the maximum gain by 3dB. An antenna should transmit energy in all directions if it does not have gain. The parameter that describes the most important lobe, the main lobe, is the half power beam width (HPBW). According to Rodriguez (2011), since ½ is 0.5 and 10log (0.5) is 3dB, the HPBW is also referred to as 3dB beam width. It is expressed in

degrees and describes the arc of the angle between the two points to the side of the point of highest radiation which are 3dB lower in radiated power.

ix. Signal-to-Noise Ratio: This is the relationship between the desired information and the noise (Singh, Solanki & Solanki, 2014).

x. Front- to-back ratio: It is the ratio of the maximum gain of the forward direction to the gain 180-degrees behind the maximum gain. It is also defined as the difference between the peak/maximum gain in the forward direction and the gain 180-degrees behind the peak, on a dB scale.

xi. Radiation Power Density: Power density is the power radiated per unit area in the field of the antenna (Neelakanta & Chatterjee, 2003; Gao, J., Zhang, Sun & Wu, 2019). This reveals the power attached with an electro-magnetic wave. It is the instantaneous poynting vector defined as

$$\mathcal{W} = \mathcal{E}X\mathcal{H} \tag{2.8}$$

Where: $\mathcal{W}$= instantaneous poynting vector (W/m^2), $\mathcal{E}$= instantaneous electric-field intensity (V/m), $\mathcal{H}$= instantaneous magnetic-field intensity (A/m) (Kraus and Marhefka, 2001).

Adekola (2012) emphasized that it is more suitable to find the average power density for applications concerning time varying fields. The author gave the time average Poynting vector (average power density) as;

$$p_{av} = \tfrac{1}{2}(E \times H^{*}) \quad (W/m^2) \tag{2.9}$$

Where: E= electric-field intensity (V/m), H *= conjugate of magnetic-field intensity (A/m)

xii. Radiation Intensity, U: This is defined as the time average per unit solid angle (Balanis, 2005). It is another measure of antenna performance which is obtained by multiplying the time average poynting vector and the square of the distance.

Thus:

$$U = r^2 P_{av} \text{ (W/ unit solid angle)} \quad (2.10)$$

Where: r= distance of antenna from origin to the field point, P_{av}=average power radiated

xiii. Radiation Resistance, R_{rad}: Radiation Resistance is the point that the value of a hypothetical resistor will dissipate a power equal to the power radiated by the antenna when fed by the same current (Adekola, 2012; United States Marine Corps, 2016).The higher the radiation resistance, the greater the energy radiated by the antenna. Hence, radiation resistance is a function of the current flowing through the antenna and this determines the energy to be radiated (Singh, Solanki, & Solanki, 2014). The equation of radiation resistance is:

$$R_{rad} = 2\frac{P_{rad}}{I_0^2} \quad (2.11)$$

Where; P_{rad} is $radiated$ $power$, I_0 is peak-value of the feed-point current.

xiv. Voltage Standing Wave Ratio (VSWR)– A portion of the transmitted power is reflected at the antenna, to the transmitter (Smith, 2006). The forward and return power generates standing wave with corresponding voltage minima and maxima (Vmin/Vmax). VSWR is the product of the minimum voltage and the inverse of the maximum voltage in a

standing wave pattern. It is also known as the ratio of power delivered to a device to the power reflected from the device.

xv. Return Loss: This is a logarithmic ratio in dB that compares the antenna reflected power to the power fed into the antenna from the transmission line. This parameter serves as an additional way of denoting mismatch, and the relationship that exist between the Signal Wave Ratio (SWR) and return loss (Collin, 2001).

$$Return\ loss\ (dB) = 20\ log_{10} = \frac{SWR}{SWR-1} \quad (2.12)$$

2.2 Classification of Antennas

Antennas could be classified based on electromagnetic wave transmission, as either Omni-directional (an antenna that radiates equally in all directions such as quad antenna, billboard antenna, and helical antenna) or a unidirectional antenna (an antenna that radiates in a particular designed direction such as radar antenna, dish antenna, Yagi antenna) (Madikwane, 2006; Uchendu & Kelly, 2016). Antenna classification could also be based on frequency (VLF, LF, HF, VHF, UHF, Microwave, Millimeter wave antennas), and also on the geometry of the shape namely: wire antennas, aperture antenna, micro- strip antennas, and array antennas and so on (Balanis, 2005).

2.2.1 Antenna Classification Based on Frequency

Table 2.1 is used to show the classification of antenna based on their frequency of operations. These include: VLF, LF, HF, VHF, UHF, Microwave, Millimeter wave antennas.

Table 2.1: Antenna Classification

Frequency Band	**Description**	**Typical service**	**Examples of antenna**
3-30KHz	Very Low Frequency (VLF)	Navigation Sonar	Vertical radiators, Top-loaded monopoles, T and Inverted L antennas, Triatic antenna Valley-span antenna
30-300KHz	Low Frequency (VF)	Radio Beacons, navigational aids	
300-3000KHz	Medium Frequency (MF)	AM Broadcasting, Maritime radio Coast guard communication Direction finding	Radiators (monopoles and dipoles) Directional antennas
3-30MHz	High Frequency (HF)	Telephone, Telegraph and Facsmile, amateur radio, ship-to-coast and ship-to-aircraft communication	Log periodic antenna, conical monopole and inverted cone antennas, vertical whip antenna, Rhombic antenna, Fan dipole antenna

Frequency Band	Description	Typical service	Examples of antenna
300-3000MHz	Very High Frequency (VHF)	Television, FM broadcast, air traffic control, police, navigational aids.	Yagi-uda antennas Log-periodic antennas Parabolic antennas Helical antennas Panel antennas Corner reflector antennas Discone antennas
3-30GHz	Ultra High Frequency (UHF)	Television, Satellite communication, Surveillance RADAR, navigational aids.	
30-300GHz	Super High Frequency (SHF)	Satellite communication, Airborne RADAR, Microwave links.	Parabolic antenna, pyramidal horn antennas, discone antennas, monopoles and dipoles antennas, Microstrip patch antennas, fractal antennas
300-3000GHz	Extremely High Frequency (EHF)	RADAR Experimental	Same as in (SHF)

Source: (Dhande, 2009)

2.2.2 Antenna Classification Based on Radiation Pattern

This sub-section narrated the classification of antennas based on the nature of their radiation pattern.

i. Isotropic Antenna: This is a theoretical antenna that radiates equally in all directions. It is a hypothetical lossless antenna which is usually employed to compare practical antennas. For a practical antenna of gain 3dB: it means that the gain of the practical antenna is three (3) times greater than the gain of an isotropic antenna. Figure 2.2 is the isotropic antenna pattern.

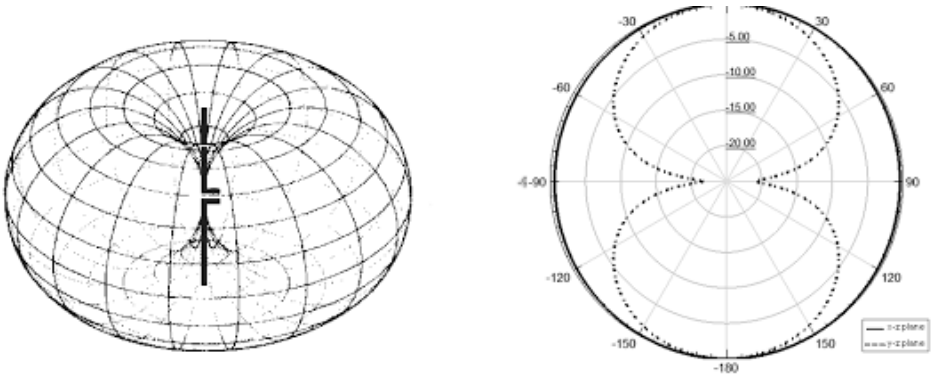

Fig. 2.2: Isotropic Antenna Pattern (Rohde & Schwarz, 2015)

ii. Omni-directional Antenna: This is defined as an antenna that radiates equally well in azimuth direction with some angle in elevation direction. Such antennas include whip antenna, dipole antennas, etc. According to Hui (2016), this is a type of antenna that is often designed for marine use. It performs well there because there are no obstacles at sea unlike land where there are many obstacles. United States Marine Corps (2016) described omni-directional antenna as that radiator that puts exactly the same radiation

in all directions around it, while directional antennas are radiators which the radiation is mainly on one direction. Figure 2.3 is the omni-directional antenna pattern.

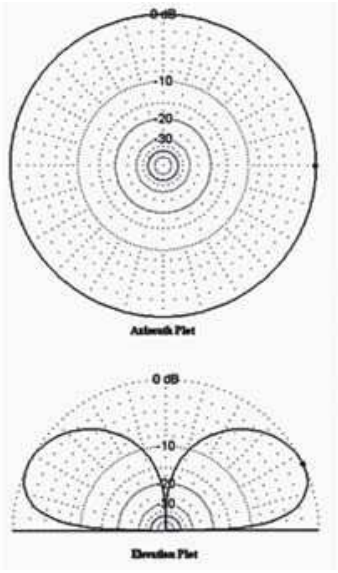

Fig. 2.3: Omni-directional Antenna Pattern (Dhande, 2009)

iii. Directional Antenna: Directional antennas are those antennas that focus their radiated energy in a specific direction. The antennas could be patch, dish, or horn. By transmitting the available energy within a semi-circle (180^0) 3dB gain is obtained, however, radiating the available energy within a quadrant (90^0) 6dB gain is actualized (scholz, 2016). Directional antenna pattern is shown in Figure 2.4.

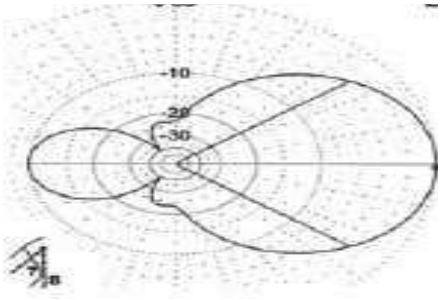

Fig. 2.4: Directional Antenna Pattern (Dhande, 2009)

iv. Hemispherical Antenna: These are antennas whose radiation pattern covers one half of the upper or lower hemisphere. Example of such antenna is monopole antenna, which can be used on aircraft for data link purpose. Figure 2.5 is the hemispherical antenna pattern.

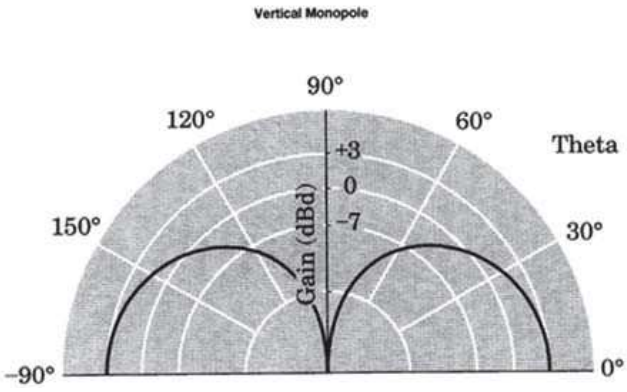

Fig. 2.5: Hemispherical Antenna Pattern (Dhande, 2009)

2.2.3 Antenna Classification Based on Geometry

Antennas can also be categorized as regards the nature of their geometry. The antennas are as listed:

i. Wire Antennas: These antennas are made of various forms of wire which shapes could be straight (dipoles), loop (circular, rectangular, square, etc), helix, and so on (Balanis, 2005). This category of antenna is symmetrically fed at the center with a sinusoidal current distribution (Kraus, 2001). Figure 2.6 is the diagram of Wire Antenna

Fig. 2.6: Diagram of Wire Antenna (Jackson, 2022)

ii. Dipole Antennas: This is an antenna made of conductive elements and whose whole length is half of a wavelength at its operation frequency. A half-wave dipole antenna has an approximate gain of 2.2dBi (CISCO Systems). Elevation pattern of dipole antennas indicates that they are best suitable to transmit and receive from the antenna broadside (Smith, 2016). This is because of its sensitivity to any movement away from a perfectly vertical position. The antennas can either be fed through an input coming to the bottom side of the antennas or into the center of the antenna. Qing and Chen (2015) revealed that dipole antennas are fundamental types of radiators common in many systems because of their uniform omni-directional coverage, moderate gain, relatively low production cost. However, the author regretted that dipole antennas have the challenge of relatively narrow bandwidth which hinders their usage in modern multi-band communication systems. According to the author, close-by objects readily detune the dipoles due to their limited bandwidth of operation. The antenna performs well in good signal areas and also very effective in weak signal areas where the dipole length suits the exact channel being radiated. Figure 2.7 is the diagram of Dipole Antenna.

Fig. 2.7: Diagram of Dipole Antenna (Elprocus, 2023).

iii. Loop antenna: This is a state where the wire antenna is used to form a loop. It can take any shape such as square, circle, among others. Figure 2.8 is the diagram of Loop Antenna.

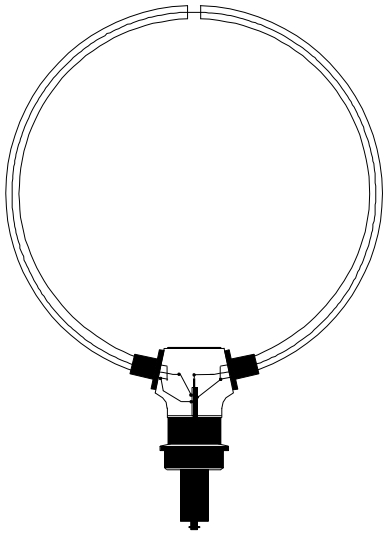

Fig. 2.8: Diagram of Loop Antenna (Rohde & Schwarz, 2015).

iv. Helical antenna: This involves the bending of a wire antenna into a helical shape or simply helix. Figure 2.9 is the diagram of Helical Antenna.

Fig. 2.9: Diagram of Helical Antenna (Elprocus, 2023).

v. Multiple Element/Collinear Omni Antennas (Collinear array): This involves combination of multiple wires or elements in a linear pattern in order to achieve a higher gain. Higher gain does not imply creation of more power by the antenna but the radiation of the same amount of power in a more focused manner. This antenna type share some general features with dipole. The use of multiple elements results to increase directionality of the antenna in the elevation pattern, and increased gain. Figure 2.10 is the diagram of Collinear array Antennas.

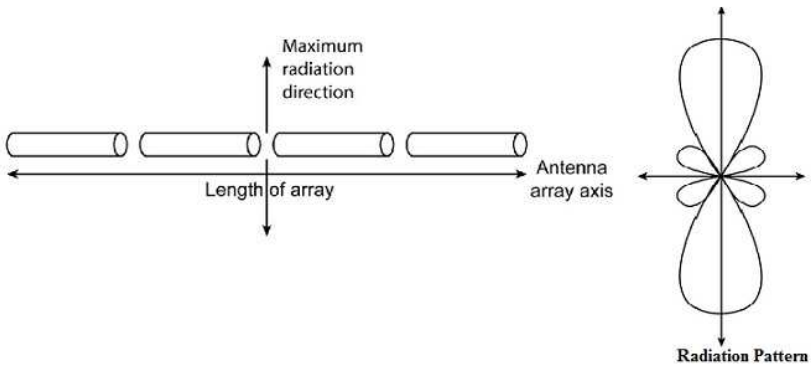

Fig. 2.10: Diagram of Collinear array Antennas (Elprocus, 2023).

vi. Yagi Antennas – This is made of an array of independent antenna elements with only one element driven to radiate EM waves. The antenna is formed by driving a simple antenna like dipole and shaping the beam using parasitic (non-driven) elements, and a reflector behind the driven element. The more the number of elements, the more the gain and directivity. Figure 2.11 is the diagram of Yagi Antenna.

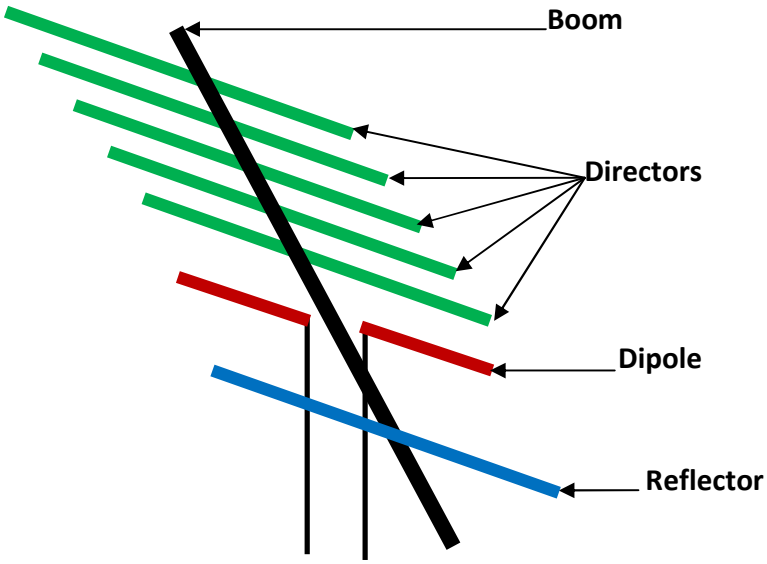

Fig. 2.11: The Yagi Antenna

vii. Flat Panel Antennas – These antennas are configured in a patch type, and they possess square or rectangular shape. These antennas possess optimal directivity and moderate gain. Figure 2.12 is the diagram of Flat Panel Antenna

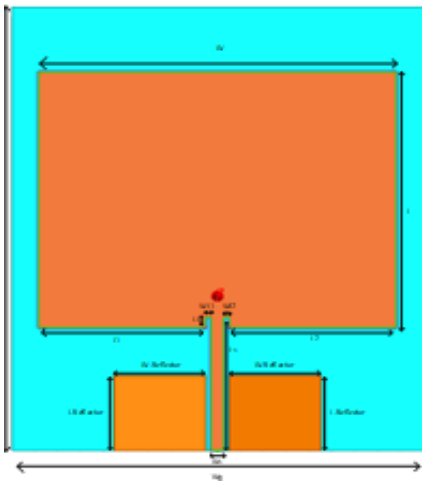

Fig. 2.12: Diagram of Flat Panel Antenna (Nugroho, Ruliyanta & Nugroho, 2023)

viii. Parabolic dish Antennas – These antennas employ physical features and multiple element antennas to actualize high gain and sharp directivity. They possess parabolic reflective dish to direct received EM waves to a single point on the antenna. This antenna is made of radiating element and a reflecting surface. Parabolic reflector antenna makes use of a parabolic reflector instead of the flat type, which is used to convert spherical waves into plane waves (Singh, Solanki, & Solanki, 2014). Figure 2.13 is the diagram of Dish Antenna.

Fig. 2.13: Diagram of Dish Antenna (Jackson, 2022)

ix. Slotted Antennas – They are made of narrow slot cut into ground plane. They possess similar radiation features like dipoles. They possess little gain, low directionality, but low cost. Figure 2.14 is the diagram of Slot Antenna

Fig. 2.14: Diagram of Slot Antenna (Elprocus, 2023)

x. Microstrip Patch Antenna: This is an antenna with patches of conducting materials etched on one side of a dielectric substrate, while the reverse side is the metal ground plane. The shape of this radiating patch can be square, rectangular, circular, triangular, and elliptical, among others. This antenna type is good for space-craft application. Microstrip patch array antennas are used extensively in the field of communication and microwave sensors, and are light weight, low profile and a compact and minimum line length feed network (Chen & Otto, 2016). A common benefit of patch antennas is their ability to have polarization diversity. In other words, Patch antennas can be designed to have vertical, horizontal, right hand circular or left hand circular polarizations, using multiple feed points, or a single feedpoint with asymmetric patch structures (Arpitha & Kumar, 2015). Microstrip Antennas are constructed with Printed Circuit Board (PCB) traces on the PCB board and can take different styles. They are very small and light weight. They operate within particular antenna frequency ranges

and thus not suitable for wideband communication systems. Microstrip antennas are used on high-performance aircrafts, spacecrafts, satellites, cars, and even handheld electronic devices such as telephone (Balanis, 2005). Figure 2.15 is the diagram of Micro Strip Antenna.

Fig. 2.15: Diagram of Micro Strip Antenna (Elprocus, 2023)

xi. Aperture antenna: This antenna is constructed from waveguide which is basically a hollow metallic tube through which waves travel. The waveguide can take the shape of a rectangle or circle. Example of such antenna is the rectangular or circular horn (Singh, Solanki, & Solanki, 2014). These types of antennas find applications in the aircraft or spacecraft. Amiri (2015), and Saunders and Zovala (2007) stated that the part of the wave that is passing through the hole in the absorbing sheet will continue, after being diffracted at the borders of the hole, and will spread out to form a "far field radiation pattern" of a "uniformly illuminated aperture antenna" possessing the shape of the hole. Figure 2.16 is the diagram of Aperture Antenna.

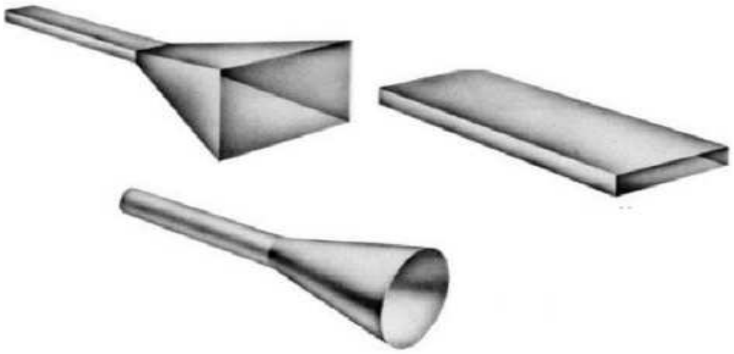

Fig. 2.16: Diagram of Aperture Antenna (Elprocus, 2023)

2.3 Wireless Communication Antennas

Antennas are indispensable part of communication systems. Mobile phones, Wireless Fidelity (Wi-Fi) Internet, TV broadcasting, Frequency modulation (FM) radio broadcasting, among others operate via wireless communication with the aid of set of antennas. The popular types of antenna used for this is the quarter wave helical antenna, the quarter wave whip (monopole) antenna and Log Periodic Antennas. Whip antenna is mainly used for cellular phones within the frequency range of mainly 400 to 500MHz. The quarter wave helical antenna is used in the frequency bands of 800 to 1000MHz. Whip antenna has similar performance like the helical antenna but has a smaller size. Log–periodic Antenna is a broadband antenna. It offers moderate gain and supports wider frequency bandwidths. (Özgönül & Seçmen, 2017; Singh, Solanki & Solanki, 2014; Bontempo, Marques, Marins & Arismar, 2015). Most antennas are resonant appliances that perform efficiently within a comparable narrow frequency band. Antenna sizes are often referred in relation to wavelength. The wavelength is the distance travelled by wave within a cycle (Dhande, 2009).

$$\lambda = \frac{c}{f} \tag{2.13}$$

Where, λ is the wavelength in meters, c is the speed of light, f is the frequency.

The dimensions of antennas are dependent upon the wavelength of the transmitted signal. As the frequency of the transmitted signal increases, its wavelength decreases, and hence the size of the wireless system reduces and becomes compact (Gruber, Froeling, Leiner & Klomp, 2018; Dhande, 2009)

2.4 Array Antennas

The radiation patterns of single-element (dipole) antennas are omni-directional. That is, they have relatively low directivity (gain). Hence, single-element antennas are not practicable in long distance communications – as antennas with high directivity are often needed. While using such antennas, the dimensions of the structure are very large. Alternative technique to enlarge the electrical size of an antenna is to assemble the radiating elements together, which invariably changes the electrical length and the antenna geometry (Lema & Hailu, 2019). The array of radiating elements are mainly similar, though not always necessary but easier for design and manufacture. Also, the radiating elements in the array could be of any form (wire dipoles, loops or apertures). Hence, the overall electromagnetic fields generated by the array constitute a vectorial superposition of the electromagnetic fields radiated by the individual elements (Safar & Al-Zayed, 2016). In order to obtain a very directive pattern, it is very important that the fractional fields – radiated by the individual elements, interfere constructively in the preferred direction and interfere destructively in every other remaining space (Felici-Castell, Navarro, Pérez-Solano,Segura-García & García-Pineda, 2017).

An array involves the combination of two or more antenna elements, positioned in a particular geometrical arrangement, in order to achieve the needed radiation characteristics. Array of

antennas can either be active or passive. The elements are active when they are electrically linked to the (driven) sources (in transmit mode) or sinks (in receive mode). They are passive or parasitic elements (non-driven) when the elements are not electrically connected (Neelakanta, 2002; Huong, 2020).

When a single element antenna does not give the required characteristics, multi-element can be used. According to (Hui, 2016), antennas with a given radiation pattern can be positioned in (a line, circular, plane) pattern to generate different radiation patterns. Hence, antenna array is a configuration of multiple antenna elements positioned/arranged to obtain a required radiation pattern. These arrays can be categorized into:

i. Linear array – a situation where the antennas are arranged along a straight line.

ii. Circular array – here, the antennas are arranged around a circular ring.

iii. Planar array – this is the situation where the antenna elements are arranged over some planar surface. An example is rectangular array.

iv. Conformal array – this is obtained when the antenna elements are arranged to conform to some non-planar surface, such as aircraft skin.

v. Phased array – this comprises of an array of identical radiating elements which achieves a particular pattern by controlling the element excitation phasing. This type of antenna array can be used to vary the main lobe of the antenna without physically moving the antenna.

vi. End Fire Arrays – these are directional antennas whose mechanical characteristics are parallel to the major/main lobe of the radiation beam (Scholz, 2016). Examples of such antennas are yagi and log-periodic antennas. While the mechanical concept of yagi antennas are not proper for extreme climatic conditions due to influence of

ice and snow on the radiation pattern, the pattern of log-periodic antennas are constant over a wide frequency range without influence of such. Thus, Log-periodic antennas are utilized where exact radiation pattern is required.

vii. Broadside Array – these are directional antennas which mechanical characteristics and main lobe of the radiation pattern are orthogonal to each other (Scholz, 2016). Examples of such antennas are panel and corner reflector antennas.

Table 2.2 compared different kinds of antenna geometry based on their radiation patterns, power gain, directivity, and polarization.

Table 2.2: Antenna Comparison

Antenna types	**Radiation patterns**	**Power gain**	**Directivity**	**Polarization**	**Frequency Range (BW)**
Dipole	Broadside	Low	Low	Linear	3kHz to 300GHz
Multi element dipole	Broadside	Low/ Medium	Low	Linear	30MHz to 3GHz
Flat panel antenna	Broadside	Medium	Medium/High	Linear/circular	4900 to 6200MHz
Parabolic dish antenna	Broadside	High	High	Linear/circular	10.7–11.7 GHz, 11.7–12.75GHz
Yagi antenna	Endfire	Medium/High	Medium/High	Linear	3MHz and 300GHz
Slotted antenna	Broadside	Low/ Medium	Low/ Medium	Linear	300MHz to 30GHz.
Microstrip antenna	Endfire	Medium	Medium	Linear	13-19GHz

Source: (Smith. Aerocomm, 2016)

Maharimi et al. (2012) listed various array design variables that can be altered to obtain the total array pattern design, such as;

i. General array shape (linear, circular, planar, etc)
ii. Element Spacing
iii. Element excitation amplitude
iv. Element excitation phase
v. Patterns of array elements

Hence, the ability to increase the performance of an array antenna is dependent on the parameters like the number of radiating elements on the array, spacing between the radiating elements, phase and amplitude of excitation (Huong, 2020). Uniform arrays, as defined by Hui, 2016, are equally spaced identical elements of equivalent size and with a linearly progressive phase from element to element. Such that:

$$\varphi_1 = 0, \varphi_2 = \alpha, \varphi_3 = 2\alpha, - - -, \ \varphi_N = (N-1)\alpha \tag{2.14}$$

The author highlighted some of the general features of the array factor AF with respect to φ to include:

i. $[AF]_{max} = N$ at $\varphi = o\ (mainlobe)$
ii. $totalnumberoflobes = N - 1\ (onemainlobe, N - 2\ sidelobes)$
iii. $mainlobewidth = \frac{4\pi}{N}, minorlobewidth = \frac{2\pi}{N}$

The phasing of the uniform linear array elements could be chosen in such a way that the main lobe of the array pattern lies along the array axis (end-fire array) or normal to the array axis (broad side array). Thus,

For End fire array, main lobe is at $\theta=0^0$ or $\theta=180^0$

For Broadside array, main lobe is at $\theta=90^0$.

Hence, the maximum numerical value for the array factor is obtained when the array phase function is zero. It is written by (Huong, 2020) as:

$$\phi=\sigma + k\, d \cos\theta = 0 \quad (2.15)$$

According to Zhang, Cui, Xu and Lu (2019), antenna arrays ensure an efficient means of detecting and processing signals that arrive from various directions. The authors emphasized that antenna array sensors have the capability of modifying its beam pattern through the aid of amplitude and phase distribution termed the weights of the array, which is unlike a single antenna with limited directivity and bandwidth.

Advantages of antenna arrays in wireless communication (Hui, 2015)

i. Provision of high gain through the use of simple antenna elements.
ii. Provision of diversity gain in multipath signal reception
iii. Provision of a steerable beam (change of radiation direction) just as in smart antennas.
iv. antenna arrays allow array signal processing

2.5 Log-Periodic Dipole Array (LPDA) Theory

Log-Periodic Dipole Array (LPDA) is an antenna whose electrical properties vary negligibly with the logarithm of the frequency (Biabanifard, Biabanifard, Javad & Jahanshiri, 2018). Research shows that log-periodic arrays are infinite at both ends as shown in Figure 2.17. That is to say, one end is infinitely large while the other end is infinitely small. This retains the periodicity of the input impedance over the frequency.

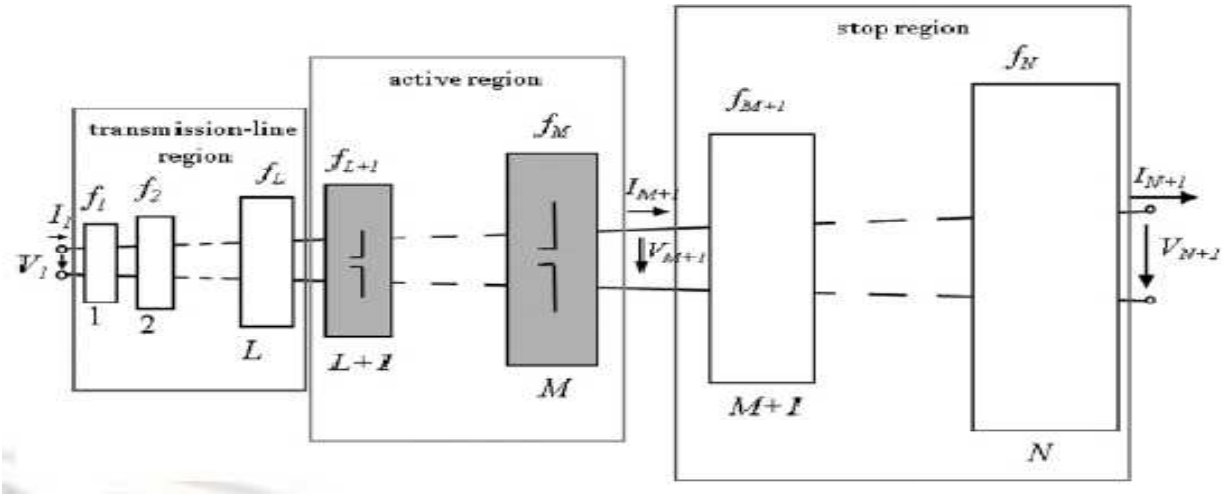

Figure 2.17: Block diagram of an N-element Log-Periodic Dipole Array (Wankhade & Nema, 2013).

While designing practical antennas, the infinite Log-Periodic Array antennas are truncated at both ends as represented in Figure 2.16.

According to Figure 2.1, three sections exist in Log Periodic Array antennas namely;

i. Transmission line region (<λ/2): There is no radiation by the elements in this zone due to the fact that the size of the elements is less than the wavelength.

ii. Active region (=λ/2): Dipole elements are permitted to radiate in this zone because the size of elements is equal to the wavelength.

iii. Stop region (>λ/2): in this region, no radiation is experienced. This is because the induced current from the active region to this region is of the same amplitude although with 180^0 phase difference (Wankhade & Nema, 2013; Okoye, 2014).

2.5.1 Background on Log-Periodic Array (LPA) Antennas

Log Periodic (LP) antenna was invented in the year 1958 by Dwight Isbell and Raymond DuHamel at the University of Illinois. LPA antennas are linearly polarized and broadband antennas due to its frequency independent features (Lakshimi & Raju, 2012; Fiorini, Morbidel, & Caso, 2017). It offers moderate gain and evolved from the principle of frequency independent antennas which theoretical background was introduced by Rumsey at the University of Illinois (Abdullahi & Ahmad, 2018; Aziz-ul-Haq, 2012). DuHamel implemented Log-Periodic Antenna based on this motive which led to the introduction of LPDA by Isbell. Afterward, (Carrel, 1961) investigated the LPDA mathematically and computed some of the antenna parameters such as its radiation pattern and input impedance.

2.5.2 Principles of Frequency Independent Antennas

Frequency-independent or Ultra-Wideband (UWB) antennas are characterized by certain key properties, including input impedance, radiation pattern, gain, polarization, and others, which remain relatively constant across a broad range of frequencies (Fiorini, Morbidel, & Caso, 2017). The magnitudes of frequency independent antennas alter with frequency when expressed in wavelength, λ, thus, they show different radiation characteristics at diverse frequencies (Amiri, 2015). The variations of radiation characteristics with frequency limit the bandwidth of the antenna and thus the information carrying capacity of the communication link to which the antenna belongs (Kim, 1999). The subject of frequency independent antennas, which ideally offer an endless bandwidth, was first addressed by Rumsey, who explained the principal requirements for the antennas (Fiorini, Morbidel, & Caso, 2017).

2.5.2.1 Angle Specified Antennas

Kim (1999) stated that if the shape of a lossless antenna can be specified entirely by angles, then the antenna characteristics such as its radiation pattern and input impedance could remain constant with frequency. In other words, the dimensions of this type of antenna, when expressed with respect to wavelength, will be the same at every frequency. This means that the electrical properties of the antenna are constant, and do not vary with frequency. This is termed frequency independent antennas for the ideal case result.

In general, if the terminals of both antennas are considerably close to the origin of a spherical coordinate system, the equation for angle specified antenna geometries is written by (Kim, 1999) as:

$$r = F(\theta, \varphi) = e^{a\varphi} f(\theta) \tag{2.16}$$

$where;$

$f(\theta) = arbitrary\ function,$

$$a = \frac{1}{k}\frac{dK}{dC} \tag{2.17}$$

K depends on angle C for congruence, but neither on ɵ nor φ. (Kim, 1999)

Examples of Angle specified Antennas are;

i. Conical spiral antenna
ii. Planar equiangular spiral antenna

2.5.2.2 Self-Complementary Configuration

According to this principle, for an antenna with the same shape as its complement empty part, its impedance is static at all frequencies (Biabanifard et al., 2018).

If complementary antennas possess input impedances $Z_1 \, and \, Z_2$, then the product of $Z_1 \, and \, Z_2$ is obtained by (Biabanifard et al., 2018) as;

$$Z_1 Z_2 = (60\pi)^2 = 3600\pi^2 \quad (2.18)$$

Hence, for two planar structures that are self-complementary, Biabanifard et al. (2018) states that

$$Z_1 = Z_2 = 60\pi \quad (2.19)$$

It should be noted that frequency independence is actualized once antennas that resemble their complements are designed, in as much as an actual frequency independent antenna would have constant input impedance.

2.6 Single Log Periodic Array (SLPA) Antennas

Log-periodic antenna is a broadband, multi-element, directional, narrow-beam antenna that has impedance and radiation characteristics which are frequently repetitive as a logarithmic function of the excitation frequency (Okoye, Ndinechi, Mbaocha, & Agubor, 2017; Halder & Pradhan, 2013; Abdullahi & Ahmad, 2018). Reeve (2016) defined log periodic antenna as an array of dipoles with mathematically related lengths and spacing.

That is; the relationship between lengths and spacingis written by (Reeve, 2016) as:

$$\frac{d1}{d2} = \frac{d2}{d3} = \ldots = \frac{dn}{dn+1} = \frac{l1}{l2} = \frac{l2}{l3} = \ldots = \frac{ln}{ln+1} = \frac{1}{\tau} \quad (2.20)$$

Where;

d_n is equal to the distance of n-dipole from the vertex formed near the feed point in meters

l_n is the length of n-dipole.

Thus, the inverse of this ratio in equation (2.20) is the design factor $\boldsymbol{\tau}$. That is (Carrel, 1961);

$$\tau = \frac{d_2}{d_1} = \frac{l_2}{l_1} < 1 \quad (2.21)$$

Where: $0.76 \leq \boldsymbol{\tau} \leq 1$

Log periodic antenna could be described by two geometric parameters which are a scale factor, τ, that defines the relative lengths and also a spacing factor, σ, which identifies the relative spacing between the antenna elements. The third parameter is α, which is half of the apex angle and that is deduced from τ and σ as shown in equation (2.22) by (Carrel, 1961).

$$\alpha = \text{Tan}^{-1}\left(\frac{(1-\boldsymbol{\tau})}{4\sigma}\right) \quad (2.22)$$

where α is half of the apex angle, $\boldsymbol{\tau}$ is the design/scale factor and σ is the spacing factor

The lengths and spacing between the elements of log-periodic antennas do increase logarithmically from one end of the antenna to the other (Kibona, 2013; Abdullahi & Ahmad, 2018). The LPAs are utilized in situations where wide range of frequencies is required with moderate gain and directionality.

Log periodic Antenna has the capability of producing different gains for the same antenna frequency simply by adjusting its elements frequency (Halder & Pradhan, 2013). Lazadiris et al. (2016) stated that Log Periodic Dipole Arrays (LPDAs) possess relatively flat gain curve over range of frequency octaves. This is as opposed to the gain of Yagi-Uda antennas which is obtained over a much narrower bandwidth with a gain curve that increases with frequency. "In modern telecommunication systems, antennas with wider bandwidth and smaller dimensions than conventional ones are preferred (Kibona, 2013; Abdullahi & Ahmad, 2018).

The author clarified that log-periodic antennas are designed in order to ensure that it has a very wide bandwidth, which theoretically is infinite.

According to Reeve (2016), the highest directivity of log periodic antenna is obtained along the longitudinal axis in the direction of the shortest elements. When the antenna is illuminated by an electromagnetic field, electric current do pass through each of the elements. Thus, currents in the active region combine together on the transmission line in accordance to their phase, and then operate together to generate the radiation pattern of the antenna, the author opined. The radiation energy generated at a particular frequency moves across the feeder till it gets to the section of the structure where the electrical lengths of the antenna elements and phase relationships generate the radiation (Kibona, 2013). As the frequency is varied, the place of the resonant element moves gradually from one element to the next one. Engargiola (2016) opined that the use of log periodic geometry is not a criterion for frequency independence of antenna. The shapes of the antenna has to be carefully selected and tuned in order to ensure low Standing Wave Ratio (SWR) and minimal variation of impedance and beam shape within a log periodic of frequency. It is the linear dimensions of the longest and shortest dipole elements that determine the boundaries of the antenna passband.

Figure 2.18 shows the schematic diagram of Single Log-Periodic Array (SLPA) antennas. It is an array of dipole elements attached to a common transmission line, and fed from the apex of the array.

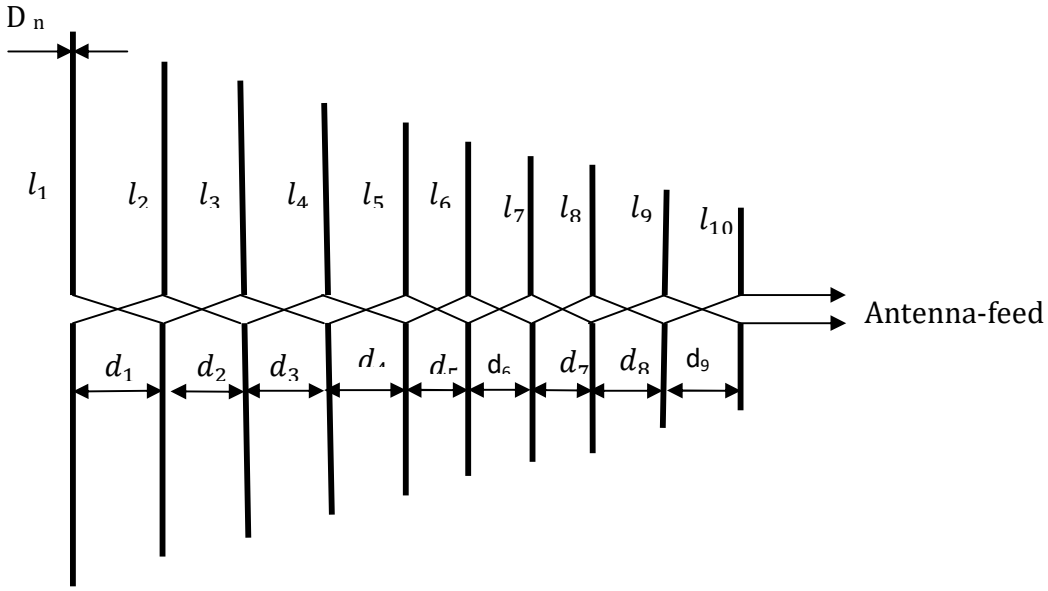

Fig. 2.18: Schematic diagram of SLPA Antennas (Okoye, 2014).

The elements are driven with a phase shift of 180^0 each by switching or by the alternation of the element connections. The set of dipoles that are attached in proximity to the input are close to each other and almost out of phase, and hence annul each other's radiation. As the element spacing increases, a spot is reached along the array where the phase difference in the transmission line is forced to combine with the 180^0 switch to generate a total of 360^0 (Carrel, 1961). Thus, this relationship is written in equation (2.23) by (Carrel, 1961) as:

$$\mathbf{d_{n-n+1}} = \frac{1}{2}\left(l_n - l_{n+1}\right)\cot\alpha \qquad (2.23)$$

where $\mathbf{d_{n-n+1}}$ is the element spacing and $l_n - l_{n+1}$ is the difference of the radiating elements (Carrel, 1961). The fields generated from the dipoles/elements in phase are directed toward the apex of the antenna, thereby producing a lobe in the active region made of set of dipoles.

2.7 Array Factor

It is a mathematical factor used to signify the relationship between total field of array and the field of single element (Huong, 2020). Array factor is a function of the array geometry and the array excitation phase. The features of the array factor and the total field of the array can be checked through varying the distance of separation d and/or the phase β that exists in between the elements. With an array factor, the far field generated by array of identical elements can easily be computed. The far field is equivalent to the product of the field of a single element, at a selected reference point (usually the origin), and the array factor of that array (Balanis, 2005). This is termed pattern multiplication.

Hui (2016) postulated the array factor for computation of parameters of uniform antenna array via pattern multiplication approach. According to the author, the total electric field E radiated from an arbitrary antenna array is given by (Balanis, 2005) as in equations (2.24) and (2.25):

$$E = Ke^{-jkr_0}\left[\hat{a}_\theta f_\theta(\theta,\varphi) + \hat{a}_\varphi f_\varphi(\theta,\varphi)\right]\sum_{i=1}^{N}\omega_i e^{-jk\rho_i.\hat{a}_r(\theta,\varphi)} \quad (2.24)$$

$$E = Ke^{-jkr_0}\left[\hat{a}_\theta f_\theta(\theta,\varphi) + \hat{a}_\varphi f_\varphi(\theta,\varphi)\right]f_{array}(\theta,\varphi) \quad (2.25)$$

Equations (2.24) and (2.25) follow the principle of pattern multiplication which states that the product of the antenna element pattern and an array factor $f_{array}(\theta,\varphi)$ gives the array pattern. For uniform linear array, the array factor is written by (Hui, 2016) as:

$$f_{array}(\theta,\varphi) = \sum_{i=1}^{N}\omega_i e^{-jk\rho_i.\hat{a}_r(\theta,\varphi)} = \sum_{i=1}^{N}\omega_i e^{-jb_i} \quad (2.26)$$

This assumed that excitation currents have equal amplitude (I=1), and phase difference of β.

For $\theta = \frac{\pi}{2}$, Hui (2016) defined the array factor as shown in equations (2.27), (2.28) and (2.29)

$$AF = f_{array}\left(\theta = \frac{\pi}{2}, \varphi\right) = \sum_{i=1}^{N} \omega_i e^{-jb\ i} = I \sum_{i=1}^{N} e^{-j(i-1)\beta}\ e^{-j(i-1)dcos\varphi} \quad (2.27)$$

$$AF = 1 + e^{j(kdcos\varphi+\beta)} + e^{j2(kdcos\varphi+\beta)} + \ - - - + e^{j(N-1)(kdcos\varphi+\beta)} \quad (2.28)$$

$$AF = \sum_{n=1}^{N}\ \ e^{j(n-1)\varphi} = e^{j(N-1)\frac{\varphi}{2}} \frac{sin\left(N\frac{\varphi}{2}\right)}{sin\left(\frac{\varphi}{2}\right)} \quad (2.29)$$

Where: $\varphi = kdcos\varphi + \beta\ and\ 0 \leq \varphi, \beta = \leq 2\pi$.Thus, normalized array factor is

$$|AF\ _N(\varphi)| = \frac{1}{\Gamma}\left|\frac{sin\left(N\frac{\varphi}{2}\right)}{sin\left(\frac{\varphi}{2}\right)}\right| \quad (2.30)$$

Where: Γ is a constant to generate the largest value of $|AF\ _N|$ equals 1.

Hui (2016) postulated thus: for antenna array of identical elements, the radiation pattern of the antenna array could be determined through pattern multiplication theorem. Hence, Array pattern is the product of Array element pattern and Array factor (AF).

The author opined that Array factor AF is independent of the antenna type provided that all the antenna elements are identical. According to the author, for an N-element linear array, the field of an isotropic radiator located at the origin is written by (Hui, 2016) as;

$$E_\theta = I_0 \frac{e^{-jkr}}{4\pi r} \quad (2.31)$$

Where:

$$\mathrm{r1} = \mathrm{r}, \mathrm{r}_2 = \mathrm{r} - \mathrm{d} * \cos\theta, \mathrm{r}_3 = \mathrm{r} - 2 * \mathrm{d} * \cos\theta, - - -, \mathrm{r}_\mathrm{N} = \mathrm{r} - (\mathrm{N} - 1)\mathrm{d} * \cos\theta, \quad (2.32)$$

$$I_N = \ I_0 * e^{j\varphi\ N},\ (N = 1, 2, 3 \ldots) \quad (2.33)$$

Hui (2016) further derived the field as represented in equations (2.34), (2.35) and (2.36);

$$E_{\theta_1} = I_0 \frac{e^{-jkr}}{4\pi r} = E_0 \quad (2.34)$$

$$E_{\theta_2} = I_0 e^{-j\varphi_2} \frac{e^{-jk(r-d\cos\theta)}}{4\pi r} = E_0 e^{j(\varphi_2 + kd\cos\theta)} \quad (2.35)$$

$$E_{\theta_N} \approx I_0 e^{-j\varphi_N} \frac{e^{-jk[r-(N-1)d\cos\theta)}}{4\pi r} = E_0 e^{j[\varphi_N + (N-1)kd\cos\theta]} \quad (2.36)$$

By applying superposition, the overall array far field is obtained by (Hui, 2016) as shown in equations (2.37), (2.38) and (2.39);

$$E_\theta = E_{\theta_1} + E_{\theta_2} + - - - + E_{\theta_N} \quad (2.37)$$

$$E_\theta = E_0[1 + e^{j(\varphi_2 + kd\cos\theta)} + e^{j(\varphi_3 + 2kd\cos\theta)} + - - - + e^{j[\varphi_N + (N-1)kd\cos\theta)}] \quad (2.38)$$

$$E_\theta = E_0[Array - Factor] \quad (2.39)$$

Florence and Raju (2014) postulated that for sinusoidal current distribution of dipole antenna positioned along the z-axis.

The element pattern is calculated thus by (Florence and Raju, 2014) as:

$$F(\theta) = \frac{\cos(0.5\pi \cos\theta)}{\sin\theta} \quad (2.40)$$

The far field A-F (θ) pattern in the horizontal x-y plane due to the element pattern F (θ) is given by (Florence & Raju, 2014) as in equation (2.41):

$$AF(\theta) = \sum_{n=1}^{N} 2I_n \cos(kd_n \cos\theta) * F(\theta) \quad (2.41)$$

Assuming that the excitation and geometry are symmetric with respect to the center of the array, the normalized radiation pattern in dB is written by (Florence & Raju, 2014) as,

$$AF_n(\theta) = 20\log_{10}\left[\frac{|AF(\theta)|}{|AF(\theta)|_{max}}\right] \quad (2.42)$$

Where:

N=number of elements, $k = \frac{2\pi}{\lambda}$=wave number, λ=wave length, d=distance of center of n^{th} element from origin, N=total number of elements, θ=the polar angle of the far field measured from broad side.

The authors stated that the radiation pattern generated by the array is expected to satisfy the condition of low Side Lobe level (SLL) and optimum Dynamic Range Ratio (DRR). They explained DRR to be the ratio of maximum value of excitation amplitude to the minimum value (Florence & Raju, 2014).

The array factor for array of antennas is well synthesized/derived from computing the total field generated by a sample of two or more identical elements of the array. With the array factor, the total field generated by the antenna array of any number of radiating elements can be computed, provided the field generated by a single element in the array is known (Florence & Raju, 2014).

2.7.1 Array-Factor for Single Log-Periodic Array (SLPA) Antennas

Figure 2.19 was the array arrangement of Single Log-Periodic Array Antennas. From the Figure, R_1, R_2, R_3, R_4 and R_n represented the distances from the source points to the field points of the antennas. The r_1, r_2, r_3, r_4 and r_n indicated the distances from the origin of the antennas to the field points. Also, z_1', z_2', z_3', z_4' and z_n' stand for the differential lengths of the antenna, while d_1, d_2, d_3, d_4 and d_n represented the distances of separation between the antenna elements in the array (Okoye, 2014).

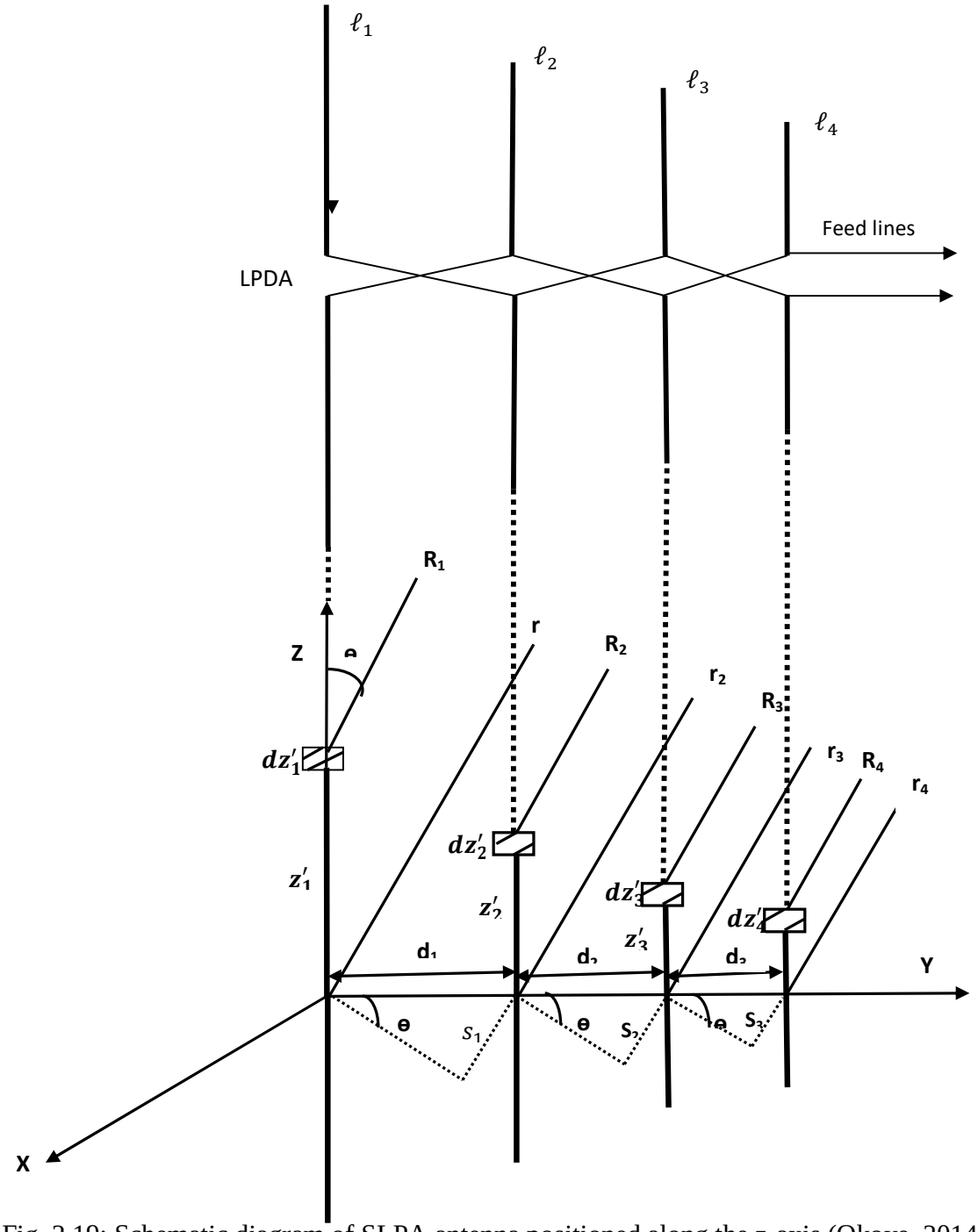

Fig. 2.19: Schematic diagram of SLPA antenna positioned along the z-axis (Okoye, 2014)

According to the author, the phase variations of the SLPA antenna elements were evaluated by determining the distances from the source points to the field points of the antenna elements $R_1, R_2, R_3, \text{and } R_n$ in terms of the distances from the origin of the antennas to the far field points $r_1, r_2, r_3, \text{and } r_n$. Also, the phase of the antennas $\hat{R}$ in the Green's function was substituted with the values of the derived R. This was as demonstrated by (Okoye, 2014) as in equations (2.43), (2.44), (2.45) and (2.46).

$$R_1 = r - z_1' \cos\theta \tag{2.43}$$

$$R_2 = r - d_1 sin\theta - z_2' \cos\theta \tag{2.44}$$

$$R_3 = r - (d_1 + d_2) \sin\theta - z_3' \cos\theta \tag{2.45}$$

Then, from design factor,τ relation, it is shown by (Okoye, 2014) that:

$$\tau = \frac{d_2}{d_1}, \tau^2 = \frac{d_3}{d_1}, \tau^3 = \frac{d_4}{d_1} \tag{2.46}$$

(That is: $\tau = \frac{d_2}{d_1} = \frac{d_3}{d_2} = \frac{d_4}{d_3} \cdots$)

According to (Okoye, 2014), substituting the d_2 in equation (2.46) with τd_1, resulted to equation (2.47);

$$R_3 = r - d_1(1 + \tau) \sin\theta - z_3' \cos\theta \tag{2.47}$$

Also, from Figure 2.19,

$$R_4 = r - (d_1 + d_2 + d_3) \sin\theta - z_4' \cos\theta \tag{2.48}$$

Substituting the d_2 with τd_1 and the d_3 with $\tau^2 d_1$, resulted to (2.49) (Okoye, 2014):

$$R_4 = r - d_1(1 + \tau + \tau^2) \sin\theta - z_4' \cos\theta \tag{2.49}$$

In order to obtain the effective phase variations for the SLPA antennas, the antenna phase $\hat{R}$ in the Green's function was replaced with the values of R_1,R_2, R_3 and R_4, of equations (2.43), (2.44), (2.47) and (2.49) to give the expressions written in equation (2.50) by (Okoye, 2014);

$$\frac{e^{-j\,k\,R_{eff}}}{r} = \frac{e^{-j\,k\,R_1}}{r} + \frac{e^{-j\,k\,R_2}}{r} + \frac{e^{-j\,k\,R_3}}{r} \tag{2.50}$$

Multiplying both sides of equation (2.50) by r gave (2.51) as written by (Okoye, 2014).

Hence;

$$e^{-j\,k\,R_{eff}} = e^{-j\,k\,R_1} + e^{-j\,k\,R_2} + e^{-j\,k\,R_3} \tag{2.51}$$

Then, substituting the values of $R_1, R_2, R_3\ and\ R_4$ into equation (2.51) resulted to equation (2.52), and then (2.53) as indicated by (Okoye, 2014).

$$e^{-j\,k\,\hat{R}_{eff}} =$$

$$e^{j\,k\,z_1'\cos\theta} + e^{j\,k\,d_1\sin\theta + z_2'\cos\theta} + e^{j\,k\,[d_1\ (1+\tau)\sin\theta + z_3'\cos\theta]} + e^{j\,k\,[d_1\ (1+\tau+\tau^2)\sin\theta + z_4'\cos\theta]} \tag{2.52}$$

Simplifying the above expression of the effective phase gave equation (2.53),

$$e^{-j\,k\,\hat{R}_{eff}} = \begin{matrix} e^{j\,k\,z_1'\cos\theta} + e^{j\,k\,d_1\sin\theta} e^{j\,k\,z_2'\cos\theta} \\ + e^{j\,k\,d_1\sin\theta} e^{j\,k\,d_1\tau\sin\theta} e^{j\,k\,z_3'\cos\theta} + e^{j\,k\,d_1\sin\theta} e^{j\,k\,d_1\tau\sin\theta} e^{j\,k\,d_1\tau^2\sin\theta} e^{j\,k\,z_3'\cos\theta} \end{matrix} \tag{2.53}$$

Factorizing out equation (2.53) resulted to (2.54) as written by (Okoye, 2014),

$$e^{-j\,k\,\hat{R}_{eff}} = \begin{matrix} e^{j\,k\,z_1'\cos\theta}\ (1 + e^{j\,k\,d_1\sin\theta} \\ + e^{j\,k\,d_1\sin\theta} e^{j\,k\,d_1\tau\sin\theta} + e^{j\,k\,d_1\sin\theta} e^{j\,k\,d_1\tau\sin\theta} e^{j\,k\,d_1\tau^2\sin\theta}) \end{matrix} \tag{2.54}$$

As the differential lengths of the antenna elements approached zero, (That is, for $z_1' = z_2' = z_3' = 0$), the expression $e^{j\,k\,z'\cos\theta}$ equals one (Okoye, 2014).

Thus, equation (2.54) is reduced to (2.55) according to (Okoye, 2014),

$$AF = \frac{1 + e^{j\,k\,d_1 \sin\theta}}{+ e^{j\,k\,d_1 \sin\theta} e^{j\,k\,d_1 \tau \sin\theta} + e^{j\,k\,d_1 \sin\theta} e^{j\,k\,d_1 \tau \sin\theta} e^{j\,k\,d_1 \tau^2 \sin\theta}} \quad (2.55)$$

Considering more antenna elements in the Single LPA antenna, the Array- Factor series equation shown above was extended as denoted in equation (2.48) by (Okoye, 2014);

$$AF = 1 + e^{j\,k\,d_1 \sin\theta} + e^{j\,k[\,d_1(1+\tau)\sin\theta\,]} + e^{jk[d_1\,(1+\tau+\tau^2)\sin\theta]} + \cdots \quad (2.56)$$

Thus, for an infinite series of array of dipole elements, the Array Factor was conveniently represented as in equations (2.57) and (2.58) by (Okoye, 2014);

$$AF = 1 + e^{j\,k\,d_1 \sin\theta} + e^{j\,k\,d_1 \sin\theta} e^{jk\,d_1 \tau \sin\theta} + e^{j\,k\,d_1 \sin\theta} e^{jkd_1 \tau \sin\theta} e^{jkd_1 \tau^2 \sin\theta} + \cdots + \prod_{i-1}^{n} e^{jk\tau^{i-1} sin\theta} \quad (2.57)$$

Assuming, $kd_1 \sin\theta = \varphi$

$$A.F = 1 + e^{j\varphi} + e^{j\,\varphi} e^{j\tau\varphi} + e^{j\,\varphi} e^{j\tau\varphi} e^{j\tau^2\varphi} + \cdots + \prod_{i=1}^{n} e^{j\tau^{i-1}\varphi} \quad (2.58)$$

Equation (2.58) was expressed in a compact form as represented in equation (2.59) by (Okoye, 2014);

$$A.F = 1 + \sum_{n=1}^{N-1} \prod_{i=1}^{n} e^{j\tau^{i-1}\varphi} \quad (2.59)$$

Where; N = number of dipole elements.

2.7.2 Derivation of SLPA Antenna Parameters

i. Total Electric/Magnetic Field for SLPA Antennas

The electric and magnetic (EM) Fields for the first element in SLPA antenna was derived in equations (2.60) and (2.61) respectively. The electromagnetic fields generated by SLPA antennas are the product of the Electric/Magnetic fields produced by the first antenna element in the array and the Array-Factor of the single antenna array (Okoye, 2014);

Thus. Equation (2.60) is written by (Okoye, 2014) as:

$$E_{s}^{T}{}_{\theta} = \left[(1 + \sum_{n=1}^{N-1}\prod_{i=1}^{n} e^{jkd\tau^{i-1}sin\theta}) \ \frac{j\,\eta\,\mathrm{k}^2\,\mathrm{I}(\mathrm{l}\tau^{n-1})^2\,e^{-jkr}}{16\pi r} \ \sin\theta \right] \quad (2.60)$$

Then the corresponding magnetic field for the SLPA antennas in (2.61) was obtained by dividing the electric field of equation (2.60) by intrinsic impedance, η as written by (Okoye, 2014).

Hence,

$$H_{s}^{T}{}_{\theta} = \left[(1 + \sum_{n=1}^{N-1}\prod_{i=1}^{n} e^{jkd\tau^{i-1}sin\theta}) \ \frac{j\,\mathrm{k}^2\,\mathrm{I}(\mathrm{l}\,\tau^{n-1})^2\,e^{-jkr}}{16\pi r} \ \sin\theta \right] \quad (2.61)$$

ii. Average Poynting Vector, ρ_{av} of SLPA Antennas

Average Poynting Vector of SLPA antennas was determined by finding the product of electric field and magnetic field generated by SLPA antennas. Thus, it is the product of equations (2.60) and (2.61). This resulted to equations (2.62) and (2.63) as written by (Okoye, 2014).

.

$$\rho av_{SLPA} = \frac{1}{2}\,\mathrm{Re}\begin{Bmatrix} \left[\left(1+\sum_{n=1}^{N-1}\prod_{i=1}^{n} e^{jkd\tau^{i-1}sin\,\theta}\right)\frac{j\ \eta\,k^2\,I\ (l\tau^{n-1})^2\ e^{-jkr}}{16\pi r}\ \sin\theta\right]\theta \\ * \left[(1+\sum_{n=1}^{N-1}\prod_{i=1}^{n} e^{jkd\tau^{i-1}sin\,\theta})\ \frac{j\,k^2\,I(l\tau^{n-1})^2\ e^{-jkr}}{16\pi r}\ \sin\theta\right]{}^{*}\hat{\varphi} \end{Bmatrix} \quad (2.62)$$

Analyzing the unit vectors θ and φ,

$$\rho av_{SLPA} = \frac{1}{2}\,\mathrm{Re}\begin{Bmatrix} \left[\left(1+\sum_{n=1}^{N-1}\prod_{i=1}^{n} e^{jkd\tau^{i-1}sin\,\theta}\right)\frac{j\ \eta k^2\,I(l\tau^{n-1})^2\ e^{-jkr}}{16\pi r}\ \sin\theta\right] \\ * \left[(1+\sum_{n=1}^{N-1}\prod_{i=1}^{n} e^{jkd\tau^{i-1}sin\,\theta})\ \frac{j\,k^2\,I(l\tau^{n-1})^2\ e^{-jkr}}{16\pi r}\ \sin\theta\right](\theta x\,\varphi) \end{Bmatrix} \quad (2.63)$$

After resolving the internal brackets of equation (2.63), equation (2.64) is obtained by (Okoye, 2014) as,

$$\rho av_{SLPA} =$$

$$\frac{1}{2}\,\mathrm{Re}\begin{Bmatrix} \left[\frac{j\ \eta k^2\,Il^2\ e^{-jkr}}{16\pi r}\ \sin\theta + \frac{j\ \eta k^2\,I(l\tau^{n-1})^2\ e^{-jkr}}{16\pi r}\ \sin\theta\ \sum_{n=1}^{N-1}\prod_{i=1}^{n} e^{jkd\tau^{i-1}sin\,\theta})\right] \\ + \left[\frac{(-j)k^2\,Il^2\ e^{jkr}}{16\pi r}\ \sin\theta + \frac{(-j)\,k^2\,I(l\tau^{n-1})^2\ e^{jkr}}{16\pi r}\ \sin\theta\ \sum_{n=1}^{N-1}\prod_{i=1}^{n} e^{-jkd\tau^{i-1}sin\,\theta})\right] \end{Bmatrix}\hat{r} \quad (2.64)$$

Also, after multiplying out and expanding the external brackets of equation (2.64), equation (2.65) was obtained by (Okoye, 2014) as:

$$\rho av_{SLPA} =$$

$$\frac{1}{2}\,\mathrm{Re}\left\{\frac{\eta\,(k^2\,I(l\tau^{n-1})^2\,)^{\,2}}{(16\pi)^{\,2}\,(r)^{\,2}}\ \sin^{\,2}\theta + \frac{\eta(k^2\,I(l\tau^{n-1})^2\,)^{\,2}}{(16\pi)^{\ \,2}\,(r)^{\,2}}\ \sin^{\,2}\theta\ \sum_{n=1}^{N-1}\prod_{i=1}^{n} e^{jkd\tau^{i-1}sin\,\theta} + \right.$$

$$\frac{\eta\,(k^2\,I(l\tau^{n-1})^2\,)^{\,2}}{(16\pi)^{\,2}\,(r)^{\,2}}\ \sin^{\,2}\theta\ \sum_{n=1}^{N-1}\prod_{i=1}^{n} e^{-jkd\tau^{i-1}sin\,\theta} +$$

$$\left.\frac{\eta\,(k^2\,I(l\tau^{n-1})^2\,)^{\,2}}{(16\pi)^{\,2}\,(r)^{\,2}}\ \sin^{\,2}\theta\ \sum_{n=1}^{N-1}\prod_{i=1}^{n}\ (1)\right\}\ \hat{r} \quad (2.65)$$

According to (Okoye, 2014), factorizing out equation (2.65) results to (2.66). Thus,

$$\rho av_{SLPA} =$$

$$\frac{1}{2}\mathrm{Re}\left\{\frac{\eta\,(\mathrm{k}^2\,\mathrm{I}(l\tau^{n-1})^2\,)^{\,2}}{(16\pi)^{\,2}\,(r)^{\,2}}\ \sin^{\,2}\theta\left[\begin{matrix}1+\sum_{n=1}^{N-1}\prod_{i=1}^{n}e^{jkd\tau^{i-1}sin\,\theta}\\ +\ \sum_{n=1}^{N-1}\prod_{i=1}^{n}\ e^{(-j)kd\tau^{i-1}sin\theta}+\sum_{n=1}^{N-1}\prod_{i=1}^{n}\ (1)\end{matrix}\right]\right\}\hat{\mathrm{r}} \quad (2.66)$$

Equation (2.66) was further analyzed as shown in equation (2.67) by (Okoye, 2014)

$$\rho av_{SLPA} = \frac{1}{2}\mathrm{Re}\left\{\begin{matrix}\frac{\eta\,(\mathrm{k}^2\,\mathrm{I}(l\tau^{n-1})^2)^{\,2}}{(16\pi)^{\,2}\,(r)^{\,2}}\ \sin^{\,2}\theta\\ \left[\,1+\sum_{n=1}^{N-1}\prod_{i=1}^{n}(1+2\cos(kd\tau^{i-1}sin\,\theta))\,\right]\end{matrix}\right\}\ \hat{\mathrm{r}} \quad (2.67)$$

According to (Okoye, 2014), rearranging the order of equation (2.67) results to (2.68)

$$\rho av_{SLPA} = \frac{1}{2}\mathrm{Re}\left\{\begin{matrix}\left[1+\sum_{n=1}^{N-1}\prod_{i=1}^{n}\left(1+2\cos\left(kd\tau^{i-1}sin\,\theta\right)\right)\right]\\ \frac{\eta\ (\mathrm{k}^2\,\mathrm{I}(l\tau^{n-1})^2\,)^{\,2}}{(16\pi)^{\,2}\,(r)^{\,2}}\ \sin^{\,2}\theta\end{matrix}\right\}\ \hat{\mathrm{r}} \quad (2.68)$$

iii. Radiation Intensity, U (ɵ, φ) of SLPA Antennas

Radiation Intensity of a dipole antenna was evaluated in equation (2.69) by (Kraus, 1997) as:

$$\mathrm{U}\,(\theta,\varphi) = \left|\frac{1}{2}Re\left\{\frac{\eta\,(\,\mathrm{I}(l)^2\,)^{\,2}\,\mathrm{k}^4}{(16\pi)^{\,2}}\ \sin^{\,2}\theta\right\}\right| \quad (2.69)$$

On further analysis, equation (2.69) was obtained thus by (Adekola, 2012) as;

$$\mathrm{U}\,(\theta,\varphi) = \frac{\eta}{32}(\pi I)^{\,2}\left(\frac{\ell}{\lambda}\right)^{\,4}\ \sin^{\,2}\theta \quad (2.70)$$

The Radiation Intensity for Single Log-Periodic Array antennas was determined by multiplying the radiation intensity of a dipole by the square of the array factor as demonstrated in equation (2.71) and (2.72) by (Adekola, 2012) as:

$$U_{SLPA}(\theta,\varphi) = \left|\frac{1}{2} Re\left\{\left[\,1 + \sum_{n=1}^{N-1}\prod_{i=1}^{n}(1 + 2\cos(kd\tau^{i-1}sin\,\theta))\,\right]\frac{\eta\,(\,I(\ell\,\tau^{n-1})^2\,)^{\,2}\,k^4}{(16\pi)^{\,2}}\ \sin^{\,2}\theta\right\}\right| \tag{2.71}$$

In order to obtain the real value of SLPA radiation intensity, equation (2.71) was multiplied out by $\frac{1}{2}$ which results to (2.72) as written by (Okoye, 2014). Hence,

$$U_{SLPA}\,(\theta) = \left|Re\left\{\left[\,1 + \sum_{n=1}^{N-1}\prod_{i=1}^{n}(1 + 2\cos\ (kd\tau^{i-1}sin\theta))\,\right]\frac{\eta\,\left(\,I(\ell\,\tau^{n-1})^2\right)^{\,2}8\pi^{\,4}}{\pi^{\,2}\,(16)^{\,2}\,\lambda^{\,4}}\ \sin^{\,2}\theta\right\}\right| \tag{2.72}$$

Equation (2.72) was further factorized and simplified to produce equation (3.73) (Okoye, 2014)

$$U_{SLPA}\,(\theta) =$$

$$\left|Re\left\{\left[\,1 + \sum_{n=1}^{N-1}\prod_{i=1}^{n}\left(1 + 2\cos\ (kd\tau^{i-1}sin\theta)\right)\,\right]\frac{\eta}{32}(\pi I)^{\,2}\left(\frac{(\ell\,\boldsymbol{\tau^{n-1}})}{\lambda}\right)^{\,4}\ \sin^{\,2}\theta\right\}\right| \tag{2.73}$$

iv. Radiated Power, P_{rad} of SLPA Antennas

Equation (2.74) is the standard formular for resolving the power radiated by antennas (Adekola, 2012). Hence,

$$P_{rad} = \int_0^{2\pi}\ \int_0^{\pi}\ P_{av} r_2 \sin\theta\, d\theta\, d\varphi \tag{274}$$

Where P_{av} is the average Poynting vector

Substituting (2.68) of average pointing vector of SLPA antennas into (2.74), the power radiated by single Log periodic array antennas was calculated by (Okoye, 2014) as:

$$P_{rad\ SLPA} = 2\pi \,.\, \mathrm{Re}\left\{ \begin{matrix} \left[\, 1 + \sum_{n=1}^{N-1} \prod_{i=1}^{n} \left(1 + 2\cos\ (kd\tau^{i-1} sin\theta)\right) \right] \\ \frac{\eta \left(\mathrm{k}^2\, \mathrm{I}(\ell\, \tau^{n-1})^2\right)^2 \mathrm{r}^2}{2\,(16\pi)^2\, r^2}\ \sin^3\theta \end{matrix} \right\} \hat{\mathrm{r}} \qquad (2.75)$$

After multiplying out, the real value of power radiated by SLPA antennas is as shown in equation (2.76) by (Okoye, 2014):

$$P_{rad\ SLPA} = \mathrm{Re}\left\{ \left[\, 1 + \sum_{n=1}^{N-1} \prod_{i=1}^{n} \left(1 + 2\cos\ (kd\tau^{i-1} sin\theta)\right) \right] \frac{\eta\, \pi\, \mathrm{w}^4}{\mathrm{f}^4\ \lambda^4\, (16\pi)^2} \left(\frac{\mathrm{l}\,(\ell\, \tau^{n-1})}{4\pi} \right)^2 \frac{4}{3} \right\} \hat{\mathrm{r}} \qquad (2.76)$$

Equation (2.76) was further factorized to generate equation (2.77) by (Okoye, 2014) as:

$$P_{rad\ SLPA} = \mathrm{Re}\left\{ \left[\, 1 + \sum_{n=1}^{N-1} \prod_{i=1}^{n} \left(1 + 2\cos\ (kd\tau^{i-1} sin\theta)\right) \right] \frac{\eta\, \pi^3 \mathrm{I}^2}{12} \left(\frac{(\ell\, \tau^{n-1})^2}{\lambda^2} \right)^2 \right\} \hat{\mathrm{r}} \qquad (2.77)$$

v. Radiation Resistance, R_{rad} of SLPA Antennas

This was calculated by dividing the radiated power of SLPA antennas by the square of the absolute current flowing through the antenna elements, and then multiplying by 2. The Radiation Resistance was calculated by (Adekola, 2012) as:

$$R_{rad\ SLPA} = \mathrm{Re}\left\{ \left[\, 1 + \sum_{n=1}^{N-1} \prod_{i=1}^{n} \left(1 + 2\cos\ (kd\tau^{i-1} sin\theta)\right) \right] \frac{\eta\, \pi^3}{6} \left(\frac{(\ell\, \tau^{n-1})^2}{\lambda^2} \right)^2 \right\} \hat{\mathrm{r}} \qquad (2.78)$$

Where: $\eta = 120\pi$

Factorizing equation (2.78) results to (2.79) as written by (Okoye, 2014). Thus,

$$R_{rad\ SLPA} = \mathrm{Re}\left\{ \left[\, 1 + \sum_{n=1}^{N-1} \prod_{i=1}^{n} \left(1 + 2\cos\ (kd\tau^{i-1} sin\theta)\right) \right] 1950 \left(\frac{(\ell\, \tau^{n-1})^2}{\lambda^2} \right)^2 \right\} \hat{\mathrm{r}} \qquad (2.79)$$

vi. Directive Gain, D (ɵ, φ) of SLPA Antennas

Equation (2.80) was used to calculate the directive gain of SLPA antennas (Balanis, 2005).

$$D(\theta, \varphi) = \frac{U(\theta,\varphi);}{U_0} = \frac{4\pi U(\theta,\varphi)}{P_{rad}} \quad (2.80)$$

Using equation (2.80) to compute the directive gain of Single Log-Periodic Array antennas; it is the ratio of radiation intensity of SLPA antennas and power radiated by SLPA antennas, all multiplied by 4π.

Hence, this is written by (Adekola, 2012) as:

$$D(\theta, \varphi)_{SLPA} = \frac{4\pi\left\{\left[1+\sum_{n=1}^{N-1}\prod_{i=1}^{n}\left(1+2\cos\left(kd\tau^{i-1}sin\theta\right)\right)\right]\frac{\eta}{32}(\pi I)^2\left(\frac{(\ell\,\tau^{n-1})}{\lambda}\right)^4 \sin^2\theta\right\}}{\left[1+\sum_{n=1}^{N-1}\prod_{i=1}^{n}\left(1+2\cos\left(kd\tau^{i-1}sin\theta\right)\right)\right]\frac{\eta\pi\,3_I\,2}{12}\left(\frac{(\ell\,\tau^{n-1})^2}{\lambda^2}\right)^2} \quad (2.81)$$

Equation (2.81) generated $1.5\sin^2\theta$ as the Directive Gain for the first element in the array. From pattern multiplication approach, the Directive Gain for Single Log-Periodic Array antennas was deduced as a product of the directive gain of first element in the SLPA antennas and the Array Factor (Balanis, 2005; Okoye, 2014)

Thus, the directive gain as written by (Okoye, 2014) is represented in equation (2.82) as:

$$D(\theta, \varphi)_{SLPA} = 1.5\sin^2\theta\left(1+\sum_{n=1}^{N-1}\prod_{i=1}^{n}\left(1+2\cos\left(\mathrm{kd}\left(\tau^{i-1}\right)\sin\theta\right)\right)\right) \quad (2.82)$$

vii. Directivity, D_{max} of SLPA Antennas

According to (Adekola, 2012), it was determined as shown in equation (2.83),

$$D_{max} = \frac{4\pi U_{max}}{P_{rad}} \quad (2.83)$$

where,

D_{max} is the maximum directive gain

U_{max} is the maximum radiation intensity,

P_{rad} is the power radiated

According to (Adekola, 2012), maximum directive gain for LPDA antennas occur at;

$$D_{max} = 1.5 \sin \theta \tag{2.84}$$

In the analysis of multiple log periodic dipole array antennas, the antenna configuration requires tactful arrangement with equivalent dimensions and element spacing. This multiple/stacked antenna arrangement pattern ensures higher power output, more directive gain and wider bandwidth – which guarantees wider signal coverage and detection.

Figure 2.20 shows a schematic diagram of an array of Multiple Log-Periodic Array (MLPA) antennas.

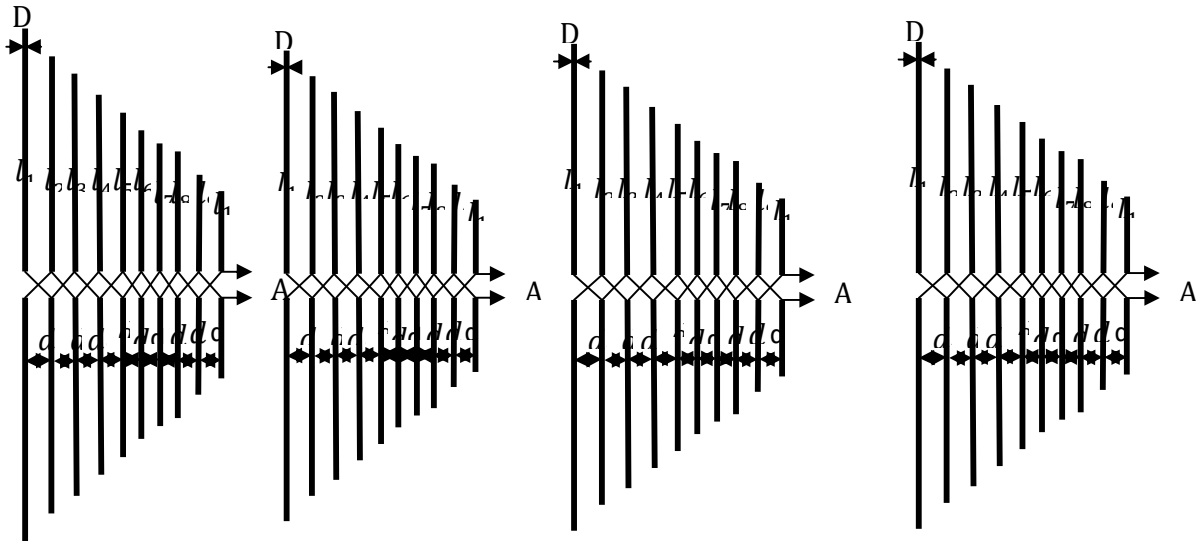

Fig. 2.20: Schematic diagram of MLPA Antennas in parallel arrangement

2.8 Magnetic Vector Potential, Â:

For easy analysis of radiation characteristics, auxiliary functions called vector potentials are mainly used. The most common of these vector potentials are the Magnetic Vector Potential (MVP), represented as Â, and the Electric Vector Potential (EVP), represented as φ. The Ê and Ĥ fields are physically measurable quantities which despite the fact that can be determined directly from the source current densities Ĵ and M̂, but can simply be obtained with the aid of the auxiliary potential functions. The only major challenge here is to integrate and determine the Â, over the bounds of current densities Ĵ and M̂ (Adekola, 2012). When these vector potentials are identified, the Ê and Ĥ fields can always be obtained by means of differentiation. Thus, direct solution of Maxwell's equations to obtain the fields generated from a given source is not always possible. However, where certain properties of the source current (or charge) are known or assumed, it is found convenient to determine the desired

fields through some auxiliary functions called potential functions. Generally, Vector Magnetic Potential of a dipole positioned along the z-axis of the Cartesian plane as written by (Balanis, 2005) is presented as;

$$\hat{A}_z = \frac{\mu}{4\pi} \int_{-l/2}^{l/2} I(z') \frac{e^{-jkR}}{R} dz' \tag{2.85}$$

Where:

$\hat{A}_z$ = the Vector Magnetic potential along z-axis;

μ = the permeability of space;

I = current flowing through the conducting wire (A).

l=length of the dipole element, and

$$\frac{e^{-JK\hat{R}}}{|R|} = the\ Green's\ function$$

$\hat{R}$ at numerator of the Green's function is the antenna phase, |R| at denominator of the Green's function stands for the amplitude of the antenna (Balanis, 2005).

2.9 Role of Antennas in Surveillance Systems

Surveillance Systems are electronic equipment used in monitoring of the activities, or other changing information of people in order to influence, direct, or protect them (Ovsenik, Kolesárová, & Turán, 2010). Figure 2.21 is the Surveillance System block diagram. According to the authors, it comprises detection module, tracking module, classification module and recognition module. These four modules are independent, but interrelating.

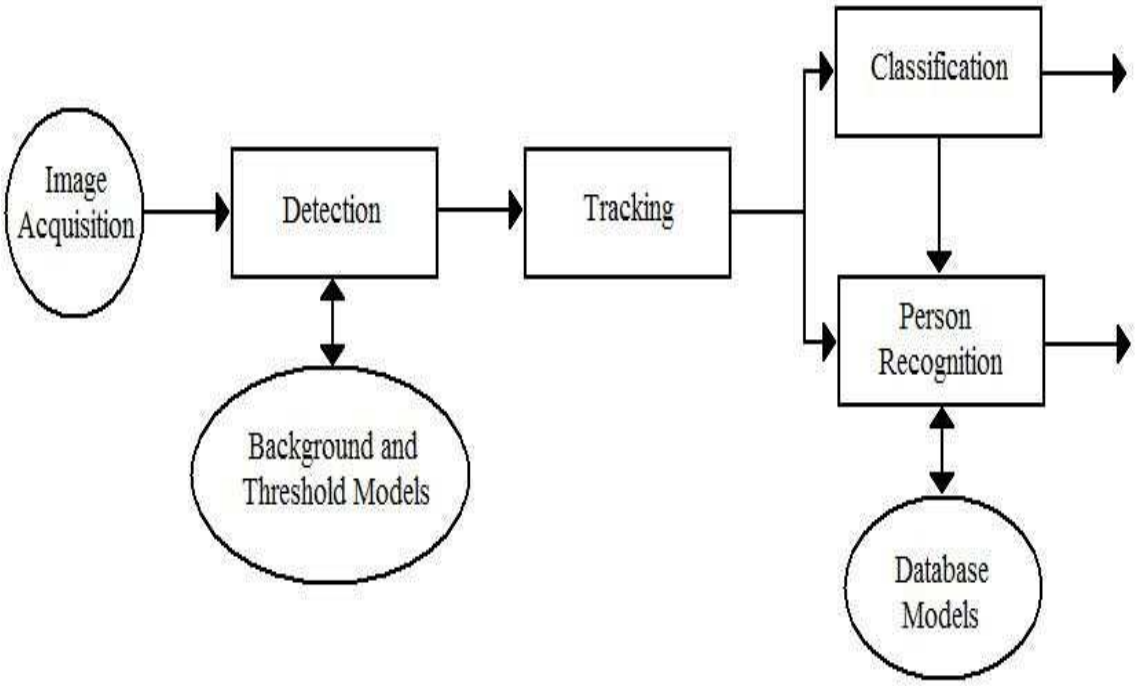

Fig. 2.21: Surveillance System Block Diagram (Ovsenik, Kolesárová & Turán, 2010)

An antenna array, electrically connected to the receiver or transmitter at the image acquisition section of the surveillance system, interfaces between electromagnetic waves propagating through space and electric currents flowing in the radiating elements.

Figure 2.22 shows an aircraft with a Wide Area Surveillance sensor orbiting above a region of concern.

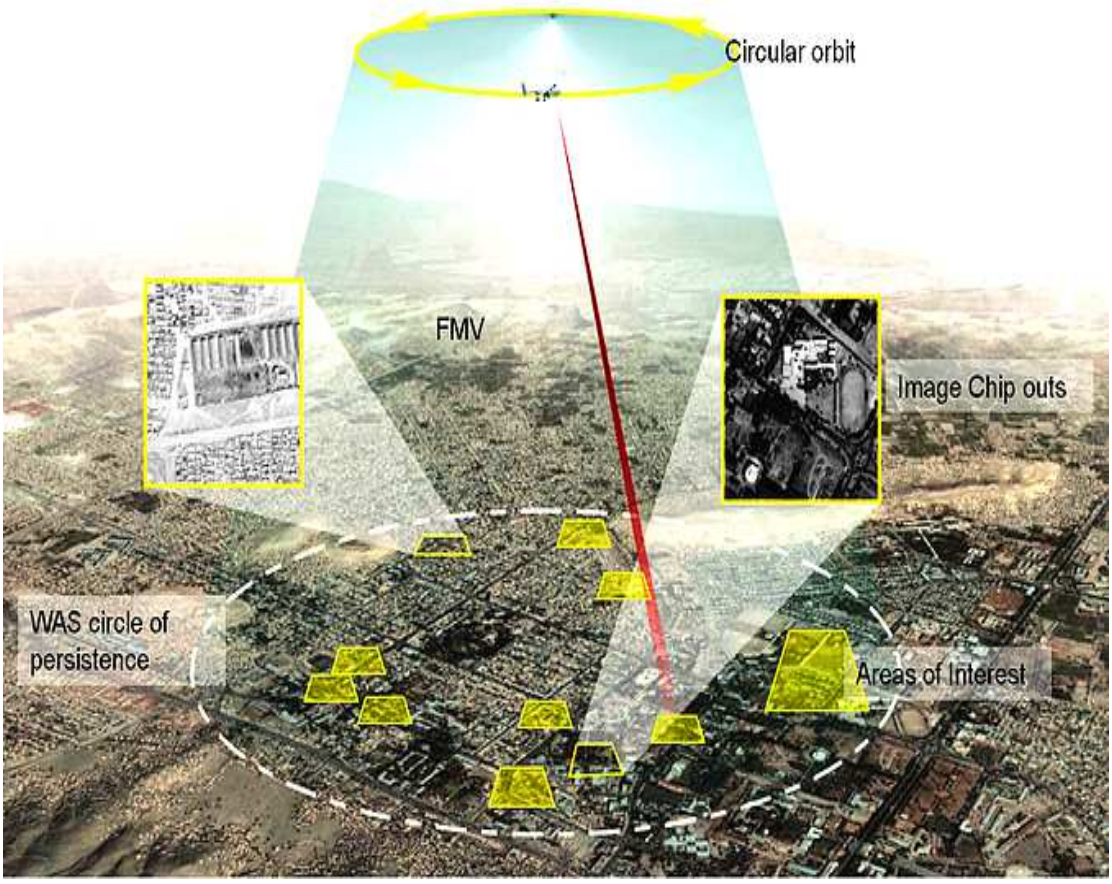

Fig. 2.22: Wide Area Surveillance (Persistent Surveillance Systems)

The dashed circle below the orbit indicates the borders of the Wide Area Surveillance coverage region. The red line designates what a traditional camera (camera ball) could view whereas the yellow blocks correspond to several areas of concern that can be observed simultaneously by the Wide Area Surveillance sensor. Thus, the traditional camera can only observe a very small area when compared to the WASS that can monitor a wide range of area.

2.10 Related Works

Many authors have worked on addressing issues relating Log-Periodic Antennas (LPAs) which include minimization of dipole length, optimization of the antenna gain, minimization of the Voltage Standing Wave Ratio (VSWR), and provision of array factors for uniformly spaced and equal dimension LPA antennas, among others.

Fundamentally, antennas are transmission lines that transform electrical energy into electromagnetic energy. The length of the transmission lines has an inverse relationship with the transmission frequency. It was upon this ground that Daasari and Thallapelli (2012) presented a paper on the analysis of radiation patterns of log – Periodic Dipole Array using Transmission Line Matrix (TLM) model. TLM method implies a space and discrete time technique for calculating electromagnetic fields. This method depicts the analogy of the electromagnetic field and a mesh of transmission lines. According to the authors, there are two main steps used in TLM technique namely: (1) substituting the field problem with the equivalent network and deriving the analogy between the field and network parameters. (2) Using iterative method to resolve the equivalent network. The authors designed a broadband LPDA that operated in the entire frequency range of 0.5 GHz to 6GHz with 30 elements. The LPA antenna was designed based on given specifications with assumed values for scale factor and spacing factor. The designed values were simulated with Personal Computer Aided Antenna Design (PCAAD) software to analyze the radiation patterns. A MatLab code was also used to analyze the radiation patterns in both Azimuth and Elevation planes using TLM method. Both results obtained from MatLab and PCAAD softwares were compared which

were similar to each other. The authors did not provide any array factor for the antenna analysis.

In the design of LPDA, its physical dimension is limited to the longest oscillator dipole in the array with the lowest resonant. Lakshmi and Raju (2012) designed and presented a novel miniaturized log periodic Antenna whose dipole size were reduced by 46%. The authors actualized the reduced lengths by employing meandering method in which the original length of the horizontal length of a LPDA was reduced by 46%. Thus;

$$\text{Meandering dipole} = \text{element length}\left\{= \left(\frac{wavelength,\lambda}{2}\right) * 0.46\right\} \quad (2.86)$$

The meandering technique involves folding the horizontal length of the dipole element into three (3) arms namely: main arm, vertical arm, and secondary arm. The authors also used the scaling factor, τ, of 0.92, spacing factor, σ, of 0.17, feeding line radius of 10mm, wedge angle, α, of 6.15^0, active region bandwidth, B_{ar} of 150Hz, B_s of 3.128Hz, λ_{max} of 0.25, and 16 dipole elements to model the log periodic antenna. The circuit simulation was based on the S-parameter representation of components using Electro Magnetic Simulator Software WIPL-D. The result obtained indicated a meandering LPDA with a reduced length of 46% from the conventional LPDA. However, the authors did not provide any array factor for the antenna analysis.

In an attempt to reduce the lateral size of an LPDA antenna, Yeo and Lee (2012) presented a miniaturized log periodic dipole array antenna operating within the frequency range of 1GHz to 6GHz for portable direction finding applications. Direction finding requires the ability to verify the angle in the azimuth plane from which a signal of interest originates and the reception of a wide range of frequencies. The authors proposed the use of bow-tie elements, a

top loading technique, and the reduction of the spacing between the LPDA elements. To analyze this, the authors first modeled a standard LPDA as presented by (Carrel, 1960) to achieve directivity of about 8dBi over frequency band of 1 GHz – 6GHz using a scale factor of 0.85, spacing factor of 0.15, and 16 dipole elements. The longest dipole element was 130mm at about 1GHz, while the length of the standard LPDA antenna was 244mm. Later, the miniaturized version of the standard LPDA antenna was modeled with bow-tie shaped dipole elements instead of the straight dipole elements to reduce the length, while a top loading technique was used to further reduce the lateral size of the LPDA. The spacing factor of 0.0106 was used instead of 0.15 and the longest dipole element was reduced to 33% and 45% respectively after simulating the data with Computer Simulation Technology (CST) microwave studio. The authors did not provide any array factor for the analysis of the antenna parameters.

For applications that requires limited space and weight, light weight and small physical size antennas are employed, Anagnostou et al. (2008) developed a printed Log Periodic Koch Dipole Array (LPKDA) for wideband applications. The authors actualized this by substituting all Euclidean dipoles of usual LPDA antenna with Koch dipoles. The Koch dipoles were designed by dividing a wire of length, ℓ into three segments of length, $\ell/3$, and then replaced the middle part with two segments of length, $\ell/3$ intersected at an angle of 60^0 to achieve first iteration (K1). Repeating the same exercise on each segment yielded more iteration (K2, K3 and so on). The antenna design covered frequency range of 2 – 3 GHz. The length of the Euclidean element L_{Eucl} at 28.4mm resonated at 1.82 GHz while the Koch element at the same frequency was (Ln) 25.6mm indicating a vertical reduction of 9.86% at first iteration Koch shape. The fractal feature length became smaller and less significant as the iteration order

increased. When the result of the LPKDA was compared with that of the Euclidean LPDA, both antennas demonstrated similar performance and covered the same frequency range. The total area covered by the LPDA was 1505mm^2 while that of the LPKDA was 1323mm^2 indicating 12.1 area reductions. The directivity of the LPKDA was 0.3dB lower than the theoretical value given by Carrel's table due to slightly enlarged bandwidth and increased VSWR. The authors, however, failed to address the method for computing the total field generated in the LPKDA which also required an array factor for easy computation.

In order to realize optimal designs of Log periodic antennas, (Aziz – ul – Haq et al., 2012) proposed the use of evolutionary technique called Particle Swarm Optimization (PSO) in the design of Log Periodic Dipole Antenna for GSM phase (I and II), WiMAX, Bluetooth, Wi–Fi and 3G mobile communication bands. According to the authors, the PSO method was preferred because of its fast divergence, simple implementation, less computation and generally few lines of code. Evolutionary algorithm is based on intelligence; every individual particle has its local best based on its position (pbest) determined by its location in the swarm. All the particles strive to attend to a position termed global best (gbest). For optimal solution, the positions of the particles are updated depending on individual's position and velocity. Hence, the velocities are scaled by inertia weight that consequently alters the direction of pbest and gbest for particular dimension. The fitness function comprises a condition to improve the gain and optimum VSWR as compared to the initial one. The authors designed a 13 dipole element LPDA using the (Carrel, 1960) classical formulars and then optimized the design using PSO. The generated result showed that the VSWR was close to 1, the gain was improved up to an average of 0.6dB when compared to the initial gain, and the physical size

of the design was smaller when compared to the initial one. However, there was no array factor derived for easy analysis of the antenna parameters.

Florence and Raju (2014) presented the design and optimization of non-uniformly spaced linear array of dipoles for side lobe reduction and improved directivity using Accelerated Particle Swarm optimization (APSO) algorithm. Unlike in standard PSO approach, APSO combined the two major equations in PSO into a single equation in order to enhance convergence. This method strives to minimize the randomness as the numbers of iteration proceed. The authors aimed at generating synthesized patterns with low Side Lobe Level (SLL) and to balance the coupling effect with a low prefixed dynamic range ratio for non - uniformly spaced array of dipoles. To synthesize the required linear array, the authors applied APSO algorithm for array of 10, 12, 20, and 24 elements. The amplitude of the excitation current and spacing between elements were varied in the range of 0 to 1, and 0.4 to 0.8 wavelengths respectively, while the excitation phases were kept at zero degree, and the required Dynamic Range Ratio (DRR) was kept at 7.0. Due to symmetry, each array required half of its total element, N and $(\frac{N}{2} - 1)$ of inter-element spacing to be optimized. The results showed that the array of dipoles patterns possessed a relatively low side lobe level while the beam width remained unenhanced. The authors provided no array factor for the analysis of the antenna parameters.

In a bid to achieve an extended frequency range, improved frequency dependence, and a steering ability in an LPA antenna, Ergul and Gurel (2007) reported on Modeling and synthesis of circular-sectoral arrays of Log-periodic antennas using Multilevel Fast Multipole Algorithm (MLFMA) and Genetic Algorithms (GAs). The authors specifically considered non

planar trapezoidal tooth Log periodic antennas in the circular-sectoral array configuration – which operated nearly frequency independent in the range of 300 – 800 MHz in the arrangement. The elements were positioned side by side in a circular arrangement. The authors employed Electric Field Integral Equation (EFIE) formulation to realize a flexible three-dimensional modeling of the antennas as well as used MLFMA in order to facilitate the design procedures. Antenna excitations were modeled by the current sources attached via the antenna feeder, and optimized with GAs so as to control the steering of the main beam. The result obtained indicated directive gain of over 9dB in angular sectors of 100^0. The directive gain of four-element array had greater fluctuations when compared to that of three-element array. This was as a result of increased mutual couplings among the antennas as the array number increased. The authors did not provide any array factor for the antenna analysis.

Gurel and Ergul (2008) presented the design and simulation of circular arrays of trapezoidal – Tooth Log Periodic Antennas using Genetic optimization. The authors remarked, "Due to the complicated structures of the trapezoidal – tooth array elements and the overall array configuration, their analytical treatments are prohibitively difficult". The authors designed and investigated a three – element LP array showing broadband characteristics using the simulation environment. The antenna operated almost frequency independent within the range of 300MHz to 800MHz. The antenna had two arms with each 1m long and angle of 45^0 between the arms. The length of the elements on the arms varied from 4cm to 27cm, and there were 38 elements on each arm and expansion angle of 30^0. Using design factor of 0.95, the authors optimized the directive gain in the x – direction as that was the best complex excitation coefficients for the antennas, likewise on main beam steering. The authors observed thus: "The concept of Array Factor suggests an optimistic scenario, where frequency

independence is conserved in the case of a circular arrangement of the LP antennas. However, our simulations show that mutual couplings between the LP antennas play an important role in shaping the antenna characteristics and that they cannot be ignored. Any analytical effects would be difficult… Therefore, using the simulation environment becomes essential for the analysis of LP arrays". The simulation results focused on the essentials needed for the antenna analysis and design but had no array factor provided. Genetic algorithms were used to optimize the excitation which improved the design and extended the steering ability.

Balanis (2005) postulated the Array-Factor for dipole arrays of uniform spacing and magnitudes using Magnetic Vector Potential model. The author described the pragmatic pattern for analyzing the array factor of identical two-element array positioned along the *z*-axis and expressed it in a compact and closed form. The electromagnetic fields generated by the antennas were calculated at the far field of the antenna using the array factor. The author however assumed point sources of infinitesimal dimensions which were not practical but theoretical antennas. The author further narrated the procedure for the design and construction of an LPDA antenna but did not consider deriving its Array Factor.

Wang (2016) on the topic "Moving-Target Tracking by Cognitive RF Stealth Radar Using Frequency Diverse Array Antenna" proposed a moving-target tracking approach to achieve cognitive radio frequency stealth using an FDA antenna for surveillance applications. According to the author, since surveillance systems were highly visible to intercept receivers, a traditional high-gain phased-array antenna beam was then replaced by a series of low-gain FDA beams with spoiled frequency increments in order to reduce the system visibility. Furthermore, a cognitive closed-loop update scheme was presented to update the operation

parameters in real time for improved moving-target tracking performance. Thus, Frequency Diverse Array Antenna generates a series of low-gain beams which consequently affects the radiating distance of the antenna.

Jha et al. (2010) postulated "Dual-Band Rectangular Microstrip Patch Antenna at Terahertz Frequency for Surveillance System" presented the analysis and simulated of a rectangular microstrip patch antenna on two-layer substrate materials at the terahertz frequency regime for the surveillance system. The proposed antenna was simulated at 600 and 800 GHz frequencies using CST Microwave Studio. The authors further simulated the antenna structure by using finite element method based simulator Ansoft HFSS and the results were compared. However, micro-strip patch antennas suffer from more drawbacks as compared to conventional antennas. Micro-strip patch antennas possess narrow bandwidth, low gain and poor end fire radiator except for tapered slot antennas. These affect its monitoring capability.

Jha and Singh (2010) on "Adaptive Array Antenna Control Methods on Delay Tolerant Networks for Road Surveillance Systems" proposed the Delay Tolerant Networks (DTN) with Adaptive Array Antenna (AAA) Control systems for the V2V networks. In the proposed system, the vehicles equipped the AAA control systems with IEEE802.11a/b/g, and the radio direction was controlled by the pattern recognitions from camera images with Kalman filter algorithm. It however has some technical problems that might hinder its large-scale use such as its high cost, and lack of array-factor for analyzing the array parameters.

In the work of (Zhong et al., 2017) on "Multi-Antenna Wireless Legitimate Surveillance Systems: Design and Performance Analysis", the authors considered a wireless legitimate surveillance system, where a full-duplex multi-antenna legitimate monitor were aimed to

eavesdrop on a dubious communication link between a suspicious pair via proactive jamming. The authors assumed that the legitimate monitor could successfully overhear the suspicious information only when its achievable data rate is no smaller than that of the suspicious receiver. The aim was to maximize the eavesdropping non-outage probability by joint design of the jamming power, receive and transmit beam formers at the legitimate monitor. The authors investigated four different scenarios which were dependent on the number of receive/transmit antennas implemented, i.e., single-input single-output, single-input multiple-output, multiple-input single-output, and multiple-input multiple-output (MIMO). For each scenario, the optimal jamming power was derived and efficient algorithms obtained for the optimal transmit/receive beamforming vectors. The findings demonstrated that by exploiting multiple antennas at the legitimate monitor, the eavesdropping non-outage probability could be significantly improved compared with the single-antenna case. However, the authors did not generate any array factor for analyzing the proposed multiple antennas applications which could hamper its parameters analysis.

Zabri et al. (2017) on "Video Monitoring Application Using Wireless Sensor Node with Various External Antenna" describes a surveillance system using Raspberry Pi with various external antennas. The Raspberry Pi with Pi Camera module and various types of antennas was used to test and experiment in line-of-sight (LOS) and non-line-of-sight (NLOS) condition. The wireless sensor node was capable of monitoring an area wirelessly when the image sensor was attached, the authors asserted. The authors also claimed that the Yagi Uda antenna gave the best output in terms of its signal strength and average Receive (Rx) rate. However, the authors could not provide any multiplier (array factor) for analyzing the array antenna.

In the work of (Okoye et al., 2017) on Derivation of Standard Array Factor for Log-Periodic Circular-Loop Antennas Using Magnetic Vector Potential Approach, the authors developed the array factor for analyzing the parameters of Log-Periodic Circular-Loop Array antennas. The authors employed the Magnetic Vector Potential (MVP) model and systematically derived the array factor for computing LPAs using Log Periodic Circular-Loop Array antennas (LPCA) as a case study. The authors further presented the normalized radiation patterns of the array-factor generated; the combined radiation patterns of the array-factor generated for different numbers of circular loop array antenna elements and the polar plot of the array-factor generated using MatLab R2010a software. However, the derived array factor was only limited to Single LPA (SLPA) antennas.

Other numerous reports highlighted in the literature investigated the synthesis of LP arrays, their operational properties, and various design procedures and optimizations. Some works were geared towards the derivation of Array-Factor for equal amplitudes and equal spacing antennas. However, research has not addressed the derivation of the array factor to be used in numerical computation of the parameters of Multiple Log-Periodic Array (MLPA) antennas as there was no such study in literature. Also, there were relatively scanty of reports on the analysis of LPA antennas with more complicated geometries, and none of them presented the array factor to ease the challenges encountered in analyzing LPA antennas.

2.11 Research Gaps

The major research gaps from the reviewed literatures are enlisted in Table 2.3.

Table 2.3: Tabular Presentation of the Research Gaps

S/N	Authors	Title of works	Findings	Research Gaps
1	(Anagnostou et al., 2008)	Printed Log Periodic Koch Dipole Array for wideband Applications	Substituted all dipoles of usual LPDA antenna with Koch dipoles.	Reduction in area coverage, directivity of the LPKDA was 0.3dB lower. No Array-Factor
2	(Gurel & Ergul, 2008)	The Design And Simulation Of Circular Arrays Of Trapezoidal – Tooth Log Periodic Antennas Using Genetic Optimization	Genetic algorithms optimized the excitation which improved the design and extended the steering ability.	No array factor for antenna analysis
3	(Balanis, 2005)	Antenna Theory Analysis and Design	Postulated the A-F for dipole arrays of uniform spacing & magnitudes.	It assumed point sources of infinitesimal dimensions which were theoretical antennas.
4	(Wang, 2016)	Moving-Target Tracking by Cognitive RF Stealth Radar Using Frequency Diverse Array Antenna	Improved moving-target tracking performance.	FDA antenna generates series of low-gain beams which affects antenna coverage area.
5	(Jha & Singh, 2010)	Adaptive Array Antenna Control Methods on Delay Tolerant Networks for Road Surveillance Systems	Proposed the use of DTNs with AAA Control systems for the V2V networks	High cost, and no array-factor for analyzing the array parameters.

S/N	Authors	Title of works	Findings	Research Gaps
6	(Ergul & Gurel, 2007)	Modeling and synthesis of circular-sectoral arrays of Log-periodic antennas using Multilevel Fast Multipole Algorithm and Genetic Algorithms	Had directive gain of over 9dB in angular sectors of 100^0	No Array-Factor
7	(Aziz – ul – Haq et al., 2012)	Particle Swarm Optimization (PSO) in the design of Log periodic Dipole Antenna for GSM phase (I and II), WiMAX, Bluetooth, Wi–Fi and 3G mobile communication bands	Designed a 13 dipole element LPDA, VSWR was close to 1, gain improved up to 0.6dB, physical size of the design was smaller.	No Array-Factor
8	(Jha et al., 2010)	Dual-Band Rectangular Microstrip Patch Antenna At Terahertz Frequency For Surveillance System	Applied a rectangular microstrip patch antenna for the surveillance system.	Micro-strip patch antennas possess narrow bandwidth, low gain & poor end fire radiator except for tapered slot antennas.

S/N	Authors	Title of works	Findings	Research Gaps
9	(Zhong et al., 2017)	Multi-Antenna Wireless Legitimate Surveillance Systems: Design and Performance Analysis	Exploited multiple antennas to improve eavesdropping non-outage probability compared with the single-antenna case.	No array factor for analyzing the proposed MIMO antennas
10	(Zabri et al,. 2017)	Video Monitoring Application Using Wireless Sensor Node with Various External Antenna	Yagi Uda antenna was used for the monitoring which gave good output in terms of signal strength & average Receive rate	No Array-Factor
11	(Okoye et al., 2017)	Derivation of Standard Array Factor for Log-Periodic Circular-Loop Antennas Using Magnetic Vector Potential Approach	Developed array factor for LPCA antennas.	Array factor was limited to SLPA antennas.

In summary, the following research gaps were noted:

1. **Lack of Array-Factor for MLPA Antennas:**

The analysis of MLPA antennas in Table 2.3 reveals a major gap – the absence of an array-factor for MLPA antennas. This omission creates a bottleneck in accurately calculating antenna losses, hindering the understanding of their parameters. Consequently, this limitation is very challenging for system designers to forecast MLPA antenna behavior at the far field.

2. **Challenges in Antenna Types:**

Various antenna types, such as dipole patterns and micro-strip patch antennas, present significant drawbacks. Dipole patterns exhibit a low side lobe level, but their beam width remains unenhanced, contributing to reduced coverage. Micro-strip patch antennas, except for tapered slot antennas, suffer from narrow bandwidth, low gain, and poor end fire radiation. These limitations pose difficulties for system designers, resulting in substantial investments in drive tests to understand and address coverage issues.

3. **Issues with Adaptive Array Antenna (AAA) Control Systems:**

The study identifies technical problems in AAA control systems, including high costs and size constraints, which could impede their large-scale use. Additionally, using a single antenna at the legitimate monitor affects eavesdropping non-outage probability in communication industries. The potential signal loss due to mismatches between the transmitter and antennas limits effective power radiation. Moreover, the existing array-factor for Log Periodic Circular-Loop Array (LPCA) antennas is limited to Single LPA (SLPA) antennas analysis, highlighting the need for a broader understanding of MLPA antennas for more comprehensive applications.

CHAPTER THREE

MATERIALS AND METHOD

3.1 Materials

The simulation of the Array Factor for MLPA antennas and the MLPA antenna parameters were carried out with the aid of the MatLab R2010a object oriented Engineering software tools. In writing the software codes, the materials/MatLab command tools were designed and executed to aid the Antenna Engineer compute and plot the patterns of the log periodic array antennas. Hence, the MatLab program constructs such as ***while*** statement, ***for*** statement, ***if*** statement, ***input*** command (for accepting input data from the keyboard), ***disp*** command (for displaying data) and ***plot*** command (for plotting two, as well as three-dimensional graphs), were used to develop a user-friendly and easy-to-use/debug programs.

Other MatLab command tools deployed included: Hold-on/ hold-off (for drawing multiple plots on the same axis), subplot (for creating an array of plots in the same figure, each of these plots is called a subplot, Loglog (for creating log-log plot), Title (for adding text at top of plots), Polar (for creating polar plot), Bar (for creating bar chart), Axes (for setting the axis scales), and close all (for closing all plots). A top-down method was adopted for the development of the program codes. The vectors in the programs were pre-allocated to ensure that the program loops execute faster.

In order to create m-files for MatLab scripts of MLPA antennas, “New” was chosen from the “File**”** menu and then “Script” was selected. This procedure brought out the text editor window where the MatLab commands were entered. To save the created m-files of the MLPA

antennas, the “File**”** menu was opened from which “Save**”** button was clicked. In the same way, opening the existing m-files of MLPA antennas was done by choosing “Open” button from the File menu.

To run the m-files of the MLPA antennas after the m-files were saved with “.m” extension, the commands in the m-files were executed by typing the file name at the MatLab command window prompt. When the Run- button on the MatLab environment is clicked, this automatically prompts for the supply of the number of antenna elements on the array. Type in the number and press the ‘Enter- key’. The program generates the table of values, as well as plots the graph of the same tabular values.

Figure 3.1 denotes the MatLab desktop environment which constitutes the command window, current folder, workspace, and command history.

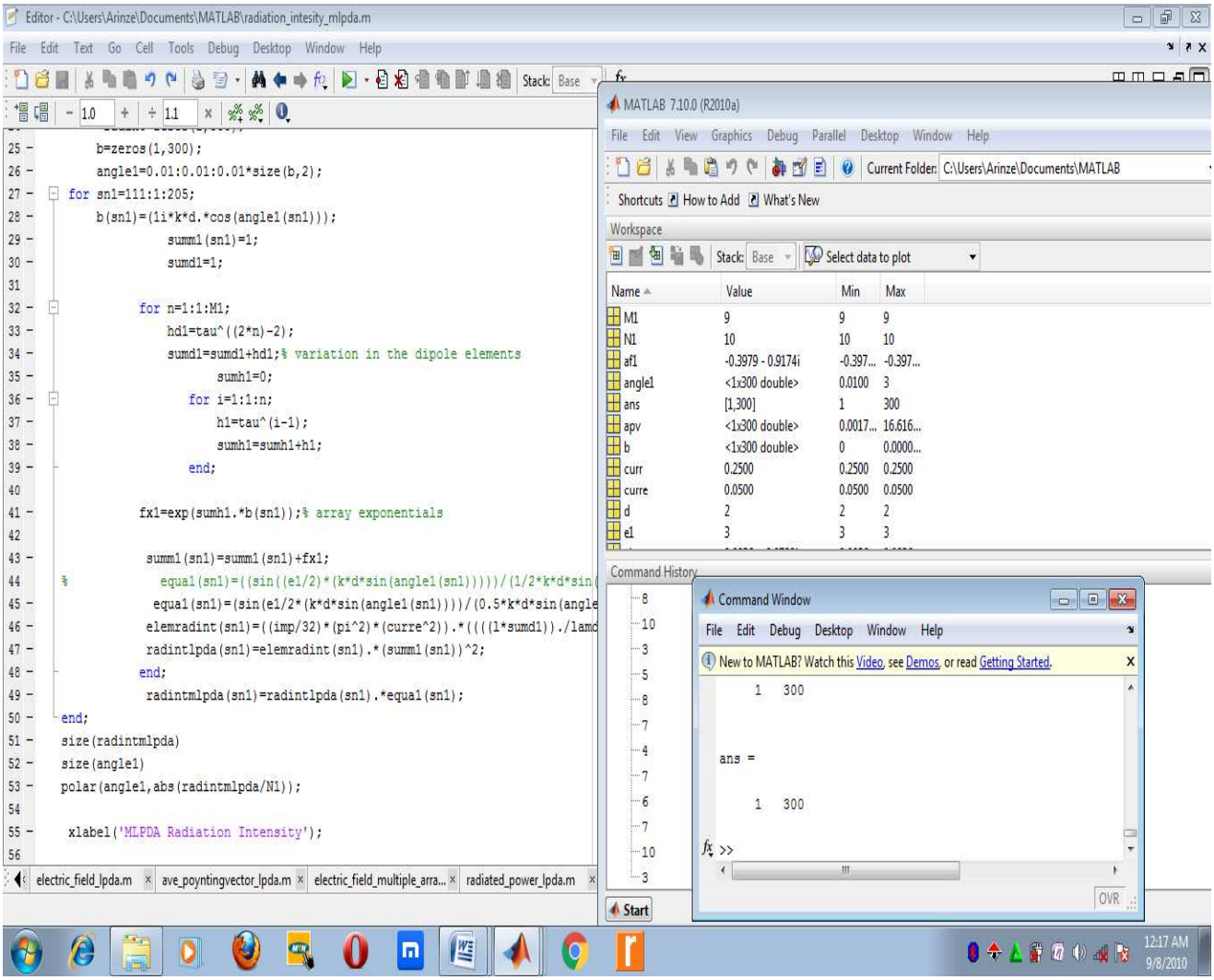

Fig. 3.1: The MatLab desktop environment

The MatLab desktop environment represented in Figure 3.1 indicates the command window used for creating the M-files for the MLPA antenna parameters. These include the Matlab programs for the Electric and Magnetic fields of a dipole element, the Array Factor for equal amplitude array elements, the Array Factor for equal dipole elements (combined), the Array Factors of SLPA Antennas plotted separately, the Array Factor of SLPA Antennas (Plotted together), the array factors of Multiple Log Periodic Array Antennas, the array factors of

MLPA Antennas, the Electric and Magnetic Fields of SLPA Antennas respectively for N equals 16, the Electric and Magnetic fields of MLPA antennas, an Average Poynting Vector of SLPA antennas for N equals 16, an Average Pointing Vector of MLPA Antennas for N Equals 10 (Antenna Set Equals 3), the Radiated Power of SLPA Antennas For N Equals 16, the Radiated Power of Multiple (3) LPA Antennas for N Equals 16, the Radiation Intensity of SLPA Antennas for N Equals 7, and the Radiation Intensity of MLPA Antennas for N Equals 16. These Matlab programs are shown in Appendix A through Appendix O respectively.

3.2 Method

The Magnetic Vector Potential (MVP) model was used as a basis in the development of the antennas Array Factors and in the analysis of the MLPA antennas parameters. The choice of the Magnetic Vector Potential model was made as it contained an auxiliary function that minimized the analytical measures. Also, the MVP model contained Green's function, which was a linear operator that enabled it transfer the antenna characteristics to the far field zone.

3.2.1 Magnetic Vector Potential Model

Generally, the conventional Magnetic Vector Potential model is expressed as (Balanis, 2005)

$$\bar{A} = \frac{\mu_0}{4\pi} \iiint \bar{J}(\mathrm{r}') \left[\frac{e^{-\mathrm{j}\, \mathrm{k}_0\, \hat{\mathrm{R}}}}{|R|}\right] \mathrm{dv}' \tag{3.1}$$

where,

k_0 represents the free-space propagation constant,

$\hat{\mathrm{R}}$ is the phase of the antenna,

$\bar{J}$ is the electric current density,

dv' is the elemental volume of the radiating wire,

$\frac{e^{-jk_0R}}{|R|}$ is the free space Green's function,

j is the imaginary number, and

|R| is the absolute value of the antenna amplitude·

r' is the distance between the antenna source point to the far field point.

For electrically thin antennas, that is to say, the antenna radius (a) is much smaller compared to the length (l) and wavelength (λ) of the radiating element, the thin-wire approximations is employed with the antenna placed along the z axis. Also, the Magnetic Vector Potential across X and Y axes are zero as it is assumed that the thickness of the element is negligibly small.

Hence, for a symmetric, center-fed linear dipole antenna, the Magnetic Vector Potential has only a Z component. Therefore, equation (3.1) of the Magnetic Vector Potential of the dipole element, $A_z$becomes (Balanis, 2005);

$$\hat{A}_z = \frac{\mu_0}{4\pi}\int_{-\frac{l}{2}}^{+\frac{l}{2}} I(Z')\frac{e^{-jk_0\hat{R}}}{|R|}\,dz' \qquad (3.2)$$

Where;

$\hat{A}_z$ = Magnetic Vector Potential along Z-axis.

$I(Z')$ is the filamentary source current flowing through the conducting wire (A).

l=length of the dipole element

μ_0= permeability of space.

$\frac{e^{-j\,k\,\hat{R}}}{|R|}$= Green's function

The current distribution along the length of the dipole element is sinusoidal. Hence, the far-field radiation patterns are determined by manipulating the $\hat{R}$ in the Green's function to (Adekola, 2012);

$$\hat{R} = |r - \hat{r}.\, r'| \qquad (3.3)$$

Where, r is the distance from the antenna origin to the field point, and r′ is the distance from the antenna source point to the field point.

3.2.2 Analytical Procedure for the MLPA Antennas

The problem of near-fields of isolated dipole antenna or array of antennas systems did not find the same popularity as far-field antenna parameters. This is because, in most of communications systems, transmitting and receiving antennas are in the far-field region with respect to each other, so most of efforts are directed towards far-field parameters investigation. Some of the far – field parameters of the MLPA antennas include the Array Radiation Patterns, Electromagnetic (EM) fields, Average Poynting Vectors, Radiation Intensity, Antenna Radiated Power, Directivity, Directive Gain, and Radiation Resistance.

To characterize the parameters of MLPA antennas for surveillance systems operations, the derived novel Array-Factor was used. The following under-listed steps/activities were followed systematically in the array factor derivation and parameter characterization. The activity flow process for the development of the novel array factor, as well as the characterization of MLPA antenna parameters was followed systematically as shown in Figure 3.2.

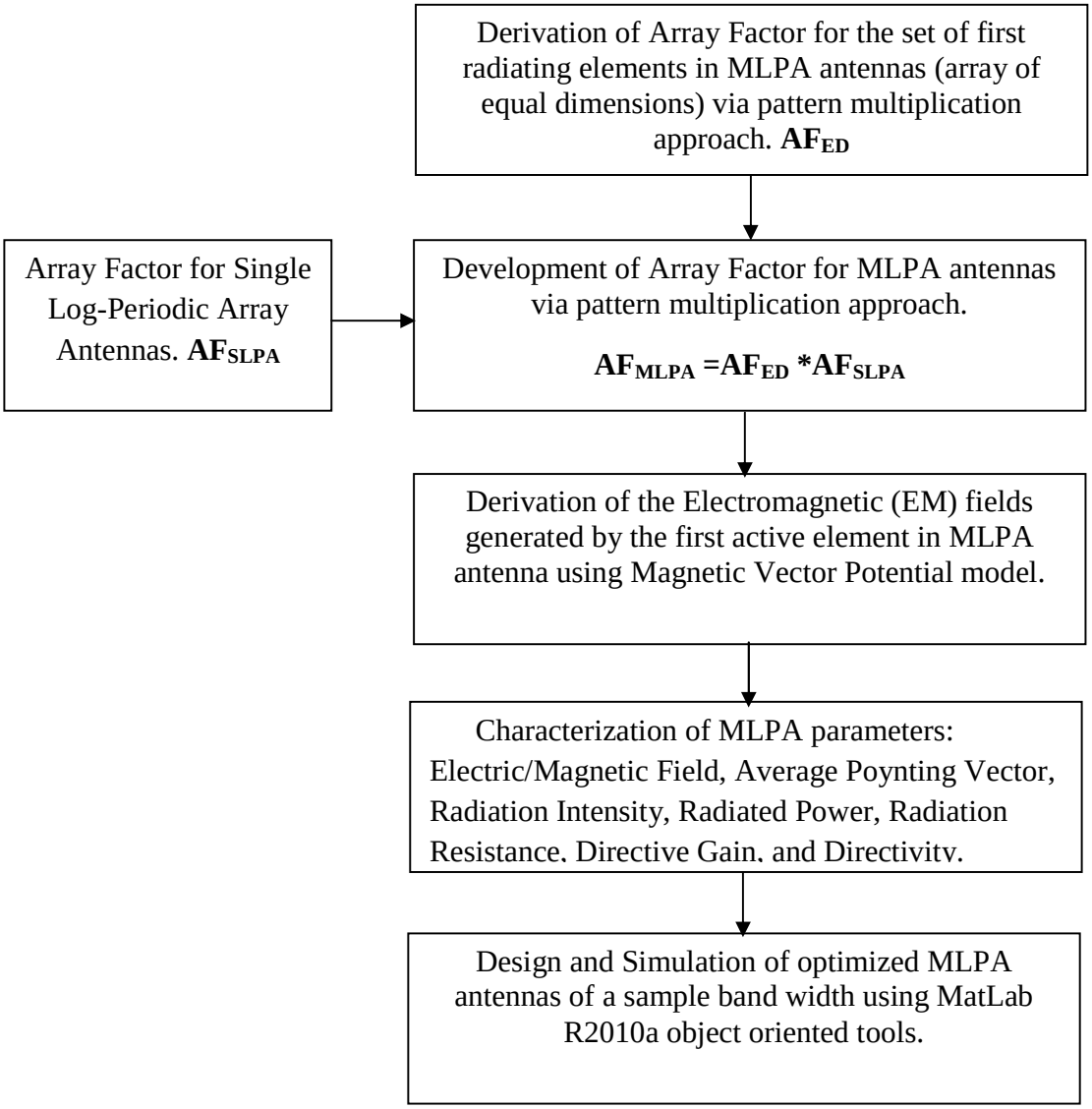

Fig 3.2: An Activity Flow Process for the Characterization of MLPA Antennas

3.2.2.1 Derivation of an Array Factor (AF) for the Set of First Radiating Elements in MLPA Antennas (Array of Equal Dimensions) via Pattern Multiplication Approach.

In order to derive the array factor for MLPA antennas, it requires that the array factor for the set of first radiating elements in MLPA (arrays of equal dimensions) be obtained. This is because of the fact that the array factor for MLPA antennas is the vectorial product of the array factors of Single Log Periodic Array antennas (already presented in equation 2.49 of section 2.71 in Chapter Two) and array antennas of equal dimensions derived and presented in this section (Hum, 2017; Cañar, 2013). This equal amplitude/dimension array constitutes set of all the first elements in the Multiple Log Periodic Array antennas. The antenna elements used for this analysis were positioned along the Z-axis of the Cartesian plane. This analysis was carried out in the far zone area of the antenna. The distances from the antennas' source points to the field point, and the distances from the antennas' origin to the field point was taken care of to ensure appropriate phase analysis. In order to derive the array factor for Multiple Log-Periodic Array Antennas, a sample of Multiple Log Periodic Dipole Array Antennas was used. Figure 3.3 shows the array arrangement of Multiple Log-Periodic Dipole Array antennas.

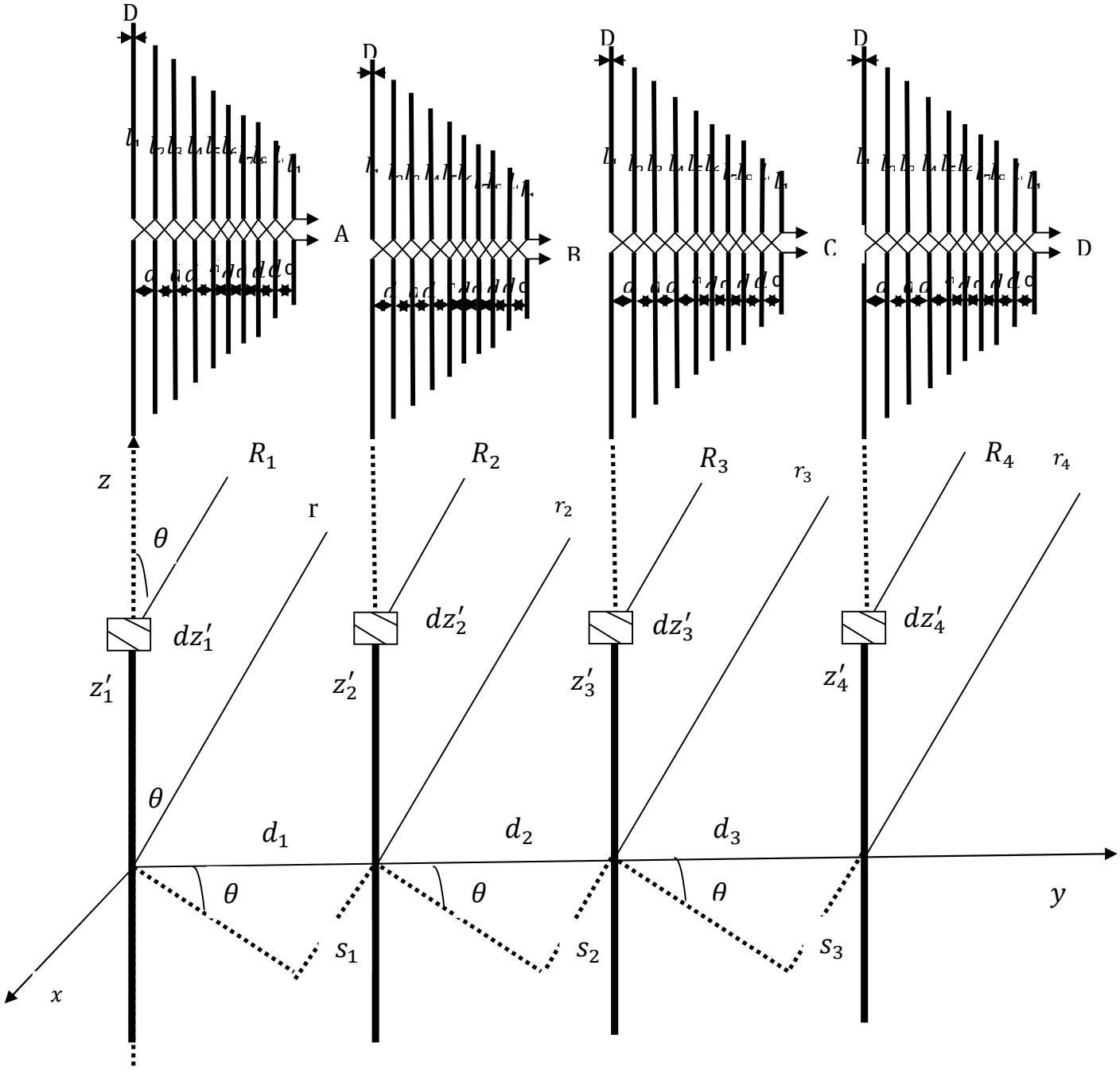

Fig. 3.3: An arrangement of Array antennas of Equal Dimensions

Figure 3.3 is used to derive the array factor for the set of all the first elements of the Multiple Log Periodic Array antennas. The phase variations of the MLPA antennas were evaluated by determining the distances from the source points to the field points of the antennas $R_1, R_2, R_3,$ and R_n in terms of the distance from the origin of the antennas to the far field point, r . Thus, the phase of the antennas $\hat{R}$ in the Green's function was substituted with the values of the derived Rs. This is as deduced from equations (3.4) to (3.12);

$$R_1 = r - z_1' \cos\theta \tag{3.4}$$

$$R_2 = r_2 - z_2' \cos\theta \tag{3.5}$$

Where;

$$r_2 = r - s_1,\ s_1 = d_1 sin\theta \tag{3.6}$$

Substituting the value of r_2 into equation (3.5) results to equation (3.7)

$$R_2 = r - d_1 sin\theta - z_2' \cos\theta \tag{3.7}$$

$$R_3 = r_3 - z_3' \cos\theta \tag{3.8}$$

Where; $r_3 = r_2 - s_2$ and $s_2 = d_2\ sin\theta$

Also, substituting the values of r_3 and r_2 subsequently into equation (3.8) results to equation (3.9)

$$R_3 = r - (d_1 \sin\theta + d_2 \sin\theta\ + Z_3' \cos\theta) \tag{3.9}$$

Factorizing out equation (3.9) results to equation (3.10)

$$R_3 = r - (d_1 + d_2)\sin\theta - z_3' \cos\theta \quad (3.10)$$

$$R_4 = r - (d_1 \sin\theta + d_2 \sin\theta + d_3 \sin\theta + Z_4' \cos\theta) \quad (3.11)$$

Also, factorizing out equation (3.11) results to equation (3.12)

$$R_4 = r - (d_1 + d_2 + d_3)\sin\theta - Z_4' \cos\theta \quad (3.12)$$

Resolving the array factor of the first antenna elements of the MLPDA by the sum of their Magnetic Vector Potential, A;

$$\text{Magnetic Vector Potential}, A = A_1 + A_2 + A_3 + A_4 \ldots + A_N \quad (3.13)$$

Placing the phase variations, R_1, R_2, R_3 *and* R_4 of equations (3.4), (3.7), (3.10) and (3.12) into the sum of (their Green's function phases) their individual Magnetic vector potential of equation (3.13); this results to equation (3.14) (Adekola, 2012).

$$A = \frac{\mu}{4\pi r}\int_{-l_1}^{l_1} I(Z_1')\, e^{-jk(r - Z_1' \cos\theta)} dz_1' + \frac{\mu}{4\pi r}\int_{-l_2}^{l_2} I(Z_2')\, e^{-jk(r-(d_1 \sin\theta + Z_2' \cos\theta) dz_2'} +$$

$$\frac{\mu}{4\pi r}\int_{-l_3}^{l_3} I(Z_3')\, e^{-jk(r-(d_1 \sin\theta + d_2 \sin\theta + Z_3' \cos\theta)} dz_3' +$$

$$\frac{\mu}{4\pi r}\int_{-l_4}^{l_4} I(Z_4')\, e^{-jk(r-(d_1 \sin\theta + d_2 \sin\theta + d_3 \sin\theta + Z_4' \cos\theta)} dz_4' \quad (3.14)$$

Factorizing out equation (3.14) produces equation (3.15)

$$A = \frac{\mu}{4\pi r} e^{-jkr} \left\{ \int_{-l_1}^{l_1} I(Z_1')\, e^{jkz_1'' \cos\theta} dz_1' + \int_{-l_2}^{l_2} I(Z_2')\, e^{jk(d_1 \sin\theta + Z_2' \cos\theta)} dz_2' + \right.$$

$$\left. \int_{-l_3}^{l_3} I(Z_3')\, e^{jk((d_1+d_2)\sin\theta) + Z_3' \cos\theta)} dz_3' + \int_{-l_4}^{l_4} I(Z_4')\, e^{jk((d_1+d_2+d_3)\sin\theta) + Z_4' \cos\theta)} dz_4' \right\} \quad (3.15)$$

For array antennas of equal dimensions, the following conditions exist for the distances of separation d between element, the differential lengths of radiating elements z', and the lengths of the radiating elements l as presented in equations (3.16), (3.17) and (3.18) (Balanis, 2005)

$$d = d_1 = d_2 = d_3 = d_4 = \cdots = d_{N-1} \tag{3.16}$$

$$z' = z_1' = z_2' = z_3' = z_4' = \cdots = z_N' \tag{3.17}$$

$$\text{lenght of radiating element}, l = l_1 = l_2 = l_3 = l_4 = \cdots = l_N \tag{3.18}$$

Thus, applying these features into equation (3.15) results to equation (3.19)

$$A = \frac{\mu}{4\pi r} e^{-jkr} \int_{-l}^{l} I(Z_1') \, e^{jkz_1'^{\prime} \cos\theta} dz_1' \left\{1 + e^{jkd \sin\theta'} + e^{2jkd \sin\theta'} + e^{3jkd \sin\theta'} + \cdots\right\} \tag{3.19}$$

Extracting the array factor, AF from equation (3.19), results to (3.20)

$$AF = 1 + e^{jkd \sin\theta'} + e^{2jkd \sin\theta'} + e^{3jkd \sin\theta'} + \cdots + e^{(M-1)jkd \sin\theta'} \tag{3.20}$$

Let $kd \sin\theta' = \varphi$

$$AF = 1 + e^{j\varphi} + e^{2j\varphi} + e^{3j\varphi} + \cdots + e^{(M-1)j\varphi} \tag{3.21}$$

This is represented in a compact form as

$$AF = \sum_{n=1}^{M} e^{(n-1)j\varphi} \tag{3.22}$$

Where M is the maximum number of LPA antennas in the array.

Equation (3.22) represents the Array-Factor for antenna array of equal dimensions, irrespective of the number of elements of the antenna array. However, equation (3.21) can further be analyzed by multiplying both sides by $e^{j\varphi}$. Hence, (Okoye, 2014)

$$AFe^{j\varphi} = e^{j\varphi} + e^{2j\varphi} + e^{3j\varphi} + e^{4j\varphi} \ldots + e^{Mj\varphi} \tag{3.23}$$

Subtracting equation (3.21) from equation (3.23),

$$AFe^{j\varphi} - AF = e^{Mj\varphi} - 1 \tag{3.24}$$

Factorizing equation (3.24) results to equation (3.25)

$$AF(e^{j\varphi} - 1) = e^{Mj\varphi} - 1 \tag{3.25}$$

AF in equation (3.25) is made the subject in (3.26)

$$AF = \frac{e^{Mj\varphi - 1}}{e^{j\varphi - 1}} \tag{3.26}$$

According to Balanis (2005), the relation $\left(\frac{e^{Mj\varphi - 1}}{e^{j\varphi - 1}} = \frac{e^{j\frac{M\varphi}{2}} e^{j\frac{M\varphi}{2}} - e^{j\frac{M\varphi}{2}} e^{-j\frac{M\varphi}{2}}}{e^{\frac{j\varphi}{2}} e^{\frac{j\varphi}{2}} - e^{\frac{j\varphi}{2}} e^{-\frac{j\varphi}{2}}}\right)$ exists. Thus, equation (3.26) becomes (3.27),

$$AF = \frac{e^{j\frac{M\varphi}{2}} e^{j\frac{M\varphi}{2}} - e^{j\frac{M\varphi}{2}} e^{-j\frac{M\varphi}{2}}}{e^{\frac{j\varphi}{2}} e^{\frac{j\varphi}{2}} - e^{\frac{j\varphi}{2}} e^{-\frac{j\varphi}{2}}} \tag{3.27}$$

Factorizing equation (3.27) results to equation (3.28)

$$AF = \frac{e^{j\frac{M\varphi}{2}} \left(e^{j\frac{M\varphi}{2}} - e^{-j\frac{M\varphi}{2}}\right)}{e^{\frac{j\varphi}{2}} \left(e^{\frac{j\varphi}{2}} - e^{-\frac{j\varphi}{2}}\right)} \tag{3.28}$$

Substituting the relation, $\left(Sin\left(\frac{M}{2}\right)\varphi = \frac{1}{2j}\left(e^{j\frac{M\varphi}{2}} - e^{-j\frac{M\varphi}{2}}\right)\right)$ into equation (3.28) results to equation (3.29)

$$AF = \frac{e^{j\frac{M\varphi}{2}}.2jSin\left(\frac{M}{2}\right)\varphi}{e^{j\frac{\varphi}{2}}.2jSin\left(\frac{\varphi}{2}\right)} \tag{3.29}$$

Equation (3.29) was rearranged as shown in equation (3.30)

$$AF = e^{j\frac{M\varphi}{2}-}e^{j\frac{\varphi}{2}}.\frac{Sin\left(\frac{M}{2}\right)\varphi}{Sin\left(\frac{\varphi}{2}\right)} \tag{3.30}$$

A situation where the reference point is the physical center of the array antenna, the AF is as represented in equation (3.31) (Balanis, 2005)

$$AF = \frac{Sin\left(\frac{M}{2}\right)\varphi}{Sin\left(\frac{\varphi}{2}\right)} \tag{3.31}$$

Then, when the value for the φ is small, the array factor is written thus,

$$AF = \frac{Sin\left(\frac{M}{2}\right)\varphi}{\left(\frac{\varphi}{2}\right)} \tag{3.32}$$

Normalizing equation above results to

$$(AF)_n = \frac{1}{N}\left[\frac{Sin\left(\frac{M}{2}\right)\varphi}{\left(\frac{\varphi}{2}\right)}\right] \tag{3.33}$$

This is approximately equal to

$$(AF)_n \approx \frac{Sin\left(\frac{M}{2}\right)\varphi}{\left(\frac{M\varphi}{2}\right)} \tag{3.34}$$

Substituting the value ($\varphi = kdsin\theta$) into equation (3.34) results to (3.35)

$$(AF)_n \approx \frac{Sin\left(\frac{M}{2}kdsin\theta\right)}{\frac{M}{2}kdsin\theta} \tag{3.35}$$

Where M is the maximum number of LPA antennas in the MLPA antennas.

The algorithms that show the step – by – step approach in determining the Array Factor of Antennas of equal dimensions are as shown;

1. Start
2. Initialize the counter, n
3. Initialize sum
4. Insert the number of LPA antennas, M
5. If M < n, go to 10.
6. p=exp[(jφ)]
7. sum=sum+p
8. Increment n
9. Go to step 5
10. Output sum
11. Stop

Flow Chart for Array Factor of Array Antennas of equal dimensions is as well shown in Figure 3.4.

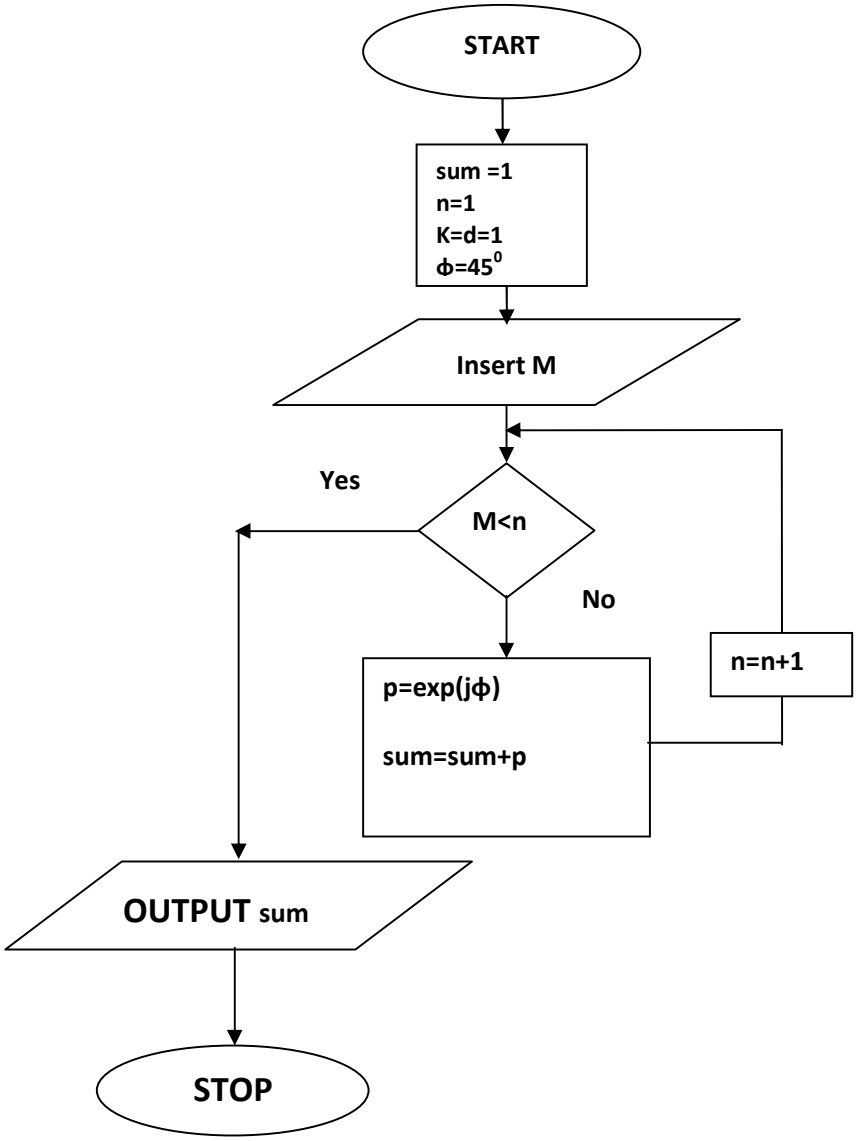

Fig. 3.4: Flow Chart for Array Factor model of Array Antennas of equal dimensions

3.2.2.2 Derivation of an Array Factor (AF) for the MLPA Antennas via Pattern Multiplication Approach.

Figure 3.5 represents the array arrangement of Multiple Log-Periodic Dipole Array (MLPDA) antennas. The diagram signifies the spatial positioning of the MLPDA antennas along the Cartesian plane. It is used to analyze the array factor for MLPDA antennas which are evenly distributed along the Z – axis of the plane.

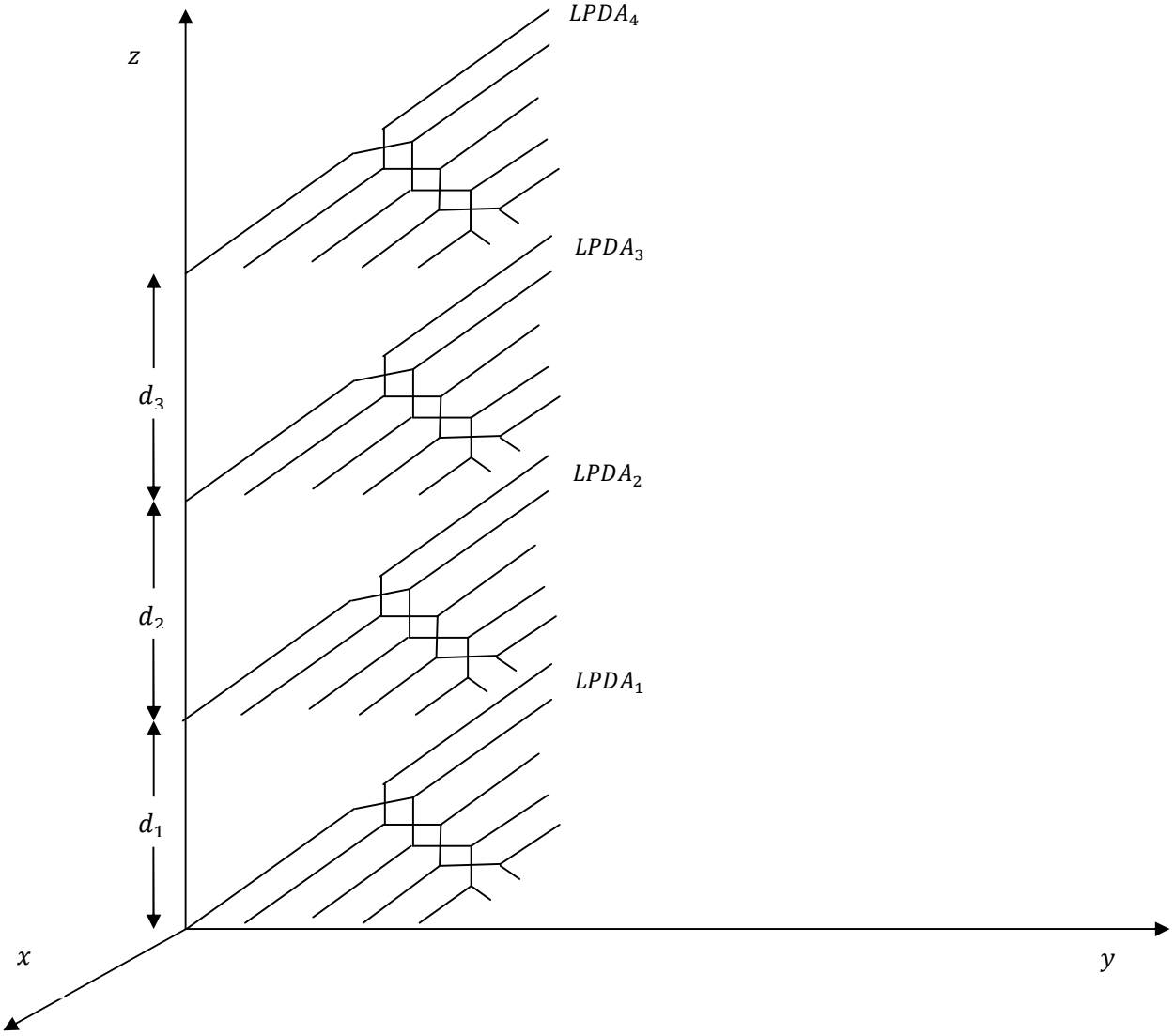

Fig. 3.5: Spatial arrangement of MLPA antenna along the Cartesian coordinate

Having presented the array factor for SLPA antennas,$\left(AF_{SLPA} = 1 + \sum_{n=1}^{N-1}\prod_{i=1}^{n} e^{\mathrm{j}\tau^{\mathrm{i}-1}\varphi}\right)$ in section 2.7.1 and the array factor for array antennas of equal amplitude, $\left(AF_{ED} = \sum_{n=1}^{M} e^{(n-1)j\varphi}\right)$ from the first principle, the array factor for the Multiple Log Periodic Array antennas is obtained as the vectorial product of the array factors for Single Log Periodic Array antennas and array antennas of equal dimensions.

Equations (3.36) and (3.37) are the array factors of the infinite series of SLPA antennas and array antennas of equal dimensions culled from equation (2.57) of Chapter Two and equation (3.20) of Chapter Three respectively. Hence;

$$AF_{SLPA} = 1 + e^{\mathrm{j\,k\,d_1\sin\theta}} + e^{\mathrm{j\,k\,d_1\sin\theta}} e^{\mathrm{jk\,d_1\tau\sin\theta}} + e^{\mathrm{j\,k\,d_1\sin\theta}} e^{\mathrm{jkd_1\tau\sin\theta}} e^{\mathrm{jkd_1\tau^2\sin\theta}} + \cdots + \prod_{i-1}^{n} e^{jk\tau^{i-1}sin\theta} \quad (3.36)$$

While the array factor of an infinite array antennas of equal dimensions is presented in equation (3.37)

$$AF_{ED} = 1 + e^{jkd\,\sin\theta'} + e^{2jkd\,\sin\theta'} + e^{3jkd\,\sin\theta'} + \cdots + e^{(M-1)jkd\,\sin\theta'} \quad (3.37)$$

The array factor of the MLPA antennas was derived by computing the vectorial product of the two array factors. Hence,

$$\mathrm{AF_{MLPA}} = AF_{SLPA} * AF_{ED} \quad (3.38)$$

$$\mathrm{AF_{MLPA}} = \left(1 + e^{\mathrm{j\,k\,d_1\sin\theta}} + e^{\mathrm{j\,k\,d_1\sin\theta}} e^{\mathrm{jk\,d_1\tau\sin\theta}} + e^{\mathrm{j\,k\,d_1\sin\theta}} e^{\mathrm{jkd_1\tau\sin\theta}} e^{\mathrm{jkd_1\tau^2\sin\theta}} + \cdots + \prod_{i-1}^{n} e^{jk\tau^{i-1}sin\theta}\right) * \left(1 + e^{jkd\,\sin\theta'} + e^{2jkd\,\sin\theta'} + e^{3jkd\,\sin\theta'} + \cdots + e^{(M-1)jkd\,\sin\theta'}\right) \quad (3.39)$$

Let,

$$\varphi = kd\ \sin\theta' \tag{3.40}$$

Substituting $(kd\ \sin\theta)'$ with φ in equation (3.39) results to equation (3.41). Thus;

$$\mathrm{AF_{MLPA}} = \left(1 + e^{\mathrm{j}\varphi} + e^{\mathrm{j}\varphi}e^{\mathrm{j}\tau\varphi} + e^{\mathrm{j}\varphi}e^{\mathrm{j}\tau\varphi}e^{\mathrm{j}\tau^2\varphi} + \cdots + \prod_{i=1}^{n} e^{\mathrm{j}\tau^{\mathrm{i}-1}\varphi}\right) * \left(1 + e^{j\varphi} + e^{2j\varphi} + e^{3j\varphi} + \cdots + e^{(M-1)j\varphi}\right) \tag{3.41}$$

$$\mathrm{AF_{MLPA}} = 1 + e^{2\mathrm{j}\varphi} + e^{3\mathrm{j}\varphi}e^{\mathrm{j}\tau\varphi} + e^{4\mathrm{j}\varphi}e^{\mathrm{j}\tau\varphi}e^{\mathrm{j}\tau^2\varphi} + e^{5\mathrm{j}\varphi}e^{\mathrm{j}\tau\varphi}e^{\mathrm{j}\tau^2\varphi}e^{\mathrm{j}\tau^3\varphi} + \cdots + \prod_{i=1}^{n} e^{\mathrm{j}\tau^{\mathrm{i}-1}\varphi}\ e^{(M-1)j\varphi} \tag{3.42}$$

Presenting equation (3.42) in a compact form results to equation (3.43)

$$(AF)_{MLPA} = \sum_{n=1}^{M} e^{(n-1)j\varphi} + \sum_{n=1}^{M} e^{(n-1)j\varphi} \sum_{n=1}^{N-1} \prod_{i=1}^{n} e^{\mathrm{j}\tau^{\mathrm{i}-1}\varphi} \tag{3.43}$$

Equation (3.43) is the Array Factor for Multiple Log Periodic Array antennas of an infinite number of dipole elements, N, and infinite number of LPA antennas, M, in the array.

However, for a small value of φ, the array factor for the MLPDA antenna can as well be written as shown in equation (3.44):

$$(AF)_{MLPA} = \left(1 + \sum_{n=1}^{N-1} \prod_{i=1}^{n} e^{\mathrm{j}\tau^{\mathrm{i}-1}\varphi}\right) \frac{Sin\left(\frac{M}{2}\right)\varphi}{\left(\frac{\varphi}{2}\right)} \tag{3.44}$$

After multiplying out, equation (3.44) becomes equation (3.45)

$$(AF)_{MLPA} = \left(\frac{Sin\left(\frac{M}{2}\right)\varphi}{\left(\frac{\varphi}{2}\right)} + \frac{Sin\left(\frac{M}{2}\right)\varphi}{\left(\frac{\varphi}{2}\right)} \sum_{n=1}^{N-1} \prod_{i=1}^{n} e^{\mathrm{j}\tau^{\mathrm{i}-1}\varphi}\right) \tag{3.45}$$

Validation of Array Factor for MLPA Antennas:

In order to validate the relationship between the array factor of SLPA antennas and that of MLPA antennas, it should be noted here that;

i. As M in the array factor reduces to 1; that is : M=n=1, the array factor of MLPA antennas is reduced to that of SLPA antennas. Given that;

$$(AF)_{MLPA} = \sum_{n=1}^{M} e^{(n-1)j\varphi} + \sum_{n=1}^{M} e^{(n-1)j\varphi} \sum_{n=1}^{N-1} \prod_{i=1}^{n} e^{j\tau^{i-1}\varphi} \quad (3.46)$$

$For\ M = n = 1;$

$$(AF)_{MLPA} = \sum_{1=1}^{1} e^{(1-1)j\varphi} + \sum_{1=1}^{1} e^{(1-1)j\varphi} \sum_{n=1}^{N-1} \prod_{i=1}^{n} e^{j\tau^{i-1}\varphi} \quad (3.47)$$

This results to equation (3.48)

$$(AF)_{MLPA} = \sum_{1=1}^{1}(1) + \sum_{1=1}^{1}(1) \sum_{n=1}^{N-1} \prod_{i=1}^{n} e^{j\tau^{i-1}\varphi} \quad (3.48)$$

And finally to equation (3.49)

$$(AF)_{MLPA} = (AF)_{SLPA} = 1 + \sum_{n=1}^{N-1} \prod_{i=1}^{n} e^{j\tau^{i-1}\varphi} \quad (3.49)$$

ii. As the design factor, τ of the SLPA antennas becomes one, the array factor of the SLPA antennas equals an array factor for equal dimension antennas. Thus equation (3.49) becomes equation (3.50);

$$1 + \sum_{n=1}^{N-1} \prod_{i=1}^{n} e^{j\varphi} = (AF)_{ED} = \sum_{n=1}^{M} e^{(n-1)j\varphi} \quad (3.50)$$

Where N equals M.

The flowchart for the Array Factor of Multiple or Stacked Log Periodic Array antennas is shown in figure 3.6. Note that N is 16 for this sample study.

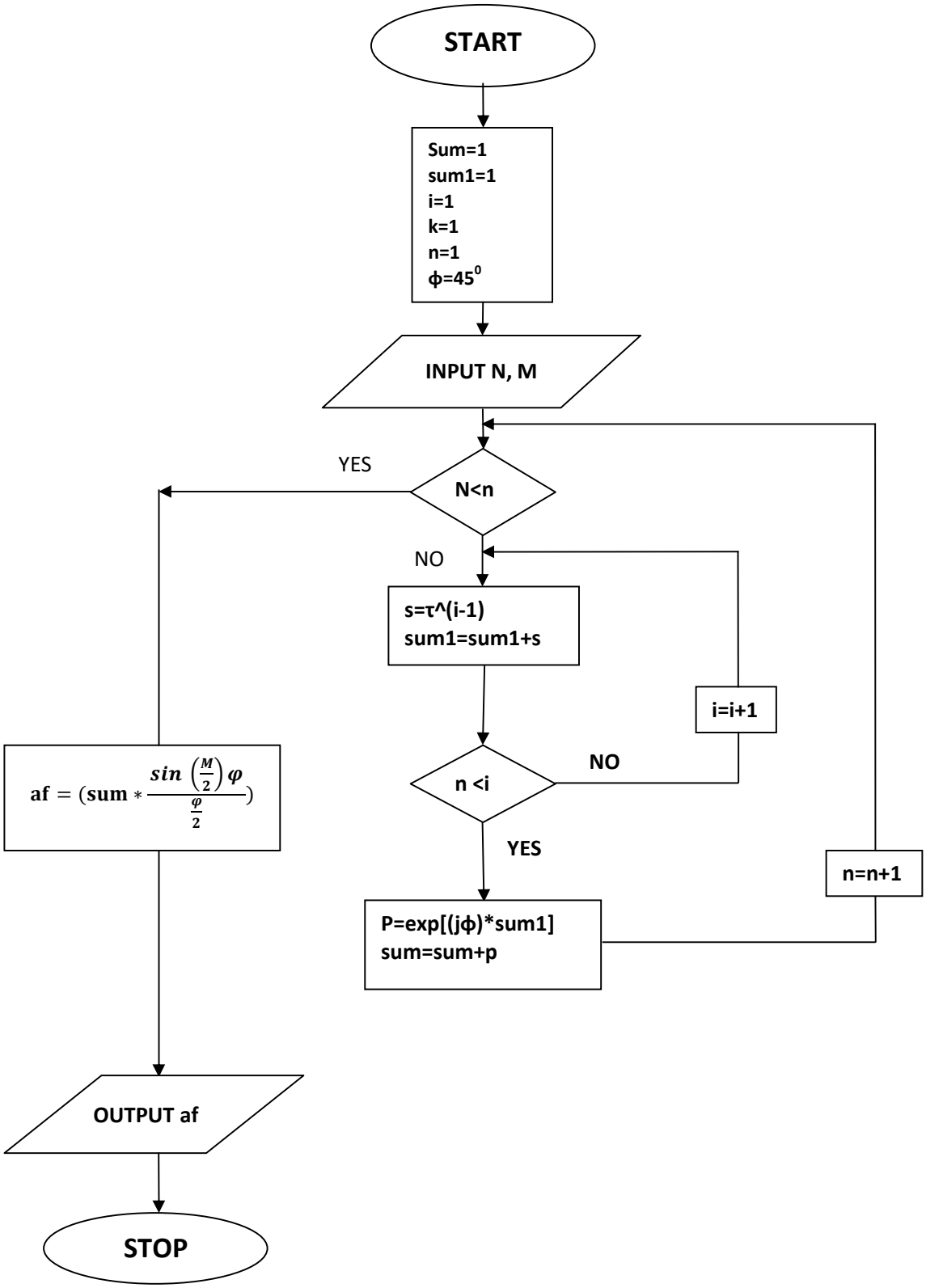

Fig. 3.6: Flow Chat for Array Factor model of MLPA Antennas

Below is the flowchart algorithm of figure 3.6. It shows the step – by – step approach in determining the Array Factor of MLPA antennas. Thus;

1. Start
2. Initialize the counters: n , i
3. Initialize sums: sum, sum1
4. Insert the number of dipoles, N, and number of LPA in the MLPA antennas, M.
5. If N < n, go to step 15
6. s=τ^(i-1)
7. sum=sum+p
8. if n < i, Go to 11
9. Increment i
10. Go to step 6.
11. P=exp[(jφ)*sum1]
12. sum=sum+p
13. Increment n
14. Go to step 5.
15. af $= (\text{sum} * \frac{sin\left(\frac{M}{2}\right)\boldsymbol{\varphi}}{\frac{\varphi}{2}})$
16. Output af (Array Factor)
17. Stop

For comparison, a flow chart for the array factor of SLPA of equation (2.51) is shown in Figure 3.7.

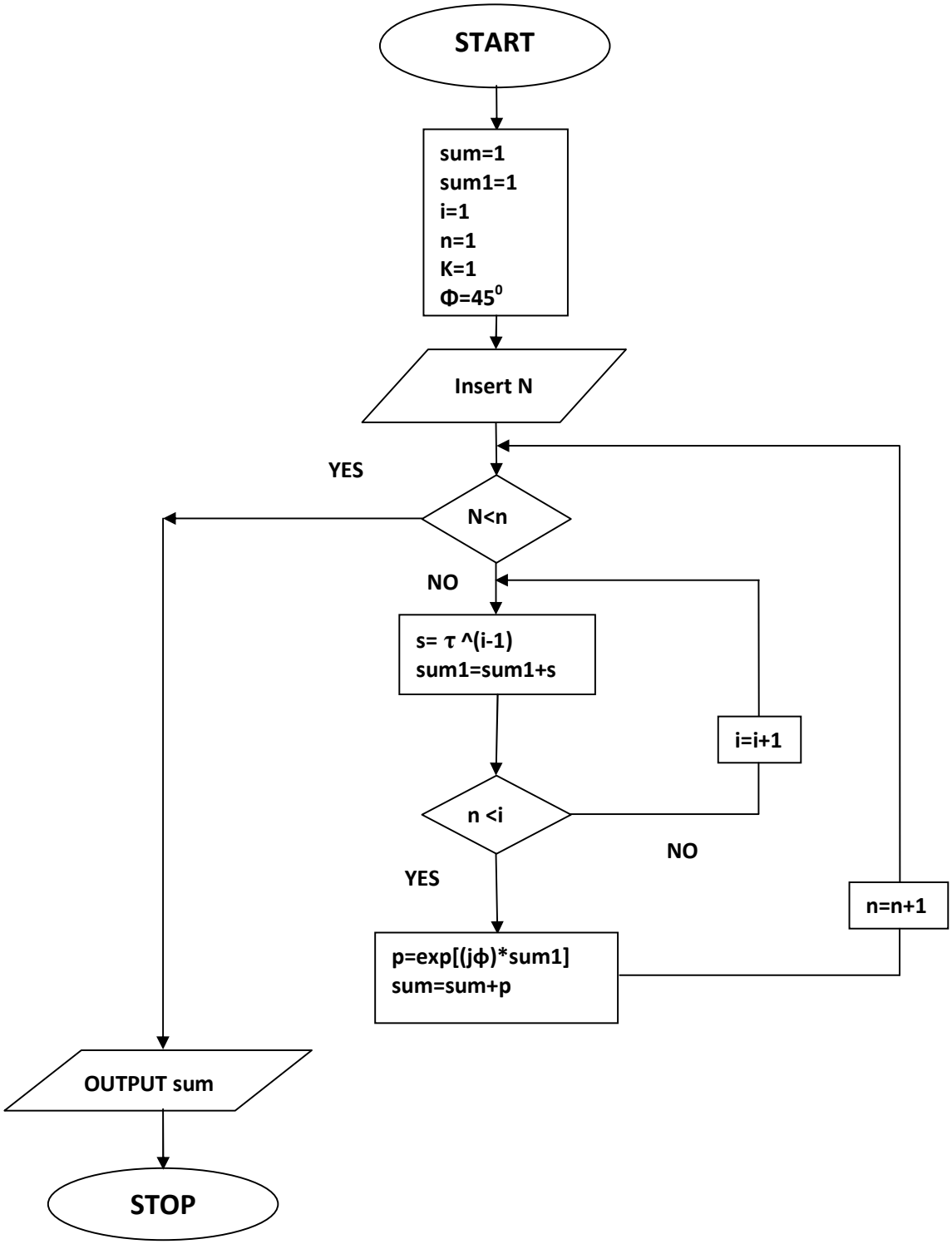

Fig. 3.7: Flow Chart for Array Factor of Single Log Periodic Array Antennas

The algorithms that show the step – by – step approach in computing the array factor of SLPA are outlined below. N is 16 for this sample study.

1. Start
2. Initialize the counter, i
3. Initialize the sums, sum and sum1
4. Insert the number of dipoles, N.
5. If N < n, go to 15.
6. s= τ^(i-1)
7. sum1=sum1+s
8. if n < i, go to 11.
9. Then increment counter, i
10. Go to step 6
11. p=exp[(jφ)*sum1]
12. Sum=sum+p
13. Increment n
14. Go to step 5
15. Output sum
16. Stop

3.2.2.3 Derivation of the Electromagnetic Fields Generated by the First Radiating Element in MLPA Antennas using MVP Model

The electromagnetic fields generated by the longest element in MLPA antennas were derived in this section. This derivation was carried out using Magnetic Vector Potential (MVP) model. This approach considered the permeability of the antenna element, the current flowing through the element, the dimension of the element, and 'Green's function'. Figure 3.8 represents the schematic arrangement of dipole antenna element located along z-axis of the Cartesian plane.

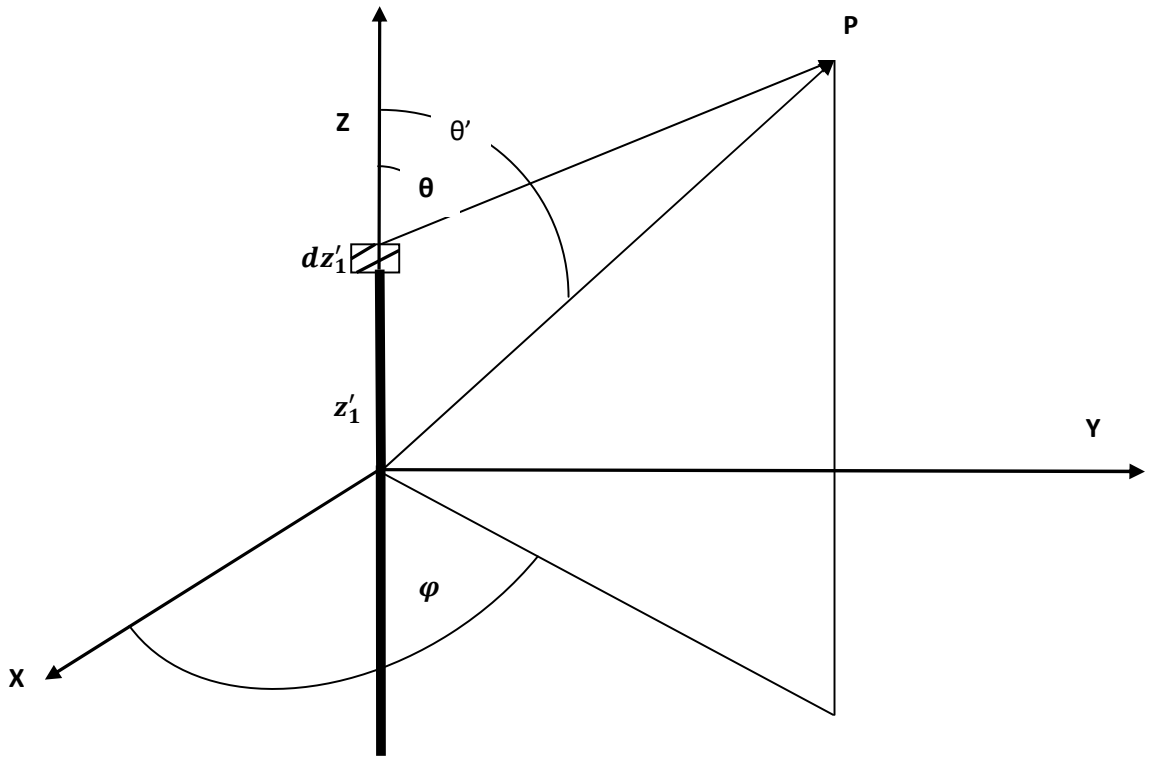

Fig. 3.8: Schematic diagram of a dipole antenna positioned along z-axis of the Cartesian plane (Okoye, 2014)

To enhance the analysis of the antenna at a far field, two important approximations are necessary namely: phase approximation and amplitude approximation. Thus, phase approximation is,

$$\hat{\mathrm{R}} = \mathrm{r} - \mathrm{z}_1' \cos\theta \tag{3.51}$$

Amplitude approximation is,

$$|\mathrm{R}| \approx \mathrm{r} \tag{3.52}$$

Substituting equations (3.51) and (3.52) into equation (3.2) of the Magnetic Vector Potential gives (Adekola, 2012; Okoye, 2014),

$$\hat{\mathrm{A}}_{\mathrm{z}} = \frac{\mu}{4\pi}\int_{-l1/2}^{l1/2} \mathrm{I}\ (\mathrm{Z}_1')\ \ \frac{e^{-\mathrm{j\,k\,(r-z_1'\cos\theta)}}}{r}\mathrm{dz}_1' \tag{3.53}$$

Factoring out the common factor results to the expression in equation (3.54),

$$\hat{\mathrm{A}}_{\mathrm{z}} = \frac{\mu_0\, \mathrm{e}^{-\mathrm{j\,k\,r}}}{4\pi \mathrm{r}}\left[\int_{-\frac{l_1}{2}}^{\frac{l_1}{2}} \mathrm{I}\left(\mathrm{z}_1'\right) e^{\mathrm{j\,k\,z_1'\cos\theta}}\ \mathrm{dz}_1'\right] \tag{3.54}$$

.

For a finite length dipole, the current distribution along the antenna element is written as (Balanis, 2005),

$$\mathrm{I}\,(\mathrm{z}') = \mathrm{I}_0 \sin\left[\mathrm{k}\left(\frac{l}{2}\right) - |\mathrm{z}'|\right] \tag{3.55}$$

Substituting the value of current in equation (3.55) into equation (3.54) results to equation (3.56);

$$\hat{\mathrm{A}}_{\mathrm{z}} = \frac{\mu\ \ \mathrm{I}\, e^{-jkr}}{4\pi r}\int_{-\frac{l_1}{2}}^{\frac{l_1}{2}} \sin\left[k\frac{l_1}{2} - |z'|\ \right] e^{jkz_1'\cos\theta}\ dz_1' \tag{3.56}$$

Expanding the integral values results to equation (3.57)

$$A_z = \frac{\mu\ I e^{-jkr}}{4\pi r} \quad \int_{-\frac{l_n}{2}}^{0} \sin\left[k\frac{l_1}{2} + |z'|\right] e^{jkz_1' cos\theta}\, dz_1' + \int_{0}^{-\frac{l_1}{2}} \sin\left[k\frac{l_1}{2} - |z'|\right] e^{jkz_1' cos\theta}\, dz_1' \tag{3.57}$$

Equation (3.57) was further expanded to equation (3.58)

$$A_z = \frac{\mu\ I e^{-jkr}}{4\pi r} \left\{ \begin{array}{l} \left(\frac{1}{2j} \int_{-\frac{l}{2}}^{0} e^{jk\left[\left(\frac{l}{2}+z'\right) + z' cos\theta\right]} - e^{-jk\left[\left(\frac{l}{2}+z'\right) - z' cos\theta\right]} dz' \right) \\ + \left(\frac{1}{2j} \int_{0}^{\frac{l}{2}} e^{jk\left[\left(\frac{l}{2}-z'\right) + z' cos\theta\right]} - e^{-jk\left[\left(\frac{l}{2}-z'\right) - z' cos\theta\right]} dz' \right) \end{array} \right\} \tag{3.58}$$

After integrating over the length of the dipole element, equation (3.59) was obtained thus (Adekola, 2012);

$$A_z = \frac{\mu\ I e^{-jkr}}{4\pi r} \left\{ \frac{\cos\left(k\frac{l}{2}\right) - \cos\left(k\frac{l}{2} cos\theta\right)}{k(1+\cos\theta)} + \frac{\cos\left(k\frac{l}{2}\right) - \cos\left(k\frac{l}{2} cos\theta\right)}{k(1-\cos\theta)} \right\} \tag{3.59}$$

Equation (3.59) was further analysed to obtain equation (3.60)

$$A_z = \frac{\mu\ I e^{-jkr}}{2\pi r k} \left\{ \frac{\cos\left(k\frac{l}{2}\right) - \cos\left(k\frac{l}{2} cos\theta\right)}{sin^2\theta} \right\} \tag{3.60}$$

Rearranging the terms in equation (3.60) results to equation (3.61) (Okoye, 2014);

$$A_z = -\frac{\mu\ I e^{-jkr}}{2\pi r k} \left[\frac{\cos\left(k\frac{l}{2} cos\theta\right) - \cos\left(k\frac{l}{2}\right)}{sin^2\theta} \right] \tag{3.61}$$

Note: a mathematical relation exist between x and $Cos\ x$. Thus,

For $\begin{cases} x \ll 1, \\ Cos\ x \simeq 1 - \frac{x^2}{2}. \end{cases}$

Consequently,

For $\begin{cases} l \ll \lambda, \\ \frac{k\,l}{2} cos\theta,\ \frac{k\,l}{2} << 1 \end{cases}$

Substituting this relation into equation (3.61) results to equation (3.62) (Okoye, 2014)

$$A_z = -\frac{\mu\ I e^{-jkr}}{4\pi rk} \frac{(k\frac{l}{2})^2 - (1 - cos^2\theta)}{sin^2\theta} \quad (3.62)$$

Simplifying equation (3.62) results to equation (3.63);

$$A_z = \frac{\mu\ k^2\ I\ l^2\ e^{-jkr}}{16\pi rk} \quad (3.63)$$

Where: l is the length of the antenna element, I is the current flowing through the antenna element, K is the wave number, r is the distance from the antenna origin to the field point.

In order to obtain the Electric, E and Magnetic, H fields of the first radiating elements of Multiple Log-Periodic Dipole Array antennas, equation (3.64) is used;

$$\hat{E} = -j\,\omega\,(\hat{A}\,z - \hat{r}\,\hat{A}\,r) \quad (3.64)$$

When the three components of $\hat{A}_z$ are substituted into equation (3.64), equation (3.65) is generated. Thus;

$$\hat{E} = (\hat{r}\,A\,r + \hat{\theta}\hat{A}\,\theta + \hat{\varphi}\hat{A}\,\varphi) - \hat{r}\,\hat{A}\,r \quad (3.65)$$

Hence,

$$\hat{E} = \hat{\theta} \hat{A}_{\theta} + \hat{\varphi} \hat{A}_{\varphi} \quad (3.66)$$

From the relation in equation (3.67) and (3.68), equation (3.69) is produced (Adekola, 2012) ;

$$\begin{bmatrix} A_r \\ A_\theta \\ A_\varphi \end{bmatrix} = \begin{bmatrix} sin\theta cos\boldsymbol{\theta} & sin\theta sin\varphi & cos\boldsymbol{\theta} \\ cos\theta cos\varphi & cos\theta cos\varphi & -sin\boldsymbol{\theta} \\ -sin\varphi & cos\varphi & 0 \end{bmatrix} \begin{bmatrix} A_x \\ A_y \\ A_z \end{bmatrix} \quad (3.67)$$

$A_x = A_y = 0$; $A_\theta = A_z \sin\theta$ (3.68)

Equation (3.69) relates the Magnetic Vector Potential of an antenna and the Electric field. That is,

$$E_\theta(\theta, \varphi) = -j\omega (A_z \sin\theta) \quad (3.69)$$

Substituting equation (3.63) of the magnetic vector potential along the z-axis into equation (3.69) results to equation (3.70);

$$E_\theta(\theta, \varphi) = \frac{jw\mu \ k^2 \ I \ l^2 \ e^{-jkr}}{16\pi rk} \sin\theta \quad (3.70)$$

After integrating over the lengths of the antenna elements, the electric field, $\hat{E}$ in the θ direction is derived as,

$$E_\theta(\theta, \varphi) = \frac{jw\mu \ k^2 \ Il^2 \ e^{-jkr}}{16\pi rk} \sin\theta \quad (3.71)$$

From the antenna relation, ($\eta = \frac{w\mu}{k}$), replacing $\frac{w\mu}{k}$ in equation (3.81) with η, the Electric field for single dipole antenna is (Adekola, 2012; Okoye, 2014),

$$E_{\theta}(\theta,\varphi) = \frac{j\,\eta\,k^2\,Il^2\,e^{-jkr}}{16\pi r}\ \sin\theta \tag{3.72}$$

While the corresponding value for the magnetic field is given thus (Okoye, 2014):

$$H_{\varphi}(\theta,\varphi) = \frac{E_{\theta}(\theta,\varphi)}{\eta} \tag{3.73}$$

where η is the intrinsic impedance. Hence,

$$H_{\varphi}(\theta,\varphi) = \frac{j\,k^2\,Il^2\,e^{-jkr}}{16\pi r}\ \sin\theta \tag{3.74}$$

Equation (3.74) of the magnetic field is obtained by dividing (3.72) by intrinsic impedance

3.2.2.4 Characterization of the MLPA Antennas Parameters using the derived Novel Array Factor

In characterizing the behaviours of Multiple Log Periodic Array (MLPA) antennas, the conventional antenna formulas were used. These formulas now assisted in determining the parameters of the MLPA antennas under study. The major antenna parameters considered were:

i. Electric/Magnetic Field,
ii. Average Poynting Vector,
iii. Radiation Intensity,
iv. Radiated Power,
v. Radiation Resistance,
vi. Directive Gain, and
vii. Directivity.

3.2.2.4.1 Total Electric/Magnetic Field for MLPA Antennas

The electric and magnetic (EM) Fields for the first element in MLPA antenna, that is a dipole antenna, was derived in equations (3.72) and (3.74) of section 3.2.2.3. In order to deduce the electromagnetic fields generated by MLPA antennas in general, these fields generated by the dipole antenna and the array factor derived for Multiple Log Periodic Array antennas are used accordingly. The electromagnetic fields generated by MLPA antennas are the product of the Electric/Magnetic fields produced by the first antenna element in the array and the Array-Factor of the MLPA antennas.

Thus, the total electric and magnetic fields of MLPA antennas of any number of elements give the expressions in equations (3.76) and (3.77) respectively.

In other words, for MLPA antennas, the total Electric field or Magnetic field generated involves the multiplication of equation (3.72) or (3.74), and equation (3.44) respectively. These electromagnetic fields take cognizance of the varying dipole lengths. Hence;

$$Total\ Field\ = \text{field of first element in the array} * \text{Array factor (A. F)} \tag{3.75}$$

Thus, for MLPA antennas;

$$E_{M\ \theta}^{\ T} = \left\{ \left(1 + \sum_{n=1}^{N-1} \prod_{i=1}^{n} e^{j\tau^{\,i-1}\varphi} \right) \frac{Sin\left(\frac{N}{2}\right)\varphi}{\left(\frac{\varphi}{2}\right)} * \frac{j\,\eta\,k^2\,I(l\tau^{n-1})^2\,e^{-jkr}}{16\pi r}\ \sin\theta \right\} \tag{3.76}$$

The corresponding magnetic field for the MLPA antennas was also obtained by dividing the electric field of equation (3.76) by intrinsic impedance, η. Thus,

$$H_{M\ \theta}^{\ T} = \left\{ \left(1 + \sum_{n=1}^{N-1} \prod_{i=1}^{n} e^{j\tau^{\,i-1}\varphi} \right) \frac{Sin\left(\frac{N}{2}\right)\varphi}{\left(\frac{\varphi}{2}\right)} * \frac{j\,k^2\,I(l\,\tau^{n-1})^2\,e^{-jkr}}{16\pi r}\ \sin\theta \right\} \tag{3.77}$$

Equation (3.76) is the total electric field for MLPA antennas while equation (3.77) is the corresponding total magnetic field for MLPA antennas,

Where;

$E^{T}_{M\ \theta}$ =total Electric field radiated by MLPA antennas in θ direction

$H^{T}_{M\ \theta}$ =total Magnetic field radiated by MLPA antennas in θ direction

3.2.2.4.2 Average Poynting Vector, ρ_{av} of MLPA Antennas

Average Poynting Vector plays a major role in the derivation of other antenna parameters. It was determined by calculating the time average of the product of the Electric Field, E and the conjugate of the Magnetic Field, H. Thus, the formular for Average Poynting Vector according to Balanis (2005) and Okoye (2014) is represented in equation (3.78),

$$\rho av = \frac{1}{2}\mathrm{Re}[\mathrm{E\ x}\ H^{*}] \tag{3.78}$$

For a dipole antenna (Okoye, 2014)

$$\rho av = \left|\frac{1}{2}Re\left\{\frac{\eta\,(\,\mathrm{I}(l)^{2}\,)^{\,2}\,\mathrm{k}^{4}}{(16\pi r)^{\,2}}\ \sin^{2}\theta\right\}\right| \tag{3.79}$$

Where; I=current flowing through the dipole antenna, l=length of dipole antenna element, k=wave number, $\eta = \text{intrinsic impedance}$.

For MLPA antennas, the Average Poynting Vector is determined by finding the product of electric field and magnetic field generated by MLPA antennas. In other words, it is the product of equations (3.76) and (3.77).

$$\rho av_{MLPA} =$$

$$\frac{1}{2}\,\mathrm{Re}\begin{Bmatrix} \left[\left(\sum_{n=1}^{M} e^{(M-1)j\varphi} + \sum_{n=1}^{N} e^{(M-1)j\varphi} \sum_{n=1}^{N-1}\prod_{i=1}^{n} e^{(\tau^{i-1})j\varphi}\right)\frac{j\ \eta\, k^2\, I\ (l\tau^{n-1})^2\, e^{-jkr}}{16\pi r}\ \sin\theta\right]\theta \\ x\ \left[\left(\sum_{n=1}^{N} e^{(M-1)j\varphi} + \sum_{n=1}^{N} e^{(M-1)j\varphi} \sum_{n=1}^{N-1}\prod_{i=1}^{n} e^{(\tau^{i-1})j\varphi}\right)\ \frac{j\ k^2\, I(l\tau^{n-1})^2\, e^{-jkr}}{16\pi r}\ \sin\theta\right]^{*}\hat{\varphi} \end{Bmatrix} \quad (3.80)$$

Also, analyzing the unit vectors θ and φ,

$$\rho av_{MLPA} =$$

$$\frac{1}{2}\,\mathrm{Re}\begin{Bmatrix} \left[\left(\sum_{n=1}^{N} e^{j\varphi(M-1)} + \sum_{n=1}^{N} e^{j\varphi(M-1)} \sum_{n=1}^{N-1}\prod_{i=1}^{n} e^{j\varphi(\tau^{i-1})}\right)\frac{j\ \eta k^2\, I(l\tau^{n-1})^2\, e^{-jkr}}{16\pi r}\ \sin\theta\right] \\ *\left[\left(\sum_{n=1}^{N} e^{-j\varphi(M-1)} + \sum_{n=1}^{N} e^{-j\varphi(M-1)} \sum_{n=1}^{N-1}\prod_{i=1}^{n} e^{-j\varphi(\tau^{i-1})}\right)\frac{(-j)k^2\, I\left(l\tau^{n-1}\right)^2\, e^{-jkr}}{16\pi r}\sin\theta\right](\theta x\ \varphi) \end{Bmatrix} \quad (3.81)$$

However, where the value for φ is small, the average Poynting vector from equation (3.81) becomes;

$$\rho av_{MLPA}$$

$$= \frac{1}{2}\,\mathrm{Re}\begin{Bmatrix} \left[\left(\frac{\mathrm{Sin}\left(\frac{M\varphi}{2}\right)}{\frac{\varphi}{2}} + \frac{\mathrm{Sin}\left(\frac{M\varphi}{2}\right)}{\frac{\varphi}{2}}\sum_{n=1}^{N-1}\prod_{i=1}^{n} e^{(\tau^{i-1})j\varphi}\right)\frac{j\ \eta k^2\, I(l\tau^{n-1})^2\, e^{-jkr}}{16\pi r}\ \sin\theta\right] \\ *\left[\left(\frac{\mathrm{Sin}\left(\frac{M\varphi}{2}\right)}{\frac{\varphi}{2}} + \frac{\mathrm{Sin}\left(\frac{M\varphi}{2}\right)}{\frac{\varphi}{2}}\sum_{n=1}^{N-1}\prod_{i=1}^{n} e^{(\tau^{i-1})j\varphi}\right)\frac{j\ k^2\, I(l\tau^{n-1})^2\, e^{-jkr}}{16\pi r}\ \sin\theta\right](\theta x\ \varphi) \end{Bmatrix} \quad (3.82)$$

Multiplying out the brackets results to equation (3.83);

$$\rho av_{MLPA} = \frac{1}{2}\,\mathrm{Re}\left\{\frac{\eta(k^2\,I(l\tau^{n-1})^2)^{\,2}}{(16\pi r)^{\,2}}\;\sin^2\theta\left[\begin{array}{c}\dfrac{\mathrm{Sin}\left(\frac{M\varphi}{2}\right)}{\frac{\varphi}{2}} \\ +\ \dfrac{\mathrm{Sin}\left(\frac{M\varphi}{2}\right)}{\frac{\varphi}{2}}\sum_{n=1}^{N-1}\prod_{i=1}^{n} e^{(\tau^{i-1})j\varphi} \\ +\ \dfrac{\mathrm{Sin}\left(\frac{M\varphi}{2}\right)}{\frac{\varphi}{2}}\sum_{n=1}^{N-1}\prod_{i=1}^{n} e^{-(\tau^{i-1})j\varphi} \\ +\ \dfrac{\mathrm{Sin}\left(\frac{M\varphi}{2}\right)}{\frac{\varphi}{2}}\sum_{n=1}^{N-1}\prod_{i=1}^{n}(1)\end{array}\right]\right\}\hat{r}$$

(3.83)

Factorizing out the sine coefficients results to equation (3.84)

$$\rho av_{MLPA} = \frac{1}{2}\,\mathrm{Re}\left\{\frac{\eta\left(k^2\,I\left(l\tau^{n-1}\right)^2\right)^{2}}{(16\pi r)^{\,2}}\;\sin^2\theta\left[\left(\frac{\mathrm{Sin}\left(\frac{M\varphi}{2}\right)}{\frac{\varphi}{2}}\right)^2\left(\begin{array}{c}1+\sum_{n=1}^{N-1}\prod_{i=1}^{n} e^{(\tau^{i-1})j\varphi} \\ +\ \sum_{n=1}^{N-1}\prod_{i=1}^{n} e^{-(\tau^{i-1})j\varphi}+ \\ \sum_{n=1}^{N-1}\prod_{i=1}^{n}(1)\end{array}\right)\right]\right\}\hat{r}$$

(3.84)

On further analysis, equation (3.84) results to equation (3.85)

$$\rho av_{MLPA} = \frac{1}{2}\,\mathrm{Re}\left\{\frac{\eta(k^2\,I(l\tau^{n-1})^2)^{\,2}}{(16\pi r)^{\,2}}\;\sin^2\theta\left[\left(\frac{\mathrm{Sin}\left(\frac{M\varphi}{2}\right)}{\frac{\varphi}{2}}\right)^2\left(1+\sum_{n=1}^{N-1}\prod_{i=1}^{n}\left(1+2\cos\left(\tau^{i-1}\right)\varphi\right)\right)\right]\right\}\hat{r}$$

(3.85)

Replacing φ with kdsin θ in equation (3.85) results to equation (3.86).

Thus,

$$\rho av_{MLPA} =$$

$$\frac{1}{2}\,\mathrm{Re}\left\{\frac{\eta\left(k^2\,I\left(l\tau^{n-1}\right)^2\right)^2}{(16\pi r)^2}\;\sin^2\theta\left[\left(\frac{\mathrm{Sin}\left(\frac{Mkd\sin\theta}{2}\right)}{\frac{\varphi}{2}}\right)^2\left(1+\sum_{n=1}^{N-1}\prod_{i=1}^{n}\left(1+2\cos\left(kd\left(\tau^{i-1}\right)\sin\theta\right)\right)\right)\right]\right\}\hat{r}$$

(3.86)

Equation (3.86) is the real value of Average Poynting Vector of MLPA antennas.

3.2.2.4.3 Radiation Intensity, U (ɵ, φ) of MLPA Antennas:

Radiation Intensity of antennas is the product of Average Poynting Vector and the square of the distance of the antenna from its origin to the field point.

Radiation Intensity of a dipole antenna was evaluated using equation (3.87) (Adekola, 2012; Kraus, 1997).

$$U(ɵ, \varphi) = r^2|\rho av| \tag{3.87}$$

To derive the Radiation Intensity for a dipole antenna, it is the product of the square of distance, r covered and equation (3.88) of average pointing vector of a dipole antenna (Kraus, 1997). Thus,

$$U(ɵ, \varphi) = \left|\frac{1}{2}Re\left\{\frac{\eta\,(\,I(l)^2\,)^2\,k^4}{(16\pi)^2}\;\sin^2 ɵ\right\}\right| \tag{3.88}$$

where;

$K = w\sqrt{\mu\varepsilon} = w/c = w/f\lambda = 2\pi / \lambda$

Hence, this implies;

$$k^4 = (2\pi/\lambda)^4 = 16\pi^4/\lambda^4 \quad (3.89)$$

Substituting equation (3.89) into equation (3.88) resulted to equation (3.90) (Adekola, 2012)

$$\mathrm{U}(\theta,\varphi) = \frac{\eta}{32}(\pi I)^2 \left(\frac{\ell}{\lambda}\right)^4 \sin^2\theta \quad (3.90)$$

Equation (3.90) shows the Radiation Intensity of a dipole antenna.

The Radiation Intensity for Multiple Log Periodic Array antennas was determined as a product of the radiation intensity of a dipole antenna and the square of the array factor for MLPA antennas. Thus,

$$\mathrm{U}_{MLPA}(\theta,\varphi) = \left|\frac{1}{2}Re\left\{\left[\left(\frac{\mathrm{Sin}\left(\frac{M\varphi}{2}\right)}{\frac{\varphi}{2}}\right)^2\left(1+\sum_{n=1}^{N-1}\prod_{i=1}^{n}\left(1+2\cos\left(\mathrm{kd}\left(\tau^{i-1}\right)\sin\theta\right)\right)\right)\right]\frac{\eta\,(\mathrm{I}(\ell\,\tau^{n-1})^2)^2\,\mathrm{k}^4}{(16\pi)^2}\sin^2\theta\right\}\right| \quad (3.91)$$

Also, in order to get the real and absolute value of MLPA radiation intensity, equation (3.91) was multiplied out by $\frac{1}{2}$ to produce equation (3.92). Thus,

$$\mathrm{U}_{MLPA}(\theta) = \left|Re\left\{\left[\left(\frac{\mathrm{Sin}\left(\frac{M\varphi}{2}\right)}{\frac{\varphi}{2}}\right)^2\left(1+\sum_{n=1}^{N-1}\prod_{i=1}^{n}\left(1+2\cos\left(\mathrm{kd}\left(\tau^{i-1}\right)\sin\theta\right)\right)\right)\right]\frac{\eta\,(\mathrm{I}(\ell\;\;\tau^{n-1})^2)^2 8\pi^4}{\pi^2(16)^2\lambda^4}\sin^2\theta\right\}\right| \quad (3.92)$$

Equation (3.92) was further simplified to generate absolute value of the radiation intensity in equation (3.93)

$$U_{MLPA}(\theta) =$$

$$\left| Re\left\{ \left[\left(\frac{\mathrm{Sin}\left(\frac{M\varphi}{2}\right)}{\frac{\varphi}{2}} \right)^2 \left(1 + \sum_{n=1}^{N-1} \prod_{i=1}^{n} \left(1 + 2\cos\left(kd\left(\tau^{i-1}\right) \sin\theta \right) \right) \right) \right] \frac{\eta}{32} (\pi I)^2 \left(\frac{(\ell\, \tau^{n-1})}{\lambda} \right)^4 \sin^2\theta \right\} \right| \tag{3.93}$$

Equation (3.93) represents the real and absolute value of the Radiation Intensity of Multiple Log Periodic Array antennas.

3.2.2.4.4 Radiated Power, P_{rad} of MLPA Antennas:

Equation (3.94) is the standard formular for resolving the power radiated by antennas (Adekola, 2012). Hence,

$$P_{rad} = \int_0^{2\pi} \int_0^{\pi} P_{av} r_2 \sin\theta \, d\theta \, d\varphi \tag{3.94}$$

Where P_{av} is the average Poynting vector

For easy evaluation, equation (3.94) was further rearranged as shown in equation (3.95) (Adekola, 2012),

$$P_{rad} = \int_0^{2\pi} d\varphi \int_0^{\pi} P_{av} r_2 \sin\theta \, d\theta \tag{3.95}$$

For Multiple Log-Periodic Array Antennas, equation (3.95) is used to compute the power radiated by Multiple Log Periodic Array antennas as shown below by substituting the Average Poynting Vector of MLPA antennas of equation (3.86) into (3.95). Hence,

$$P_{rad\ _{MLPA}} = 2\pi\,.\,\mathrm{Re}\left\{\left[\left(1+\sum_{n=1}^{N-1}\prod_{i=1}^{n}\left(1+2\cos\left(\mathrm{kd}\left(\tau^{i-1}\right)\sin\theta\right)\right)\right)\left(\frac{\mathrm{Sin}\left(\frac{\mathrm{M}\varphi}{2}\right)}{\frac{\varphi}{2}}\right)^{2}\right]\frac{\eta\left(\mathrm{k}^{2}\,\mathrm{I}(\ell\,\tau^{n-1})^{2}\right)^{2}\mathrm{r}^{2}}{2\,(16\pi)^{2}\,r^{2}}\ \sin^{3}\theta\right\}\hat{\mathrm{r}} \quad (3.96)$$

From the antenna relation, $\left(k=\frac{w}{f\lambda}\right)$ (Adekola, 2012), substituting the value of k in equation (3.96) with this relation results to (3.97)

$$P_{rad\ _{MLPA}} =$$

$$\mathrm{Re}\left\{\left[\left(1+\sum_{n=1}^{N-1}\prod_{i=1}^{n}\left(1+2\cos\left(\mathrm{kd}\left(\tau^{i-1}\right)\sin\theta\right)\right)\right)\left(\frac{\mathrm{Sin}\left(\frac{\mathrm{M}\varphi}{2}\right)}{\frac{\varphi}{2}}\right)^{2}\right]\frac{\eta\,\pi\,\mathrm{w}^{4}}{\mathrm{f}^{4}\ \lambda^{4}\,(16\pi)^{2}}\left(\frac{\mathrm{l}\,(\ell\,\tau^{n-1})}{4\pi}\right)^{2}\frac{4}{3}\right\}\hat{\mathrm{r}} \quad (3.97)$$

To further analyze equation (3.97), it is recalled that $(w=2\pi f)$ (Balanis, 2005). Thus, replacing the parameter *w* in equation (3.108) with $2\pi f$, it results to equation (3.98). This helps to establish the relationship between the length ℓ of the antenna radiating elements and the wavelength λ.

$$P_{rad\ _{MLPA}} =$$

$$\mathrm{Re}\left\{\left[\left(1+\sum_{n=1}^{N-1}\prod_{i=1}^{n}\left(1+2\cos\left(\mathrm{kd}\left(\tau^{i-1}\right)\sin\theta\right)\right)\right)\left(\frac{\mathrm{Sin}\left(\frac{\mathrm{M}\varphi}{2}\right)}{\frac{\varphi}{2}}\right)^{2}\right]\frac{\eta\,\pi^{3}\mathrm{I}^{2}}{12}\left(\frac{(\ell\,\tau^{n-1})^{2}}{\lambda^{2}}\right)^{2}\right\}\ \hat{\mathrm{r}} \quad (3.98)$$

where φ equals k d sin θ

Equation (3.98) shows the real value of power radiated by Multiple Log Periodic Dipole Array antennas.

3.2.2.4.5 Radiation Resistance, R_{rad} of MLPA Antennas:

Radiation Resistance is defined as the point that the value of a hypothetical resistor will generate a power equal to the power radiated by the antenna when fed by the same current.

The Radiation Resistance for Multiple Log-Periodic Array antennas was calculated as shown in equation (3.99). This was calculated by dividing the radiated power of MLPA antennas by the square of the absolute current flowing through the antenna elements, and then multiplying by 2. Thus,

$$R_{rad}{}_{MLPA} =$$

$$\mathrm{Re}\left\{\left[\left(1+\sum_{n=1}^{N-1}\prod_{i=1}^{n}\left(1+2\cos\left(\mathrm{kd}\left(\tau^{i-1}\right)\sin\theta\right)\right)\right)\left(\frac{\mathrm{Sin}\left(\frac{\mathrm{M}\varphi}{2}\right)}{\frac{\varphi}{2}}\right)^{2}\right]\frac{\eta\,\pi^{3}}{6}\left(\frac{(\ell\,\tau^{n-1})^{2}}{\lambda^{2}}\right)^{2}\right\}\hat{\mathrm{r}} \qquad (3.99)$$

where, $\eta = 120\pi$

Substituting the values of intrinsic impedance and pi into equation (3.99), results to equation (3.100)

$$R_{rad}{}_{MLPA} =$$

$$\mathrm{Re}\left\{\left[\left(1+\sum_{n=1}^{N-1}\prod_{i=1}^{n}\left(1+2\cos\left(\mathrm{kd}\left(\tau^{i-1}\right)\sin\theta\right)\right)\right)\left(\frac{\mathrm{Sin}\left(\frac{\mathrm{M}\varphi}{2}\right)}{\frac{\varphi}{2}}\right)^{2}\right]1950\left(\frac{(\ell\,\tau^{n-1})^{2}}{\lambda^{2}}\right)^{2}\right\}\ \hat{\mathrm{r}}$$

(3.100)

Hence, equation (3.100) is the real value of Radiation Resistance for Multiple Log Periodic Array antennas.

3.2.2.4.6 Directive Gain, D (ɵ, φ) of MLPA Antennas:

Directive Gain is the ratio of antenna radiation intensity to that of a hypothetical isotropic radiator that radiates the same power (Balanis, 2005).

Equation (3.101) was used to calculate the directive gain of MLPA antennas (Balanis, 2005).

$$D(\theta,\varphi) = \frac{U(\theta,\varphi);}{U_0} = \frac{4\,\pi\,U(\theta,\varphi)}{P_{rad}} \tag{3.101}$$

Using the equation (3.101) to compute the directive gain of Multiple Log-Periodic Array antennas

$$D(\theta,\varphi)_{\mathrm{MLPDA}} = \frac{4\pi\left\{\left[\left(1+\sum_{n=1}^{N-1}\prod_{i=1}^{n}\left(1+2\cos\left(\mathrm{kd}\left(\tau^{i-1}\right)\sin\theta\right)\right)\right)\left(\frac{\mathrm{Sin}\left(\frac{M\varphi}{2}\right)}{\frac{\varphi}{2}}\right)^{2}\right]\frac{\eta}{32}(\pi I)^{2}\left(\frac{(\ell\,\tau^{n-1})}{\lambda}\right)^{4}\sin^{2}\theta\right\}}{\left[\left(1+\sum_{n=1}^{N-1}\prod_{i=1}^{n}(1+2\cos(\mathrm{kd}(\tau^{i-1})\sin\theta))\right)\left(\frac{\mathrm{Sin}\left(\frac{M\varphi}{2}\right)}{\frac{\varphi}{2}}\right)^{2}\right]\frac{\eta\,\pi\,^{3}I^{2}}{12}\left(\frac{(\ell\,\tau^{n-1})^{2}}{\lambda^{2}}\right)^{2}} \tag{3.102}$$

Equation (3.102) generated $1.5\sin^{2}\theta$ as the Directive Gain for the first element in the MLPA antennas.

Using pattern multiplication approach, the Directive Gain for Multiple Log-Periodic Array antennas was deduced as a product of the directive gain of first element in the MLPA antennas and the Array Factor.

Therefore;

$$D(\theta,\varphi)_{MLPDA} = 1.5\sin^2\theta\left[\left(1+\sum_{n=1}^{N-1}\prod_{i=1}^{n}\left(1+2\cos\left(kd\left(\tau^{i-1}\right)\sin\theta\right)\right)\right)\left(\frac{\sin\left(\frac{M\varphi}{2}\right)}{\frac{\varphi}{2}}\right)^2\right] \quad (3.103)$$

Equation (3.103) stands for the Directive Gain for Multiple Log Periodic Array antennas.

3.2.2.4.7 Directivity, D_{max} of MLPA Antennas:

The maximum value of directive gain of an antenna is termed its directivity. MPDA antennas possess maximum values of their respective directive gains. It was determined thus (Balanis, 2005),

$$D_{max} = \frac{4\pi U_{max}}{P_{rad}} \quad (3.104)$$

where,

D_{max} is the maximum directive gain

U_{max} is the maximum radiation intensity,

P_{rad} is the power radiated

Hence, from the analysis of equation (3.104), it was deduced that the ratio of the product of 4 π and maximum radiation intensity to the radiated power results to equation (3.105).

$$D_{max} = 1.5\sin\theta \quad (3.105)$$

The maximum directive gains for MLPA antennas occur at ɵ equals 90^0. This results to equation (3.106)

$$D_{max} = 1.5 \quad (3.106)$$

3.2.2.5 Design and Simulation of Typical Multiple Log Periodic Dipole Array Antennas using MatLab Tools

In the design of Multiple Log Periodic Array antennas, the spacing and design factors that were chosen ensure that the lengths and spacing of the elements of log-periodic array antennas increase logarithmically from one end of the antenna boom to the other end. Frequency range was carefully selected as most of modern systems operate within very high frequency band.

3.2.2.5.1 Design Specifications

For desired design, the specifications for the array antennas were carefully chosen to ensure optimum signal radiation performance, as well as ensure appropriate physical dimensions for the array antennas. Table 3.1 is the specification parameters for the antenna design.

Table 3.1: Design Specifications

Items	**Value**
expected Directivity/Gain, G	9dbi
The operating frequency of the antenna	1.350-2.690 GHz
Lowest frequency, f1	1.350MHz
Highest frequency, f2	2.690MHz
Upper to lower frequency ratio	2:1
Design Factor, τ	0.93
Spacing Factor, σ	0.17
Antenna input impedance, R_0	50Ω,

The notations used in the design of the Multiple Log-Periodic Array antennas are represented in Table 3.2.

Table 3.2: Design Elements Notations

s/n	**Design Elements**	**Notations**
1	antenna frequency	f
2	dipole length	l
3	operating Bandwidth	β
4	design factor	τ
5	Spacing Factor	σ
6	apex angle	α
7	Bandwidth of the active region	β_{ar}
8	structure (array) bandwidth	β_s
9	boom length	L
10	number of elements	N
11	terminating stub	Z_t
12	Average characteristic impedance of longest dipole	Z_{ave}
13	Mean spacing factor	σ'
14	Feeder impedance	Z_0
15	Center to center boom spacing	S
16	dipole element spacing	d_{n-n+1}
17	distance between the dipole elements from the vertex	γ_n

Figure 3.9 represents the lateral view of LPDA antenna arrangement at design.

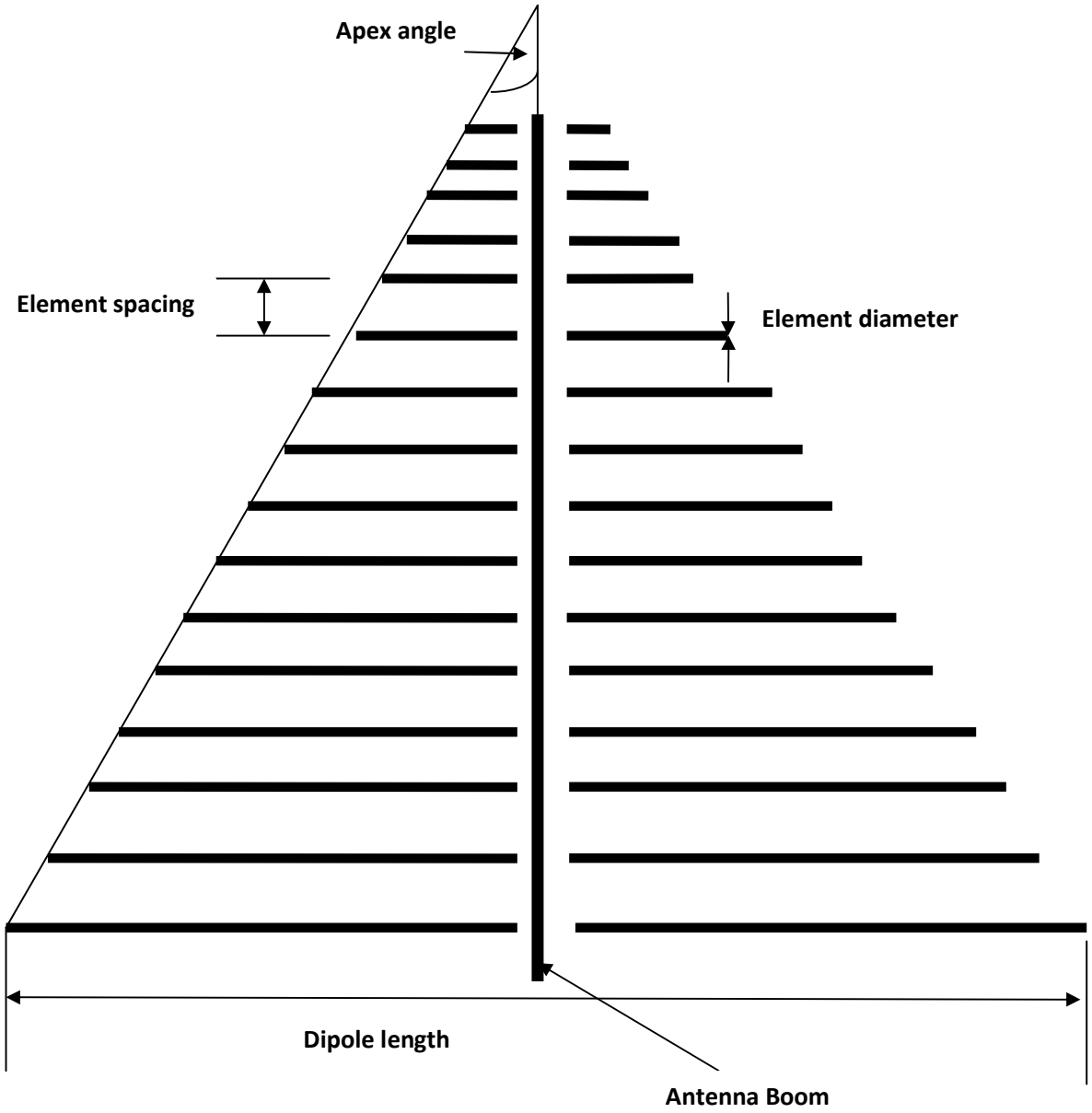

Fig. 3.9: Lateral view of LPDA antenna arrangement at design

The successive dipole elements are connected alternately to a feeder (balanced transmission line). In other words, the dipole elements are closely spaced and conversely connected so that the whole radiation is in the direction of the shorter elements whereas the broadside radiations

tend to annul each other. The radiation energy, at any given frequency travels along the transmission line. This movement continues until it reaches a section of the antenna structure where the electrical lengths of the elements and phase relationships generate the required radiation. Hence, as signal frequency is varied, the location of the resonant element is shifted gradually from one element to the other next to it. It is pertinent to note that dipole lengths of the shortest and longest elements determine the frequency bound of the signal. Thus, these lengths must be chosen to satisfy the bandwidth requirement for the upper and lower frequencies.

During signal propagation, whenever the transmitting signal meets the first few dipole elements in the array,(they are spaced quite close together in terms of the operating wavelength) the fields from these dipole elements will cancel one another out as the feeder sense is overturned between the dipole elements. However, as the signal advances down the array antenna, a point is reached where the feeder reversal and the distance that exists between the dipole elements gives a total phase shift of about 360 degrees. The section in which this happens is termed the active region of the antenna. For a practical antenna, the active region can consist of more dipole elements. However, the actual number of dipole elements involved is dependent upon the apex angle α and the design constant τ. Though dipole elements outside the active region obtain small direct power, the larger dipole elements are inductive and are resonant below the operational frequency. Also, those elements beyond the operational frequency are capacitive. Thus, the dipole elements immediately behind the active region act as reflectors while those in front act as directors.

The design/scaling factor used is 0.95 while the spacing factor is 0.17. The number of elements to be considered for each of the Log-Periodic Array (LPA) antennas is sixteen. This choice is made because the higher the design factor τ, the lower the apex angle, α and hence the higher the number of dipole elements in the antenna array, for the given antenna boom. The geometrical dimensions of the Log-Periodic Array antenna is derived with the basic standard LPDA design formulas provided by Carrel (1961) as taken from equations (3.107) to (3.126).

i. The Pass-Band of the Frequency Range

This was calculated as the difference between the highest frequency and the lowest frequency of antenna operation.

$$f_2 - f_1 = 2.690\text{GHz} - 1.350\text{GHz} = 1.340\ \text{GHz} \quad (3.107)$$

Where; f_2 is the highest frequency and, f_1 is the lowest frequency

ii. The operating Bandwidth, β

The operating bandwidth was calculated as the ratio of the highest antenna frequency and the lowest frequency of operation.

$$\beta = \frac{\text{Highest frequency},f_2}{\text{Lowest frequency},f_1} = \frac{2.690}{1.350} \approx 2.00 \quad (3.108)$$

iii. The Design Factors

The dimensions of dipole log-periodic array antenna have a special fixed relationship. It has an invariable ratio between each of the adjacent element.

$$\frac{\mathrm{d1}}{d2} = \frac{\mathrm{d2}}{d3} = \ldots = \frac{dn}{dn+1} = \frac{l1}{l2} = \frac{l2}{l3} = \ldots = \frac{ln}{ln+1} = \frac{1}{\tau} \quad (3.109)$$

Where;

d_n is equal to the distance of n-dipole from the vertex formed near the feed point in meters

l_n is the length of n-dipole.

Thus, the inverse of this ratio in equation (3.109) is the design factor $\boldsymbol{\tau}$. That is;

$$\tau = \frac{d_2}{d_1} = \frac{l_2}{l_1} < 1 \quad (3.110)$$

Where: $0.76 \leq \boldsymbol{\tau} \leq 1$

Design factor is used to resolve the spacing between two successive elements.

Thus, the design factor is chosen to be 0.95 in order to maximize the number of dipole elements required for the array design.

iv. The Optimum Spacing Factor σ,

The optimum spacing factor was calculated using equation (3.111).

$$\sigma = 0.258\,\boldsymbol{\tau} - 0.066 \quad (3.111)$$

$= 0.258\ (0.93) - 0.066 = 0.1739$

≈ 0.17

v. The apex angle, 2α

$$\text{Tan } \alpha = \frac{(1-\tau)}{4\sigma} = \frac{(1-0.93)}{4(0.17)} = \frac{0.07}{0.68} = 0.1029 \quad (3.112)$$

$\alpha = \tan^{-1} 0.1029 \approx 6^0$

Thus, the apex angle of the antenna is

$2\alpha = 2\,(6^0) = 12^0$

vi. The Bandwidth of the active region, β_{ar}

$$\beta_{ar} = 1.1 + 7.7\,(1-\tau)^2 \cot \alpha \quad (3.113)$$

$$\beta_{ar} = 1.1 + 7.7\,(1-0.93)^2 \cot 6^0$$

$$= 1.1 + 7.7\,(0.07)^2 (\tan 6^0)^{-1}$$

$$= 1.1 + 0.0377\,(9.5144)$$

$= 1.46$

vii. The structure (array) bandwidth, β_s

This is the product of the operating bandwidth, β and the bandwidth of the active region, β_{ar}. Thus,

$$\beta_s = \beta * \beta_{ar} \quad (3.114)$$

$\beta_s = 2.00(1.46) \quad = 2.92$

viii. The boom length, L

This is the distance between the longest and shortest dipoles.

$$L = [\frac{1}{4}(1 - (\frac{1}{\beta_s}))\cot\alpha]\,\lambda_{max} \quad (3.115)$$

Where;

λ_{max} = longest free-space wavelength

$$\lambda_{max} = \frac{984}{f1} = \frac{984}{1350} = 0.73$$

$$L = [\frac{1}{4}(1 - (\frac{1}{2.92}))\cot 6^0]\,0.73$$

$$L = \left[\frac{1}{4}(0.6575) * 9.5144\right] 0.73$$

= 1.56 ft

ix. The number of elements, N

$$N = 1 + \left\{\log \beta s / \log\left(\frac{1}{\tau}\right)\right\} \quad (3.116)$$

$$N = 1 + \left\{\log 2.92 / \log\left[\frac{1}{0.93}\right]\right\}$$

$$N = 1 + \left\{\frac{\log 2.92}{\log 1.0753}\right\}$$

N = 1 + 14.76 = 15.76 ≈ 16

The number of elements, N is rounded off to the nearest higher integer

x. The Longest Element Length, L_1 and Other elements

The relationship between frequency, velocity and wavelength is written as;

$$f = \frac{C}{\lambda} \quad (3.117)$$

Where;

f is frequency,

C is the velocity of light, and

λ is the wavelength

Lowest frequency,f $= 1350\text{MHz}$

Thus, wavelength is calculated as

$$\lambda = \frac{\text{C}}{\text{f}} = \frac{(3*10^{8})}{(13.50*10^{8})}$$

$$\lambda = 0.22\text{m}$$

The antenna length and its wavelength are directly related by;

$$l_{\text{n}} = \frac{\lambda}{2} \quad (3.118)$$

$$l_1 = \frac{\lambda}{2} = 0.11\ ;$$

$$\text{h}_1 = \frac{l_1}{2} = 0.055$$

From the relation;

$$l_{\text{n}+1} = \tau l_{\text{n}} \quad (3.119)$$

$$l_2 = \tau l_1 = 0.93\ (0.11) = 0.1023$$

$h_2 = 0.0512$

$l_3 = \tau l_2 = 0.93\ (0.1023)\ = 0.0951$

$\mathrm{h}_3 = \frac{l_3}{2} = 0.0476$

$l_4 = \tau l_3 = 0.93\ (0.0951)\ = 0.0884$

$\mathrm{h}_4 = \frac{l_4}{2} = 0.0442$

$l_5 = \tau l_4 = 0.93\ (0.0884)\ = 0.0822$

$\mathrm{h}_5 = \frac{l_5}{2} = 0.0411$

$l_6 = \tau l_5 = 0.93\ (0.0822)\ = 0.0765$

$\mathrm{h}_6 = \frac{l_6}{2} = 0.0382$

$l_7 = \tau l_6 = 0.93\ (0.0765)\ = 0.0712$

$\mathrm{h}_7 = = \frac{l_7}{2} = 0.0356$

$l_8 = \tau l_7 = 0.93\ (0.0712)\ = 0.0662$

$\mathrm{h}_8 = \frac{l_8}{2} = 0.0331$

$l_9 = \tau l_8 = 0.93\ (0.0662)\ = 0.0616$

$$h_9 = \frac{l_9}{2} = 0.0308$$

$$l_{10} = \tau l_9 = 0.93\ (0.0616) = 0.0573$$

$$h_{10} = \frac{l_{10}}{2} = 0.0286$$

$$l_{11} = \tau l_{10} = 0.93\ (0.0573) = 0.0533$$

$$h_{11} = \frac{l_{11}}{2} = 0.0265$$

$$l_{12} = \tau l_{11} = 0.93\ (0.0533) = 0.0496$$

$$h_{12} = \frac{l_{12}}{2} = 0.0248$$

$$l_{13} = \tau l_{12} = 0.93\ (0.0496) = 0.0461$$

$$h_{13} = \frac{l_{13}}{2} = 0.0231$$

$$l_{14} = \tau l_{13} = 0.93\ (0.0461) = 0.0429$$

$$h_{14} = \frac{l_{14}}{2} = 0.0215$$

$$l_{15} = \tau l_{14} = 0.93\ (0.0429) = 0.0399$$

$$h_{15} = \frac{l_{15}}{2} = 0.0200$$

$$l_{16} = \tau l_{15} = 0.93\ (0.0399) = 0.0371$$

$$h_{16} = \frac{l_{16}}{2} = 0.0186$$

xi. The terminating stub, Z_t

The terminating stub was calculated by dividing the maximum wavelength by 8.

$$Z_t = \frac{\lambda_{max}}{8} = \frac{0.22}{8} = 0.0275 \text{ m} \quad (3.120)$$

xii. Average characteristic impedance of longest dipole, Z_{ave}

Using element of radius, a = 3mm

Longest element to radius ratio, l /a = 36.66

$$Z_{ave} = 120 (\ln \frac{l}{a} - 2.25) \quad (3.121)$$

$$= 120 (\ln 36.66 - 2.25)$$

$$= 120 (3.602 - 2.25)$$

$$= 120 (1.3517) = 162.2\Omega$$

xiii. Mean spacing factor σ'

$$\sigma' = \frac{\sigma}{\sqrt{\tau}} \quad (3.122)$$

$$= \sigma / \sqrt{(0.93)} = \frac{0.17}{0.9644} = 0.1763$$

***xiv.* Feeder impedance, Z_0**

$$Z_0 = \frac{R_0^2}{(8\sigma' Z_a)} + R_0 \sqrt{\left[\left(\frac{R_0}{(8\sigma' Z_a)}\right)^2 + 1\right]} \quad (3.123)$$

$$= \frac{50^2}{8(0.1763)(162.2)} + 50\sqrt{\left[\left(\frac{50}{(8(0.1763)(162.2))}\right)^2 + 1\right]}$$

$$= \frac{2500}{228.77} + 50\sqrt{\left[\left(\frac{50}{228.77}\right)^2 + 1\right]}$$

$$= 10.9280 + 50\sqrt{[1.0478]}$$

$$= 10.9280 + 51.1811 = 62.11 \approx 62\Omega$$

xv. Center to center boom spacing, S

$$s = (\frac{\text{diam}}{2})X10^{\frac{z_0}{276}} \quad (3.124)$$

Where; diam is the boom diameter in mm

$$s = (\frac{10}{2})X10^{\frac{62}{276}}$$

$$s = 5X10^{0.217}$$

$$s = 5X1.6774$$

$$s = 8.39 \text{ mm}$$

xvi. Dipole element spacing d_{n-n+1}

$$d_{1-2} = \frac{1}{2}(l_1 - l_2)\cot\alpha \quad (3.125)$$

$$= \frac{1}{2}(0.11 - 0.1023)\cot 6^0$$

$$= \frac{1}{2}(0.0077)9.5144$$

$$= 0.0366$$

$d_{2-3} = \sigma 2l_2$

$= 0.17(2)(0.1023) = 0.03478$

$d_{3-4} = \sigma 2l_3$

$= 0.17(2)(0.0951) = 0.0323$

$d_{4-5} = \sigma 2l_4$

$= 0.17(2)(0.0884) = 0.0301$

$d_{5-6} = \sigma 2l_5$

$= 0.17(2)(0.0822) = 0.0280$

$d_{6-7} = \sigma 2l_6$

$= 0.17(2)(0.0765) = 0.0260$

$d_{7-8} = \sigma 2l_7$

$= 0.17(2)(0.0712) = 0.0242$

$d_{8-9} = \sigma 2l_8$

$= 0.17(2)(0.0662) = 0.0225$

$d_{9-10} = \sigma 2l_9$

$= 0.17(2)(0.0616) = 0.0206$

$d_{10-11} = \sigma 2l_{10}$

$= 0.17(2)(0.0573) = 0.0195$

$d_{11-12} = \sigma\, 2l_{11}$

$= 0.17(2)(0.0533) = 0.0181$

$d_{12-13} = \sigma\, 2l_{12}$

$= 0.17(2)(0.0496) = 0.0169$

$d_{13-14} = \sigma\, 2l_{13}$

$= 0.17(2)(0.0461) = 0.0157$

$d_{14-15} = \sigma\, 2l_{14}$

$= 0.17(2)(0.0429) = 0.0146$

$d_{15-16} = \sigma\, 2l_{15}$

$= 0.17(2)(0.0399) = 0.0136$

xvii. Distance between the dipole elements from the vertex, γ_n:

$$\gamma_n = h_n \cot \alpha \qquad (3.126)$$

Where;

γ_n is the distance from the antenna vertex to the nth dipole.

$$\gamma_1 = h_1 \cot \alpha = 0.055 \cot 6^0 = 0.055\ (9.5144) = 0.5233 \text{ m}$$

$$\gamma_2 = h_2 \cot 6^0 = 0.0512 \cot 6^0 = 0.0512\ (9.5144) = 0.4871\text{m}$$

$$\gamma_3 = h_3 \cot 6^0 = 0.0476 \cot 6^0 = 0.0476\,(9.5144) = 0.4529\text{m}$$

$$\gamma_4 = h_4 \cot 6^0 = 0.0442 \cot 6^0 = 0.0442\,(9.5144) = 0.4205\text{m}$$

$$\gamma_5 = h_5 \cot 6^0 = 0.0411 \cot 6^0 = 0.0411\,(9.5144) = 0.3910\text{m}$$

$$\gamma_6 = h_6 \cot 6^0 = 0.0382\cot 6^0 = 0.0382\,(9.5144) = 0.3635\text{m}$$

$$\gamma_7 = h_7 \cot 6^0 = 0.0356\cot 6^0 = 0.0356\,(9.5144) = 0.3387\text{m}$$

$$\gamma_8 = h_8 \cot 6^0 = 0.0331\cot 6^0 = 0.0331\,(9.5144) = 0.3149\text{m}$$

$$\gamma_9 = h_9 \cot 6^0 = 0.0308 \cot 6^0 = 0.0308\,(9.5144) = 0.2930\text{m}$$

$$\gamma_{10} = h_{10} \cot 6^0 = 0.0286 \cot 6^0 = 0.0286\,(9.5144) = 0.2721\text{m}$$

$$\gamma_{11} = h_7 \cot 6^0 = 0.0265\cot 6^0 = 0.0265(9.5144) = 0.2521\text{m}$$

$$\gamma_{12} = h_8 \cot 6^0 = 0.0248\cot 6^0 = 0.0248\,(9.5144) = 0.2360\text{m}$$

$$\gamma_{13} = h_9 \cot 6^0 = 0.0231\cot 6^0 = 0.0231\,(9.5144) = 0.2198\text{m}$$

$$\gamma_{14} = h_{10} \cot 6^0 = 0.0215 \cot 6^0 = 0.0215\,(9.5144) = 0.2046\text{m}$$

$$\gamma_{15} = h_7 \cot 6^0 = 0.0200 \cot 6^0 = 0.0200\,(9.5144) = 0.1903\text{m}$$

$$\gamma_{16} = h_8 \cot 6^0 = 0.0186 \cot 6^0 = 0.0186\,(9.5144) = 0.1770\text{m}$$

Figure 3.10 represents the schematic model of the designed 16 element MLPDA antennas in parallel arrangement.

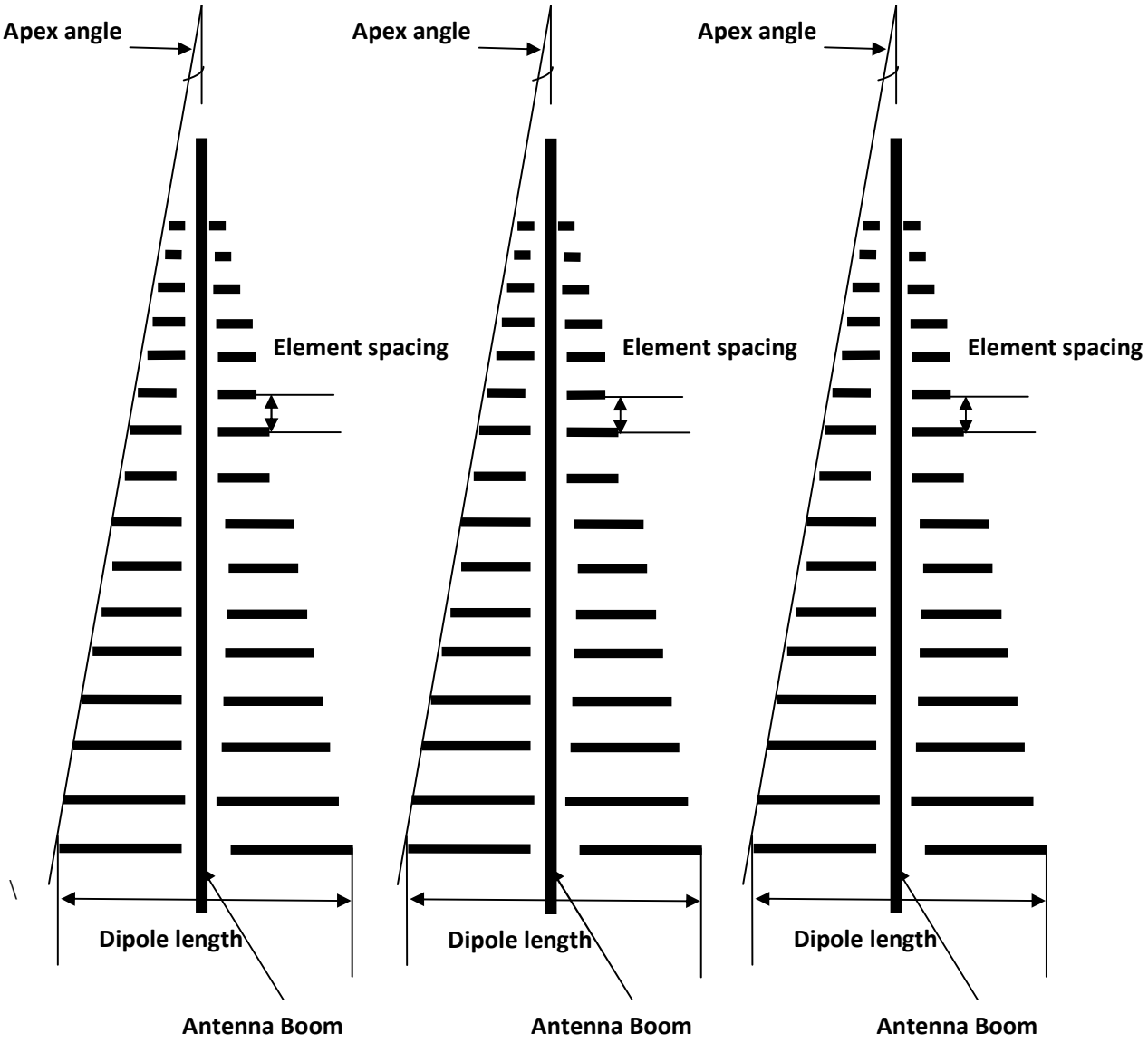

Fig. 3.10: A schematic diagram of MLPDA antennas in linear array

This MLPA antenna was designed to transfer signals within VHF and UHF bands, and surveillance systems operate effectively within these frequency bands.

CHAPTER FOUR

RESULTS AND DISCUSSION

4.1 Results

The sets of results presented in this chapter were as enlisted;

1. Radiation patterns for the array factors of Single Log-Periodic Array antennas, ($AF_{SLPA} = 1 + \sum_{n=1}^{N-1}\prod_{i=1}^{n} e^{j\tau^{i-1}\varphi}$), array antennas of equal dimensions, ($AF_{ED} = \sum_{n=1}^{M} e^{(n-1)j\varphi}$) and Multiple Log-Periodic Array antennas, ($AF_{MLPA} = \sum_{n=1}^{M} e^{(n-1)j\varphi} + \sum_{n=1}^{M} e^{(n-1)j\varphi}\sum_{n=1}^{N-1}\prod_{i=1}^{n} e^{j\tau^{i-1}\varphi}$).
2. Electromagnetic (EM) fields generated by the first radiating element in MLPA antennas.
3. Characterized parameters of the MLPA antennas.
   i. The Cartesian and polar plots of the Electric/Magnetic Fields of the MLPA antennas
   ii. Average Poynting Vector of MLPA antennas
   iii. Radiated Power of MLPA antennas
   iv. The Directive Gain of MLPA antennas
   v. Radiation Intensity of MLPA antennas
4. The tabular results obtained from the design of MLPA antennas of a sample band width

These results were simulated using MatLab R2010a object oriented tools. The results for the SLPA and MLPA antennas and their parameters were plotted at an intrinsic impedance of

377Ω; a far field distance of 5km (distance between the antenna source point to the far field point); design factor τ of 0.95, phase angle φ of $45^0$and antenna wave number of 1. The SLPA antenna results were used to compare that for the MLPA antennas.

4.1.1 Array Antenna Patterns

This section discussed the array antenna patterns for antenna arrays of equal dimensions, Single Log-Periodic Array antennas and Multiple Log-Periodic Dipole Array antennas. From the results obtained, the directivity of the array patterns increased from that of the Arrays of Equal Dimension to SLPA antennas and then to MLPA antennas.

i. Array Pattern for Array Antennas of Equal Dimensions

Figure 4.1 shows the results of the array pattern for four distinct types of Equal Amplitude Array antennas with 4, 7, 10 and 20 radiating elements respectively.

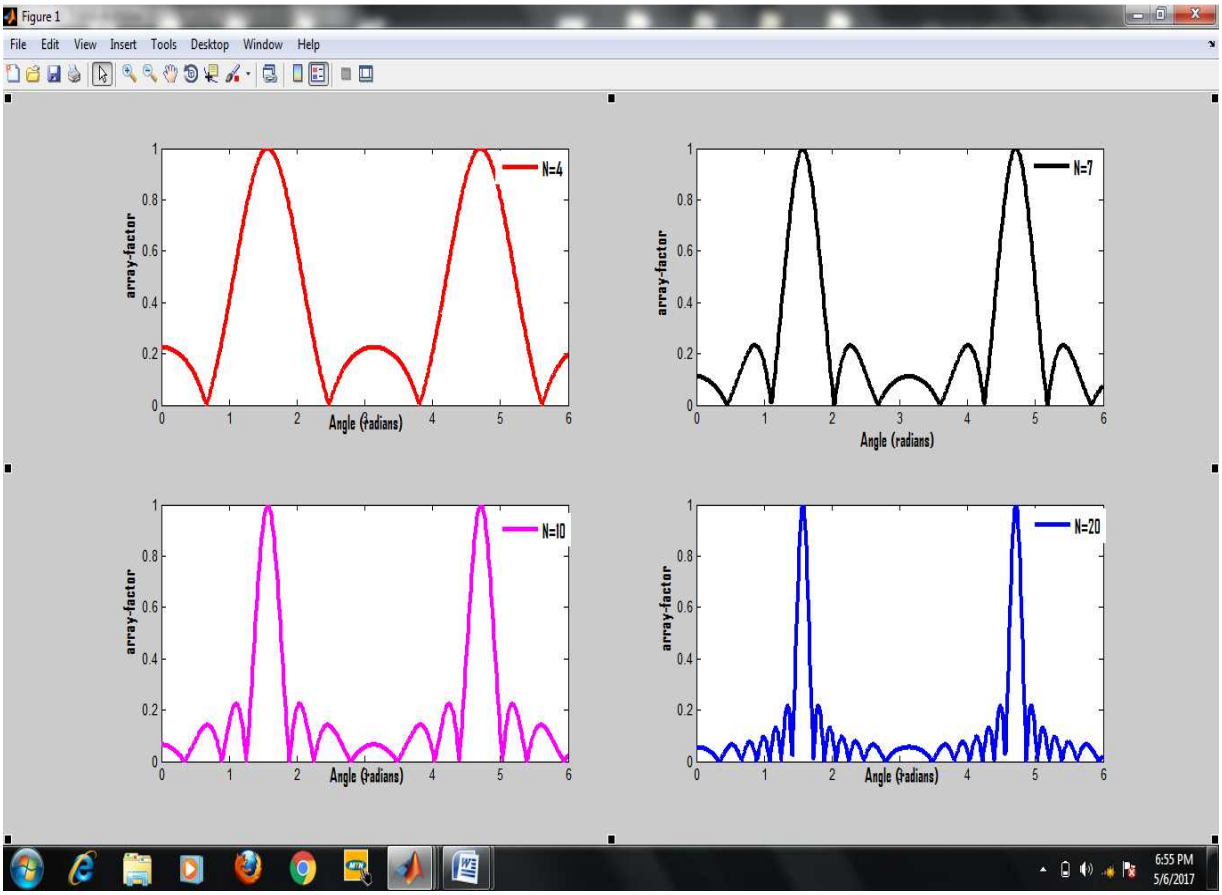

Fig.4.1: Array Antenna Patterns for four distinct sets of Equal Amplitude Array antennas of 4, 7, 10 and 20 dipoles respectively (plotted separately)

These equal dimension radiating elements are tantamount to (obtained from) the sum of the first (longest) dipole elements in each of the multiple similar LPA antennas in linear array. The radiating elements are similar in the sense that the elements had equal dimensions – the widths, lengths and spacing of the elements were equal, and like characteristics. In other words, the antenna elements in the array are uniform. For close observation, the array patterns for the same four distinct sets of equal amplitude array antennas were plotted together in Figure 4.2.

Figure 4.2 shows the normalized Array Factor patterns for four different sets of Equal Amplitude Array antennas when the numbers of the radiating elements in the four arrays were 4, 7, 10 and 20 dipoles respectively.

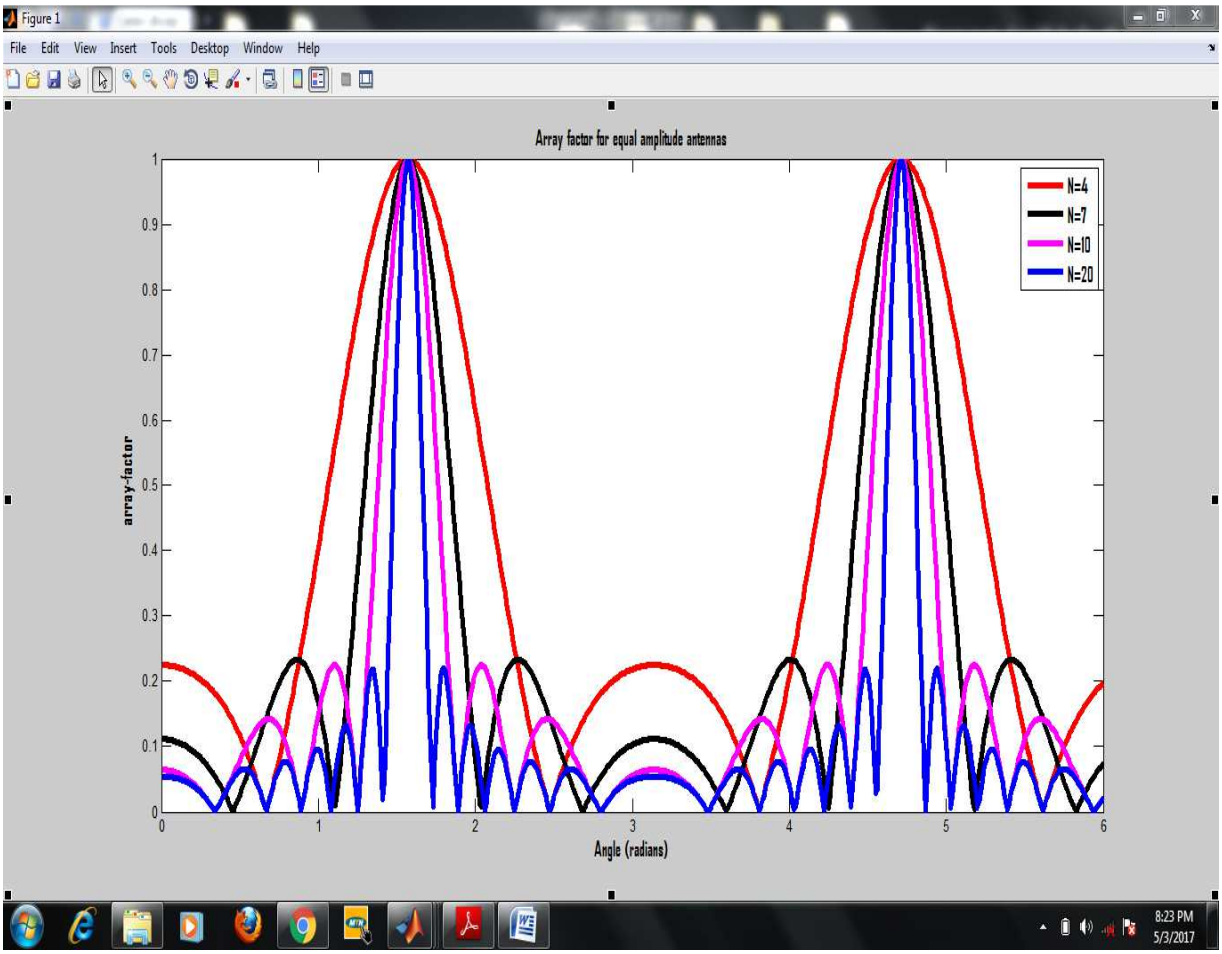

Fig.4.2: Array Patterns for four sets of Equal Amplitude Array Antennas of 4, 7, 10 and 20 dipoles (plotted together)

In Figure 4.2, the patterns of the Array Factor for four distinct sets of equal amplitude array antennas for different number of equal amplitude dipole array antennas elements (that is: for 4, 7, 10, and 20 dipoles) were plotted together. The array patterns showed systematic increase

in the number of side lobes as the number of the dipole element increased. Also, there was subsequent increase in the directivity of the main lobe in that order.

When the total radiating elements in the array was 4, the side lobes generated was minimal but least directive. Also, when the total radiating elements in the array was 20, the highest numbers of side lobes were generated, and the main lobe generated was most directive. Thus, array pattern directivity has a direct relationship with the number of dipole radiating elements.

From the diagrams, it became obvious that: as the number of radiating elements in the array increased, the angle within which the signal radiation occurred decreased. Consequently, the main lobe became more directive whereas the number of side lobes produced also increased, as the dipole elements increased along the arrays. The array pattern was most directive at the highest number of equal amplitude array antennas elements (that is: for 20 dipoles) but has minimal directivity at the least number of dipole elements (that is: for 4 dipoles).

ii. Array Patterns for SLPA Antennas

Figure 4.3 represents the Array Factor patterns for four (4) different Single Log-Periodic Array antennas. As the case for the array antennas of equal dimension, the radiating patterns for different kinds of arrays of LPA antennas are represented. These four distinct LPA antennas contain 4, 7, 10, and 20 radiating elements respectively.

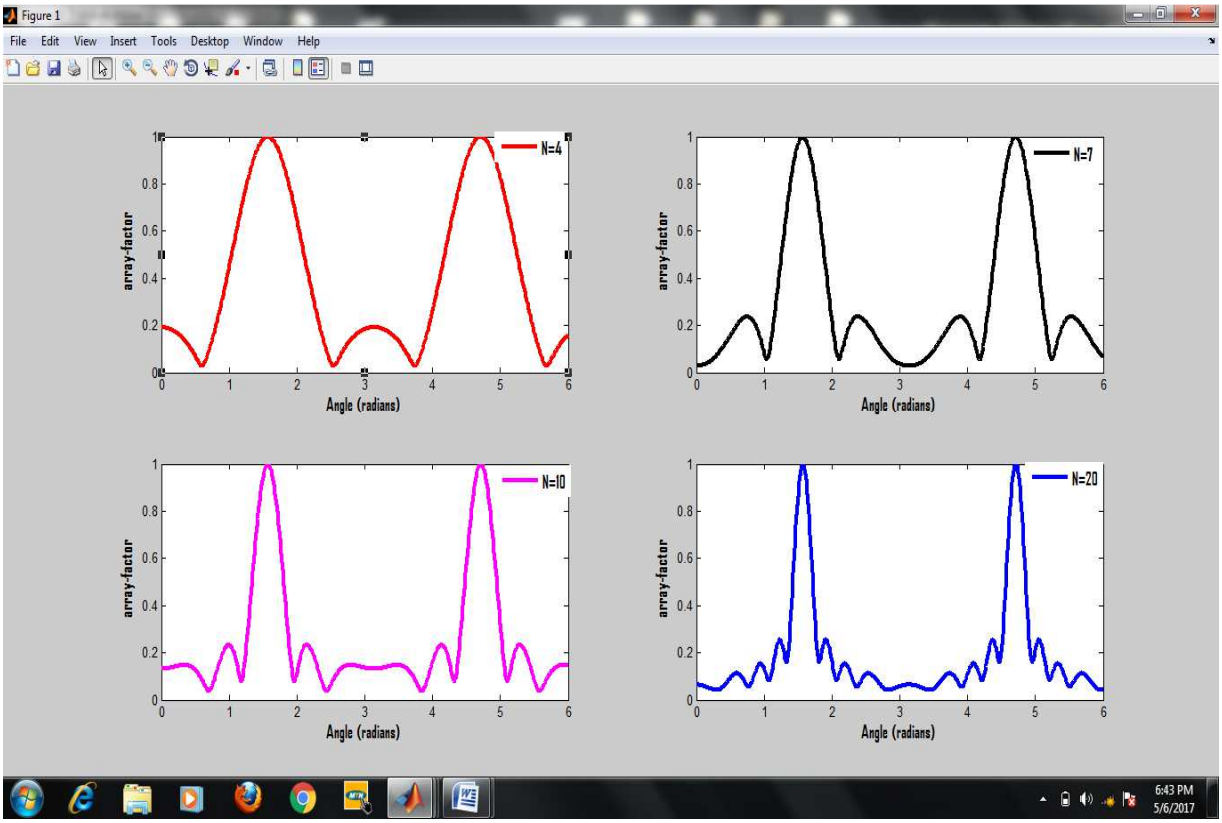

Fig. 4.3: Array Patterns of SLPA Antennas for 4, 7, 10 and 20 dipoles (plotted separately)

Figure 4.3 is the array patterns for different sets of Single Log Periodic Array antennas for 4, 7, 10 and 20 radiating elements plotted separately. The diagram showed that the number of radiating elements, the angle of signal radiation, the main lobe and the side lobes of the antennas have direct relationship. The generated array patterns were similar to those produced from the sets of Equal Amplitude Dipole Array antennas. The exception was that the patterns for the Log Periodic Dipole Array antennas were sharper and more directive. For clarity sake, the array patterns for the four different SLPA antennas are plotted together as shown in Figure 4.4.

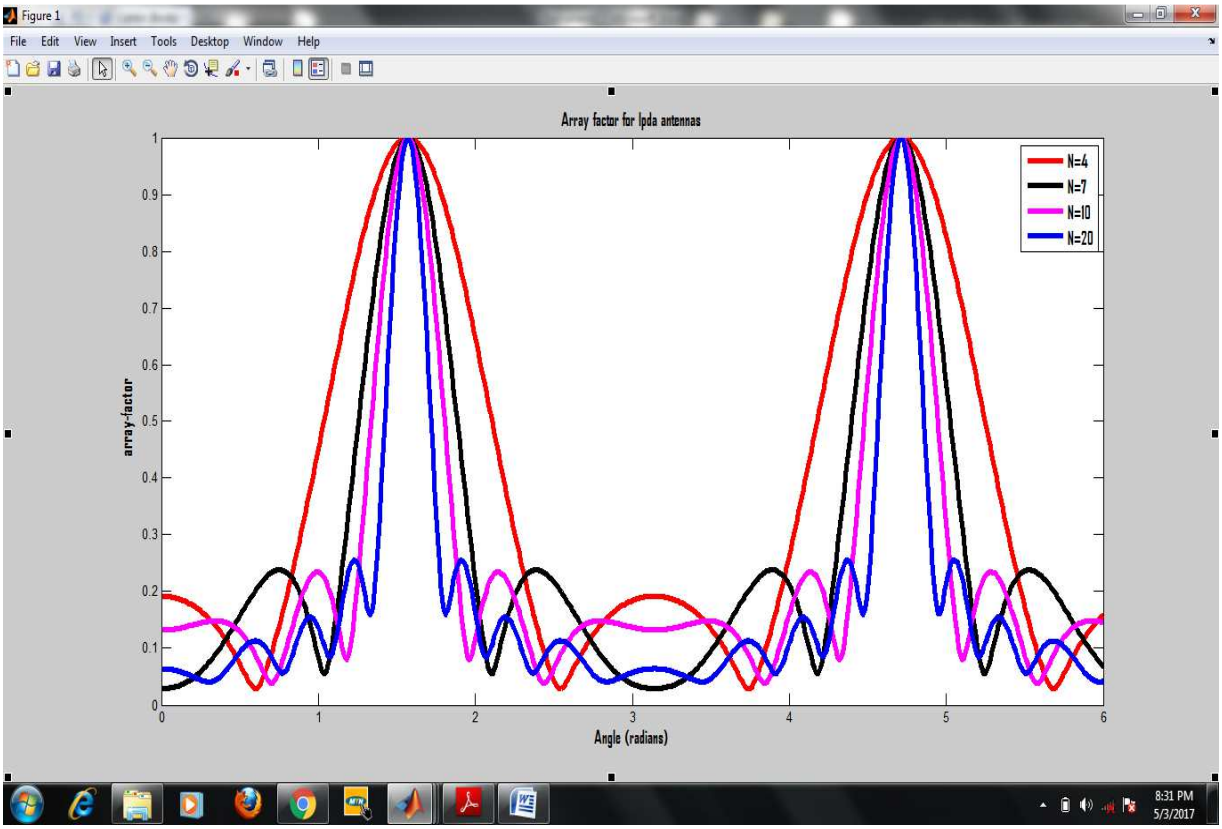

Fig.4.4: Array Patterns for four distinct SLPA antennas of 4, 7, 10 and 20 dipoles respectively (plotted together)

Figure 4.4 is the Cartesian plots of the array patterns for four sets of Single Log Periodic Dipole Array antennas of 4, 7, 10 and 20 dipole elements respectively. As it was the case of Equal Amplitude Array antennas, the array patterns indicated methodical increase in directivity of the main lobe and the number of side lobes generated, when the number of the dipole elements in the array increased. When the number of radiating elements in the array was 4, the pattern produced the least side lobes which were least directive. As the total radiating elements in the array was gradually increased from 7, 10, and then to 20, the array directivity and numbers of side lobes generated increased drastically. The maximum numbers

of side lobes were generated when the radiating elements were 20 in numbers, and thus formed the most directive main lobe.

iii. Array Patterns for MLPA Antennas

Figure 4.5 is the Array Factor patterns for Multiple Log-Periodic Array Antennas.

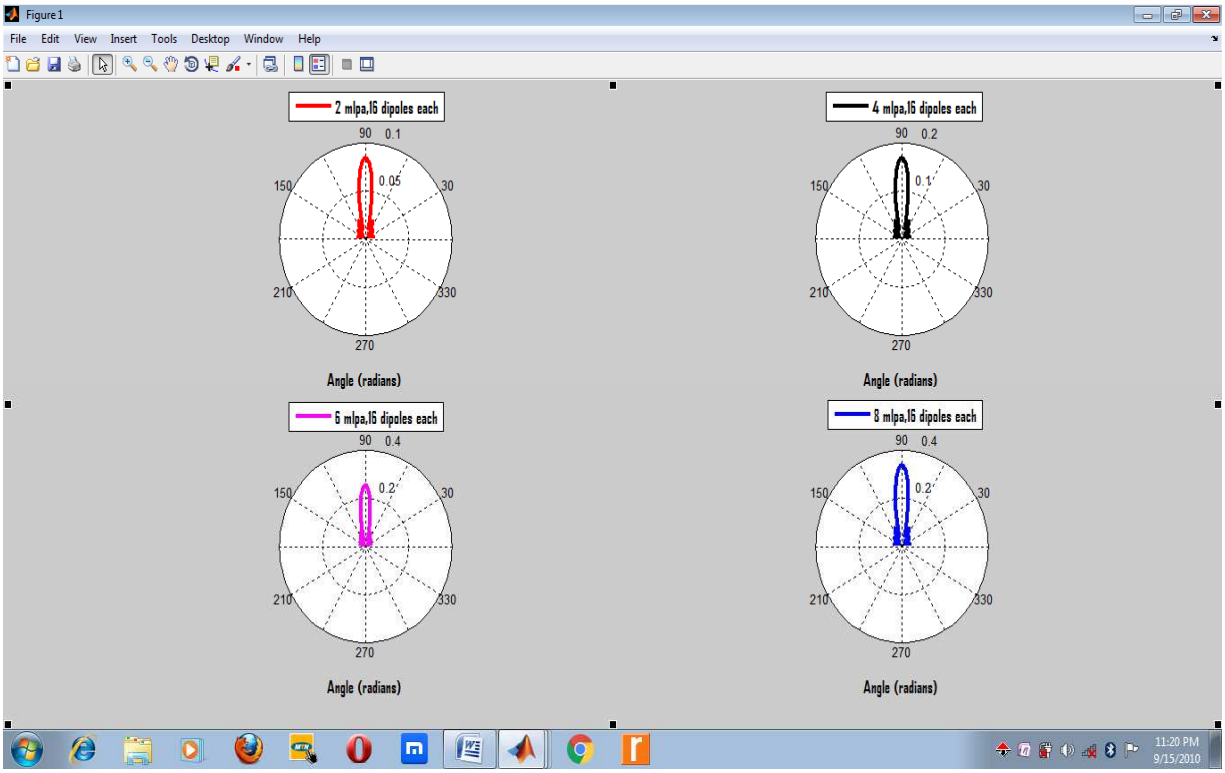

Fig.4.5: Array Patterns of 2, 4, 6. 8 sets of respective MLPA Antennas of 16 dipoles each (plotted separately)

For the MLPA antennas, the polar plots of the separated Array-Factors patterns for 2, 4, 6, and 8 stacked MLPA antennas (of 16 dipole elements each); when the design factor τ equals 0.95, are shown in figure 4.6 correspondingly. In these patterns, the plots are made for similar LPA antennas of 16 dipole elements each. However, there are 2 multiple (that is: 2 LPA by 16 dipoles each), 4 multiple (that is: 4 LPA by 16 dipoles each), 6 multiple (that is: 6 LPA by 16

dipoles each), and 8 multiple(that is: 6 LPA by 16 dipoles each) respectively in the sets of MLPA antennas described. These are indicated at the legend. The antennas patterns showed gradual variations on the directivity and radiated power/intensity. As the number of LPA antennas in the MLPA antennas increased, the directivity of the main lobe also increased in that order.

Alternatively, the polar plots for the array antenna patterns of 2, 4, 6, and 8 sets of MLPA antennas of 16 dipole elements each are combined in figure 4.6 accordingly.

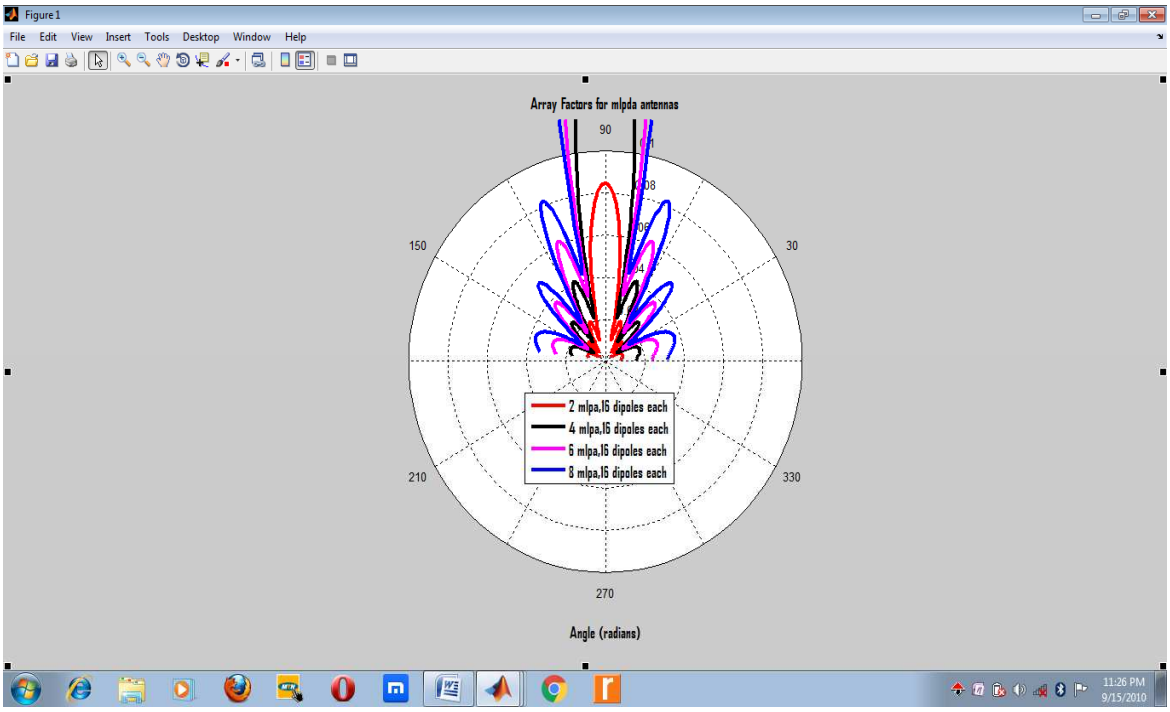

Fig. 4.6: Array Patterns of 2, 4, 6. 8 sets of MLPA antennas of 16 dipoles each (plotted together)

Figure 4.6 represents the combined polar plots for the array factor patterns of 2, 4, 6, and 8 sets of MLPA antennas of 16 dipoles each, in that order. The array patterns generated were similar to those of the SLPA antennas. However, there were systematic increment in the magnitude of both the main and the side lobes when the number of set of LPA antennas increased from 2, 4, 6 and then to 8. The highest array pattern magnitude is obtained at 8 MLPA antennas, followed by 6 MLPA, and then by 4 MLPA antennas. 2 MLPA antennas had the lowest array pattern magnitude. Thus, the array patterns for the MLPA antennas are of greater magnitude compared to those of the SLPA antennas. The more the number of the LPA in the array antenna set, the more the magnitude of the generated lobes and vice versa.

4.1.2 Electromagnetic (EM) Fields Generated by the First Radiating Element in MLPA Antennas

Figure 4.7 is the Electric and Magnetic fields generated by the First Radiating Element in MLPDA Antenna (a dipole).

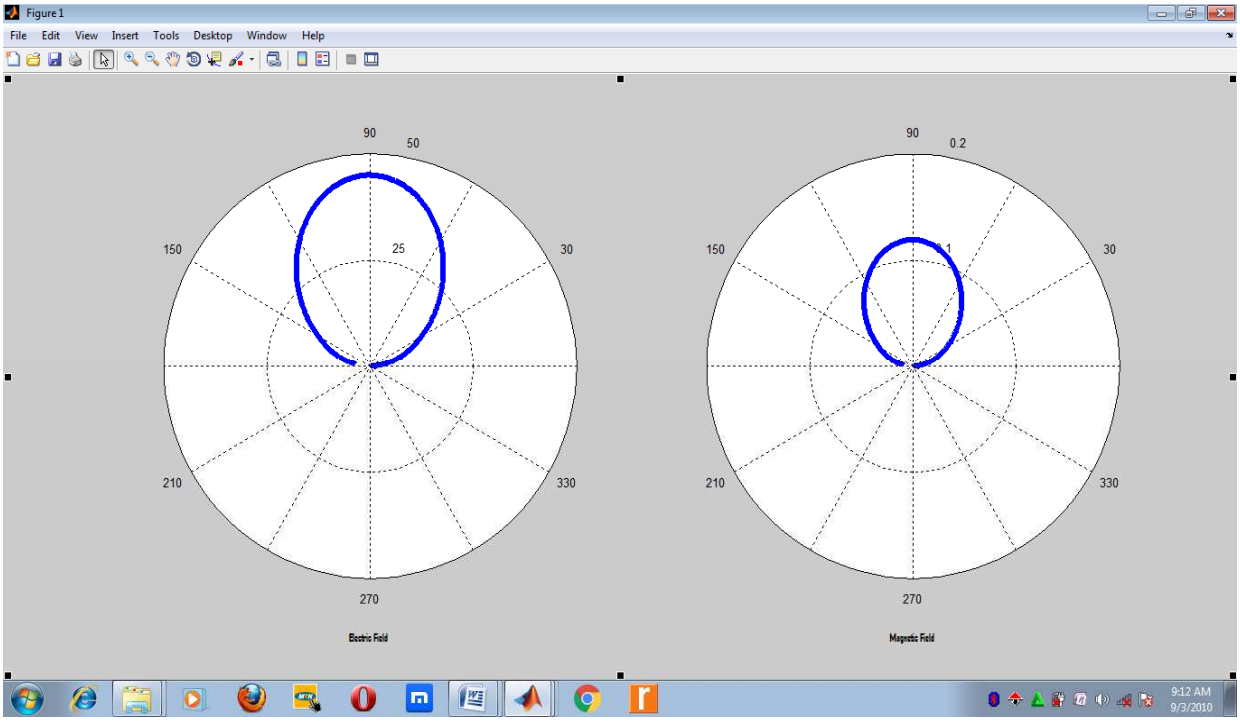

Fig 4.7: Electric and Magnetic fields generated by the First Radiating Element in MLPA antennas.

The normalized Electric and Magnetic fields for the first active element in MLPA antennas are shown in Figure 4.7. The antenna patterns for both fields were not very directive and as such could not propagate very far from the point of signal radiation. As observed from the antenna pattern, the Electric field was 45.24 Newtons/coulomb while the Magnetic Field was 0.12 Tesla. This is the typical behaviour for dipole antennas. The dipole radiating elements

are particularly essential for radio transmitting and receiving applications but their wavelengths are too long for very low frequencies which limited the antenna application. This type of antenna is not fit for long distance and Line – Of – Sight (LOS) communication as the lobe is not particularly directive.

4.1.3 Results from the Characterization of MLPA Antenna Parameters

This section analyzed the patterns for the MLPA antennas which include the Electric and Magnetic fields, Average Poynting Vector, Radiated Power, Directive Gain, and Radiation Intensity of Multiple Log Periodic Array antennas in contrast with that of Single Log Periodic Array Antennas. The outcome of the patterns indicated that; while the electromagnetic fields generated by the log Periodic Array antennas were very directive, the directivity of the fields generated from the MLPA antennas were not only directive but of greater magnitude in comparison. These are as shown in figures 4.7 and 4.8 respectively.

i. Electric and Magnetic Fields of MLPA Antennas

Figure 4.8 shows the polar plots of Electric and Magnetic fields of the Single Log Periodic Array antenna discussed in chapter two of this work.

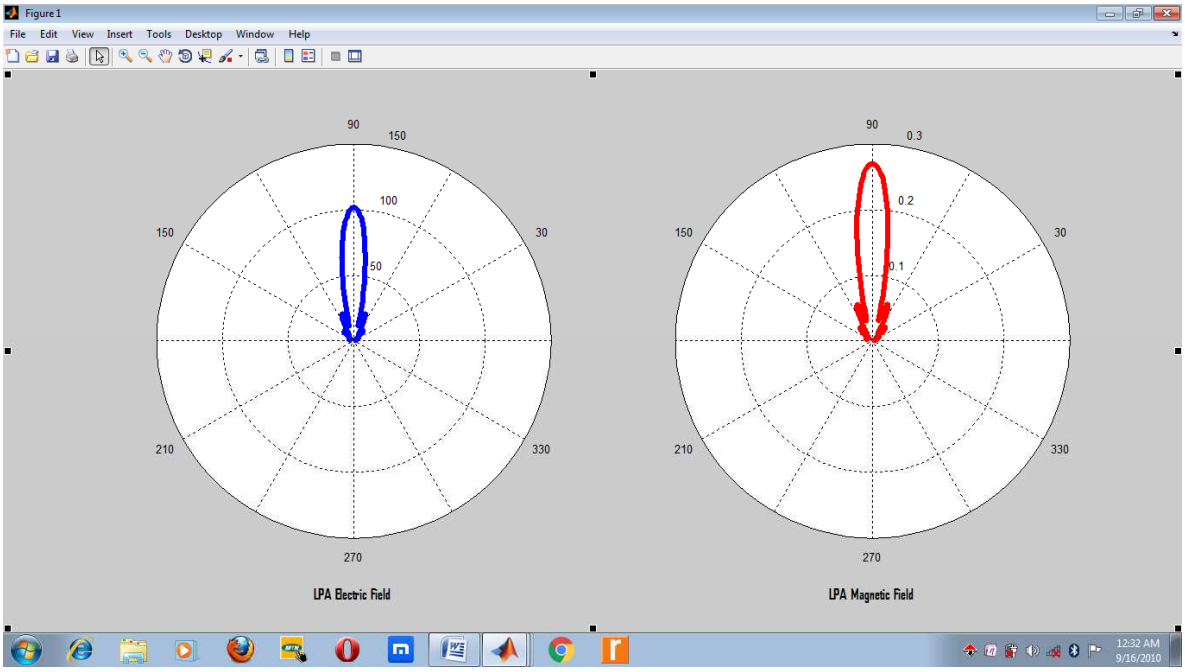

Fig.4.8: Electric and Magnetic fields of SLPA antennas of 16 dipoles respectively

The polar plots of Electric and Magnetic fields above represent the patterns for single Log Periodic Array antennas. Both field patterns are similar in shape except that the Electric field is of higher magnitude. The magnetic field as shown in equation (2.61) was obtained by dividing the electric field of equation (2.60) by the intrinsic impedance, 120π.

Hence, the radiated Electric and Magnetic fields were generated from the simulation of the log periodic array antennas of equations (2.60) and (2.61) respectively. Care was taken in selecting the angle within which the fields were radiated in order to ensure that the creation of recurring lobes was avoided. Thus, the adverse effect of subtracting from the total radiated power, as well as radiation effects on the operators behind the transmitting system was curtailed. From the antenna patterns produced, the Electric field was 98.02Newtons/coulomb while the Magnetic Field was 0.26Tesla. The produced lobes were directional with minimal

sidelobes, thus focusing the generated lobes in the direction of concern. The generated patterns of the electromagnetic fields were very directive compared to that produced from the dipole antenna of figure 4.1. This outcome is feasible as array antennas possess higher gain than single radiating element.

Figure 4.9 shows the polar plot of the Electric Field and the corresponding Magnetic Field of the Multiple Log Periodic Dipole Array Antennas of equations 3.86 and 3.87 respectively.

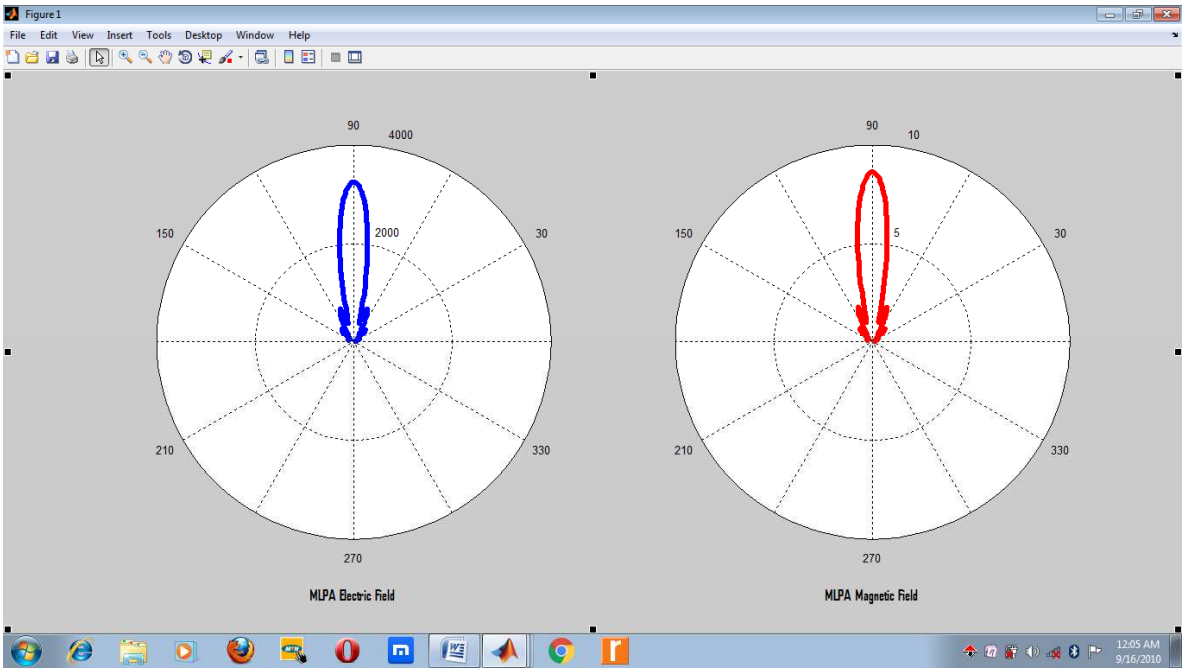

Fig.4.9: Electric and Magnetic fields of Multiple (3) Log Periodic Array Antennas of 16 dipoles respectively

Both field patterns in Figure 4.9 are similar in shape except that the magnitude of the Electric field is higher. The magnetic field was obtained as a product of the electric field of equation (3.77) and the inverse of the intrinsic impedance, 120π. Hence, the antenna patterns generated the normalized Electric field as 3,204 Newtons/coulomb while the normalized

Magnetic Field was 8.5Tesla. These values are quite appreciable and large. Compared to the magnitude and directivity of the electric and magnetic fields of single log periodic dipole array antenna, the Multiple Log Periodic Dipole Array antennas are better. This attribute attested to its suitability for application in wide area surveillance systems.

ii. Average Poynting Vector of Multiple Log Periodic Array Antennas

Figures 4.10 and 4.11 in comparison described the Average Poynting Vectors for both SLPA and MLPA antennas.

Figure 4.10 indicates the polar plot of Average Poynting Vector of the single Log Periodic Array antennas as discussed in chapter three.

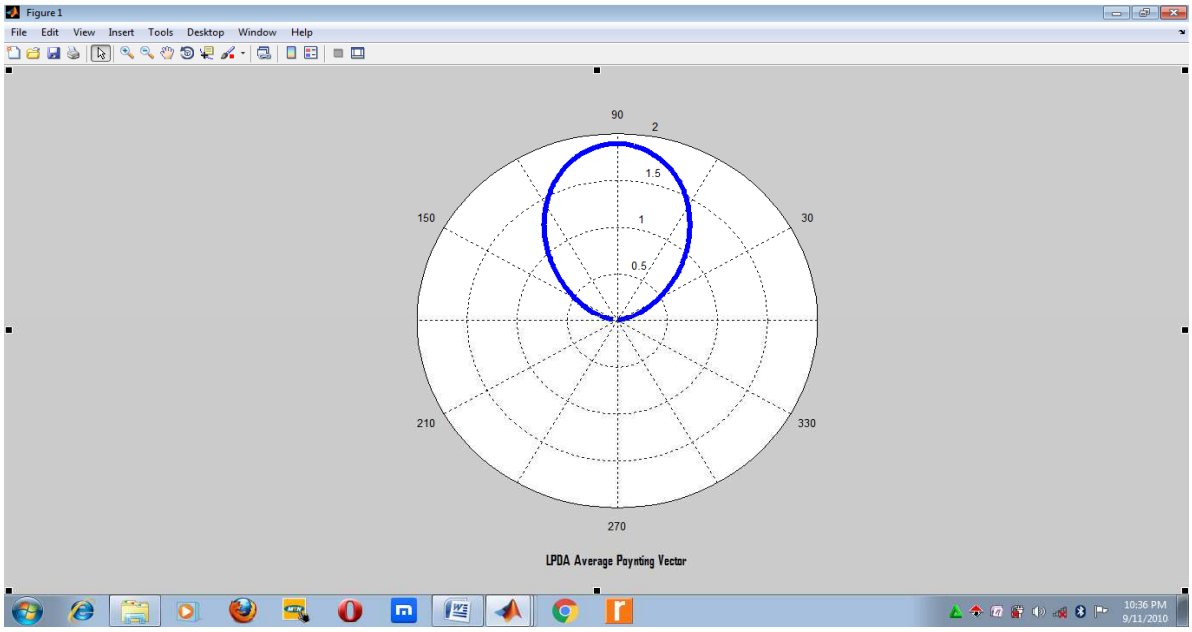

Fig.4.10: An Average Poynting Vector of SLPA Antennas of 16 dipoles

The Average Poynting Vector of the SLPA antennas obtained from the average value of the vectorial product (of the real values) of the Electric and Magnetic fields of the LPA antennas, as represented in equation (3.62).

From the antenna pattern generated, the value of the Average Poynting Vector of the LPA antennas was equivalent to 1.90 watt per square metre as read from the antenna pattern. The antenna in view had sixteen (16) active elements. Hence, the implication of this is that the power density of 1.90watt is focused within the preferred direction of interest.

Figure 4.11 shows the polar plot of Average Poynting Vector of the MLPA antennas as discussed in chapter three.

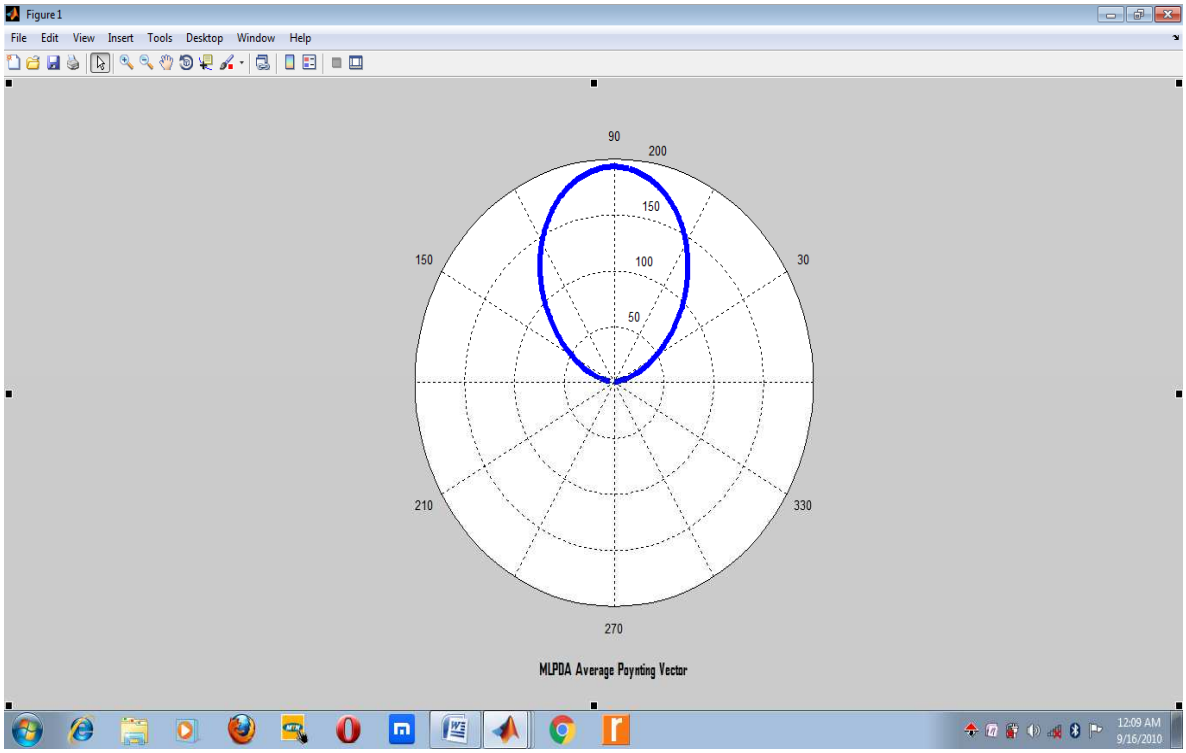

Fig.4.11: An Average Poynting Vector of Multiple Log Periodic Array Antennas of 16 dipoles

The Average Poynting Vector of the Multiple Log Periodic Dipole Array antennas was also obtained from the average value of the vectorial product (of the real values) of the Electric and Magnetic fields of the multiple log periodic dipole array antennas shown in equation (3.86).

The value of the Average Poynting Vector of MLPA antennas was equivalent to 193.75Watts per square metre as also read from the antenna pattern. The set of the MLPA antennas in view had sixteen (16) active elements per LPA antennas, and were three set in the array. This also implied that the power density of 193.75Watts was contained within the preferred direction.

iii. Radiated Power of MLPA Antennas

This section illustrated the Radiated power for Multiple Log Periodic Array antennas in contrast with that of Single Log Periodic Array antennas.

Figure 4.12 shows the polar plot of Radiated Power of the single Log Periodic Dipole Array antennas.

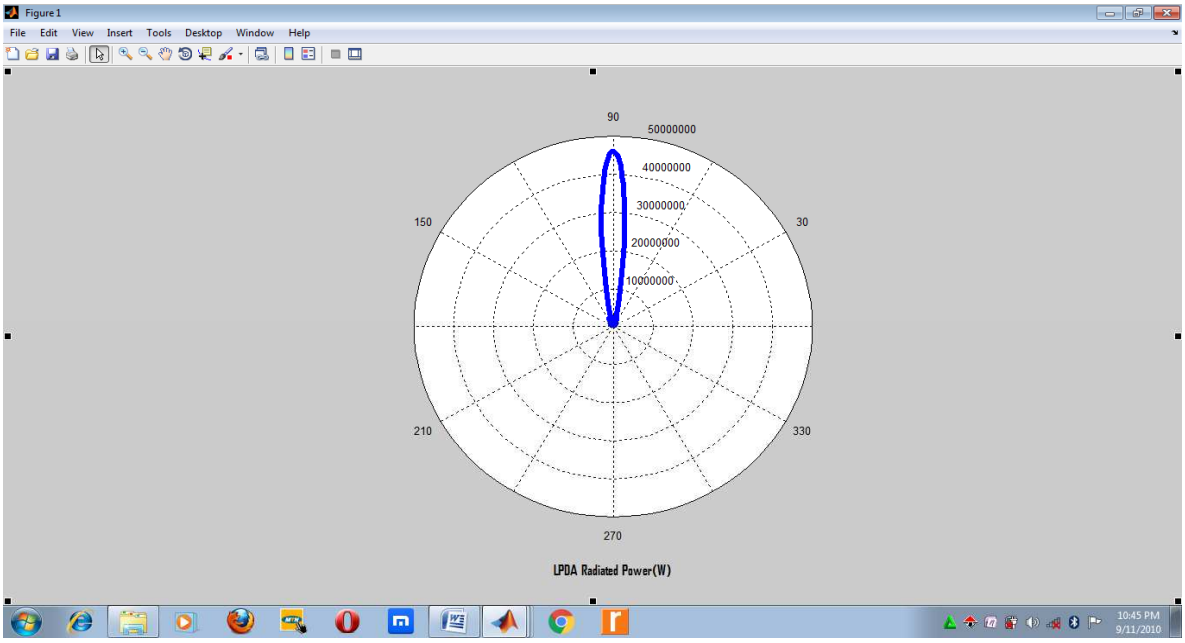

Fig.4.12: Radiated Power of Single Log Periodic Array antennas of 16 dipoles

The radiated power of SLPA antennas of equation (3.77) is plotted in figure 4.12. The average value of power radiated by the SLPA antennas was about 462W and this is equivalent to 26.65dB or 56.65dBm. The radiated power was almost directed towards the main lobe of the array with very tiny or minimal sidelobes. Thus, the bulk of the power was channeled towards the desired direction with little amount of power lost to the sidelobes.

Figure 4.13 illustrated the polar plot of Radiated Power of the MLPA antennas.

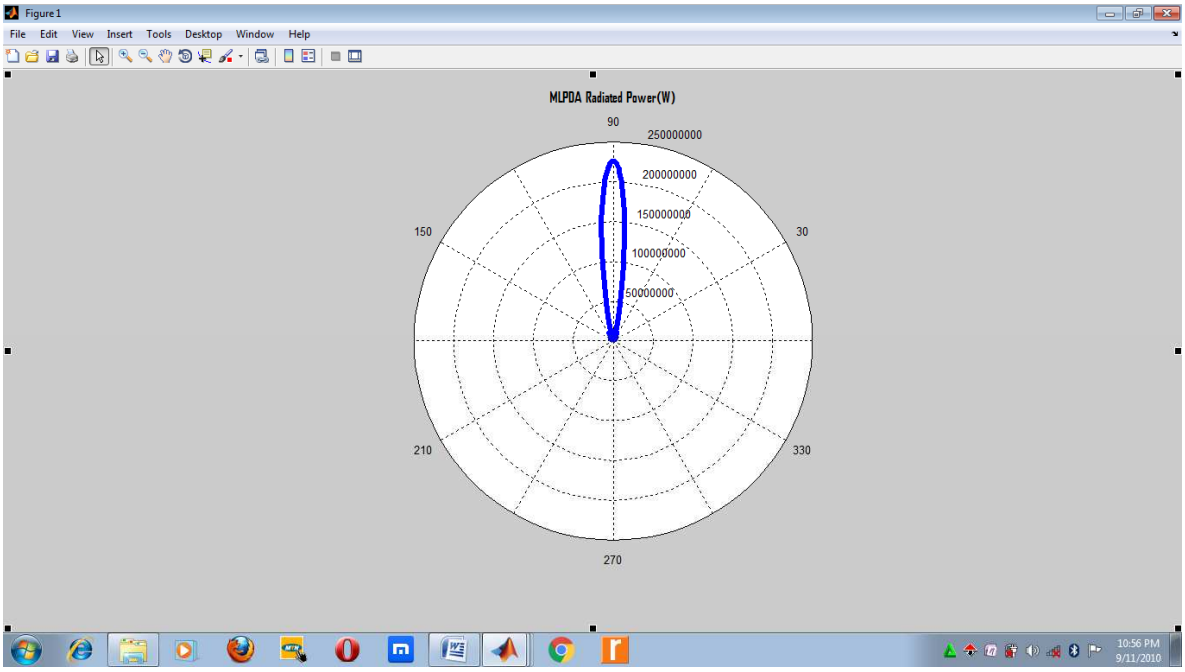

Fig.4.13: Radiated Power of Multiple (3) Log Periodic Dipole Array antennas of 16 dipoles

Figure 4.13 signifies the polar plot of radiated power of Multiple Log Periodic Dipole Array antennas of equation (3.98). The value of the power generated from the array antenna pattern was equivalent to 22,500W which corresponds to 43.52 dB or 73.52dBm. This is quite a huge number as the antenna could have application in most of communication systems due to its stability in radiating high capacity of power. Most of the radiated power of the Multiple (3) Log Periodic Dipole Array antennas is channeled to the main lobe of the array. As a result, very little amount of power was s lost to the sidelobes.

Figure 4.14 compared the powers radiated by the LPA antennas and Multiple (3) LPA antennas of sixteen (16) dipoles each.

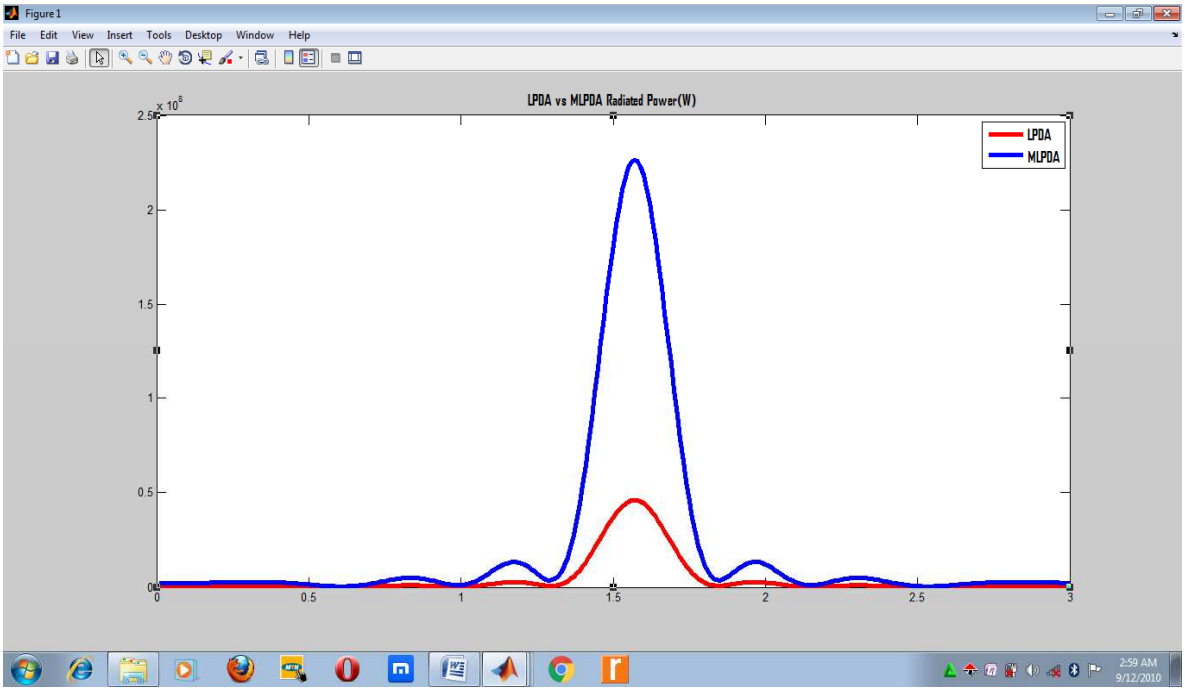

Fig.4.14: Radiated Power of Single LPA Versus Multiple (3) LPA Antennas of 16 dipoles

From the figure, it could be interpreted that the power radiated by the Multiple (3) LPA antennas had a very high magnitude compared to that of the single LPA antennas. While the MLPA antennas pattern has 43.52dB, the LPA antennas were having about 26.65dB of power. Hence, the power radiated by the MLPA antennas has a wide coverage area and could also travel far region compared to that of the SLPA antennas.

iv. Directive Gain of MLPA Antennas

Owing to ohmic losses on the antenna surface, a part of the power supplied to the antenna terminals is lost in heating of the antenna. Thus, the full power supplied to the antenna is then not radiated. The plot of the directive gain pattern of figure 4.15 was obtained from the MatLab program written on the product of the LPA directivity of the antenna and the square

of the sine of the angle of radiation, Θ. Alternatively, directive gain is obtained from the ratio of antenna radiation intensity to that of a hypothetical isotropic radiator that radiates the same power.

Figure 4.15 illustrated the polar plot for the Directive Gain of SLPA antennas.

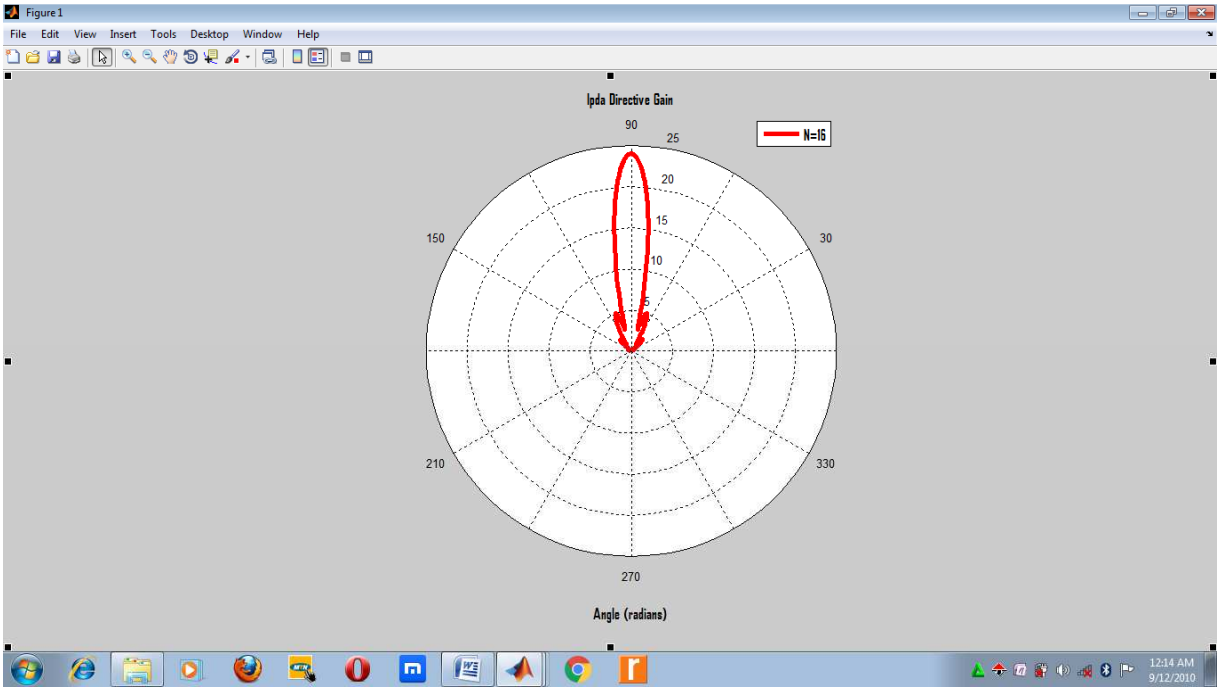

Fig.4.15: Directive Gain for Single Log Periodic Array Antennas

Figure 4.15 described the Directive gain of the Single Log Periodic Dipole Array antennas as the signal is radiated within the angle of 2π. The value of the Directive gain generated from the LPA antennas patten was 13.8dB or 43.80dBm (24W). Hence, this parameter described how well the transmitting antenna convertes input power into radio waves headed in a specified direction. However, when the antenna is in a receiving mode, this value described how well the antenna converted radio waves arriving from a specified direction into electrical

power. The directive gain of the SLPA antennas discussed in Figure 4.15 is moderate and protruded compared to that of a hypothetical isotropic radiator.

Figure 4.16 illustrated the Directive gain of the MLPA antennas.

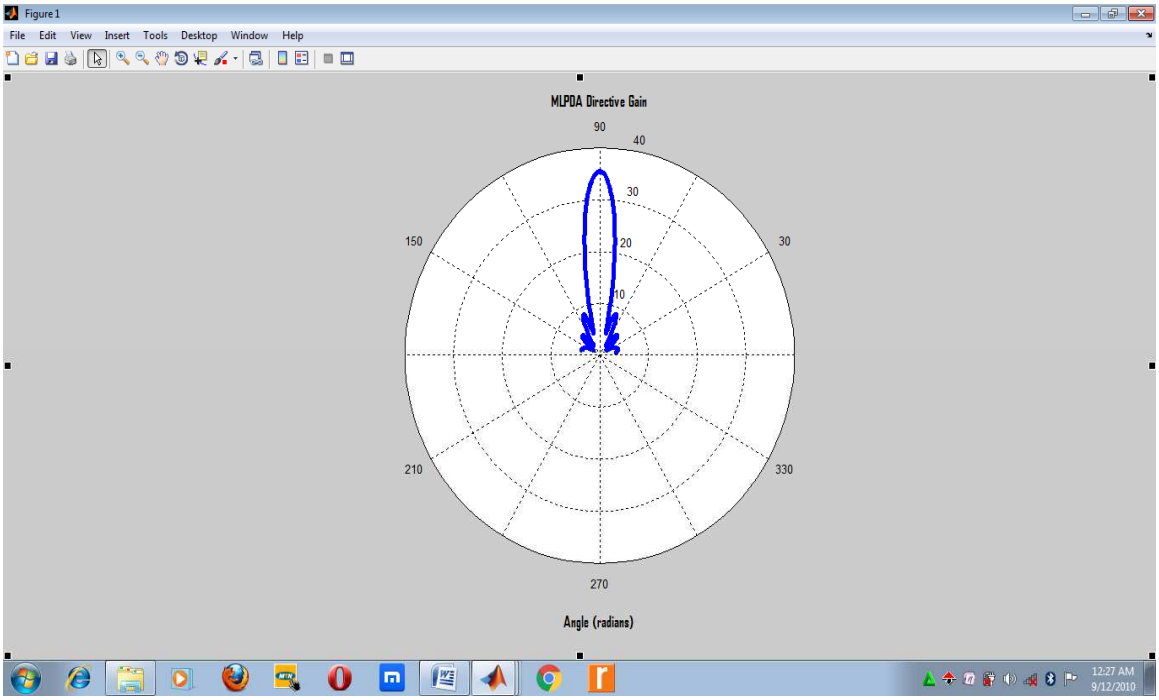

Fig.4.16: Directive Gain for Multiple (3) Log Periodic Dipole Array Antennas

Figure 4.16 demonstrated close similarity with the figure 4.15 of the directive gain of SLPA antennas. The reason was that the directive gains of both antennas were generated from the product of the directivity of the array antennas and the square of the sine of the radiation angle, Θ (see equation 3.103). The directive gain of the MLPA antennas was computed as the signal was radiated within the angle of 2π. The value of the Directive gain generated from the MLPA antennas patten was 15.68dB or 45.68dBm (37W). The antenna has a higher directive gain compared to SLPA antennas.

v. Radiation Intensity for MLPDA Antennas

This section described and compared the Radiation Intensity for a dipole antenna, SLPA antennas and MLPA antennas.

Figure 4.17 is the three-dimensional plot of the radiation intensity for a dipole antenna.

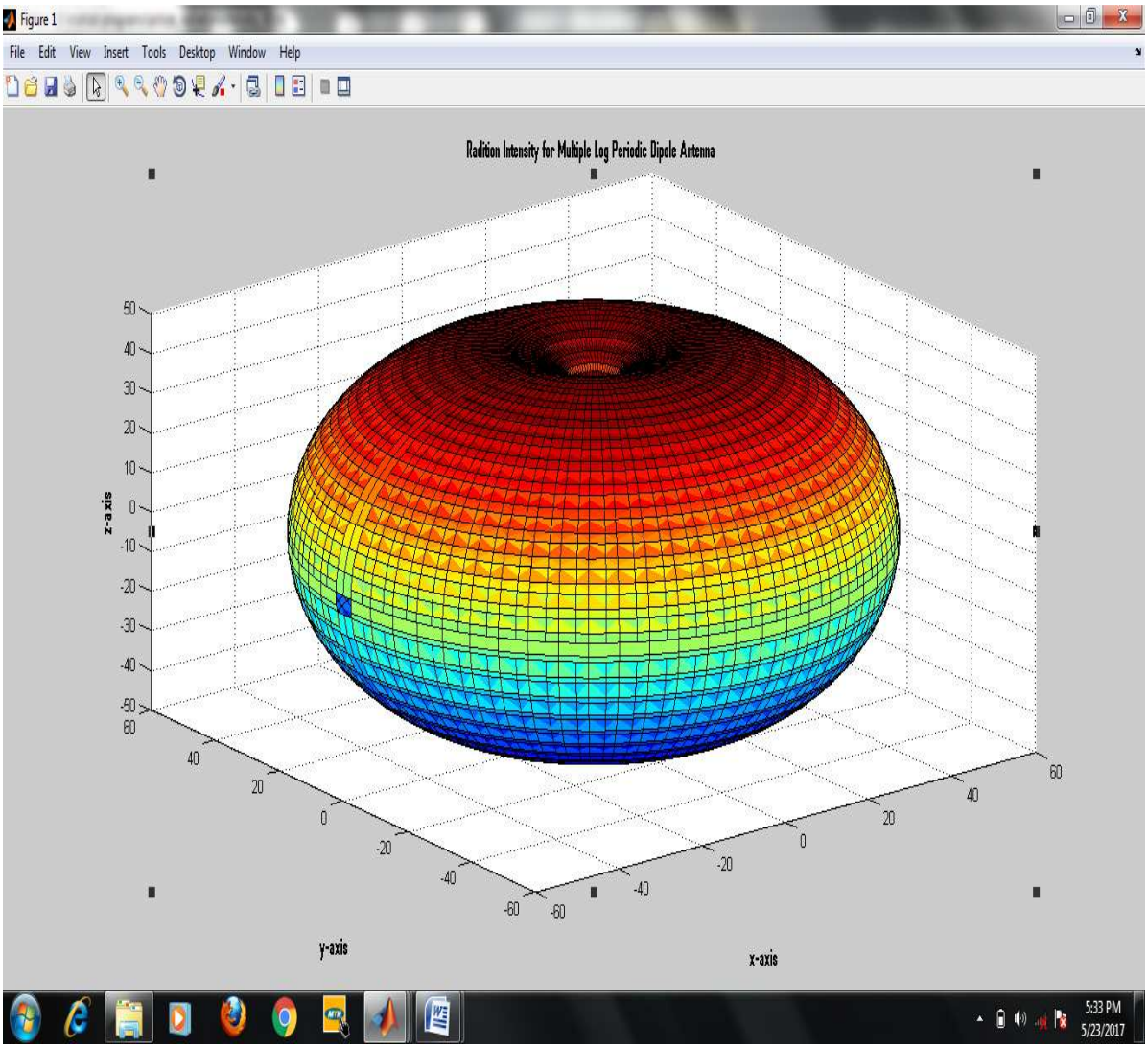

Fig.4.17: 3D Plot of Radiation Intensity for a dipole antenna

The plot of the Radiation Intensity of dipole antenna is obtained as shown in equation (3.90). It was obtained as the product of Average Poynting Vector and the square of the distance of

the antenna from its origin to the field point. The dipole radiation intensity pattern is little directive.

Figure 4.18 represents the Radiation Intensity of SLPA antennas.

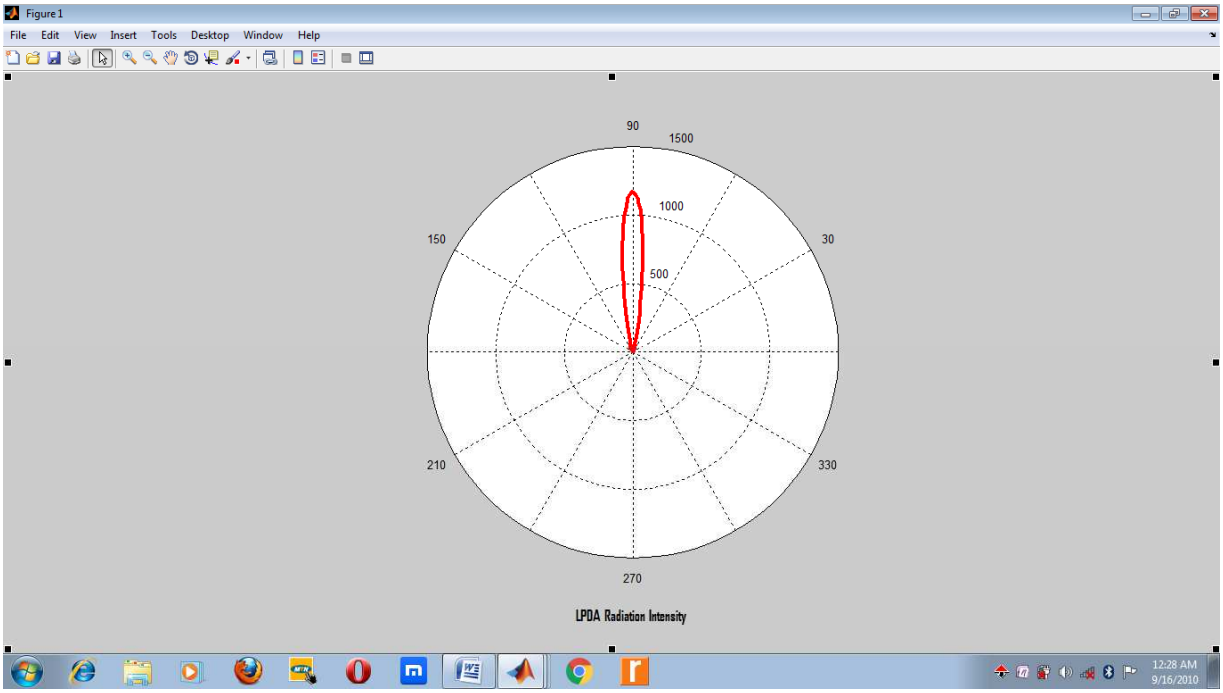

Fig.4.18: Normalized Radiation Intensity for Single Log Periodic Array Antennas

The Radiation Intensity pattern of SLPA antennas was obtained as written in equation (2.73). It was obtained as the product of Average Poynting Vector of a dipole antenna and square of distance of the antenna from its origin to the field point. From the radiation pattern developed, value of the LPA antennas radiation intensity was 1,170W/sr. This implied that, per unit solid angle, 1,170W/sr of power was radiated from this antenna. The radiation intensity pattern of the LPA antennas was very directive compared to that of a dipole antenna. Thus, antenna elements increased the radiation intensity of the array configuration.

Figure 4.19 highlighted the polar plot of Radiation Intensity for MLPA Antennas.

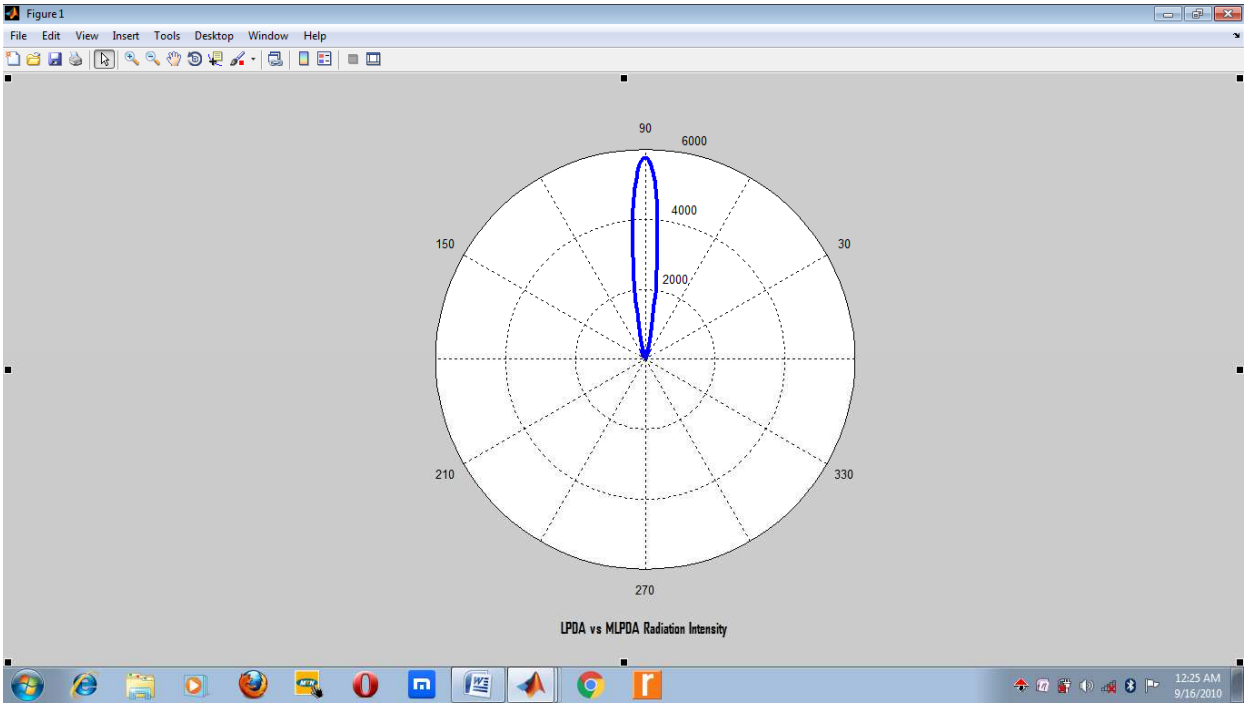

Fig.4.19: Normalized Radiation Intensity for Multiple Log Periodic Array Antennas

Figure 4.19 denotes the plot of Radiation Intensity of MLPA antennas. The figure was generated from equation (3.93). It was obtained by multiplying the Average Poynting Vector of SLPA antennas and square of distance from the antenna origin to the far field point denoted by 'r'. The radiation intensity developed by the MLPA antennas was 5,733W/sr. This value was obtained for three (3) stacked LPA of sixteen (16) dipoles each. The implication is that 5,733 W/sr of power was radiated from this antenna per unit solid angle. From the figure, the radiation intensity pattern was very directive and of higher magnitude compared to that of single Log Periodic Dipole Array antennas. Radiation Intensity is a far field parameter.

4.1.4 The Tabular Results Obtained from the Design of MLPA Antennas of a Sample Band Width

The values generated from the design of sample MLPA antennas were tabulated in Table 4.1.

Table 4.1: Dimensions for the MLPA Antennas Design

No. of Elements	**Dipole length** $\iota_d(m)$	**Element length** $h_n(m)$	**Dipole distance from vertex,** $\gamma_n(m)$	**Element spacing** $d_{n,n+1}(m)$
1	0.11	0.055	0.5233	0.0366
2	0.1023	0.0512	0.4871	0.0348
3	0.0951	0.0476	0.4529	0.0323
4	0.0884	0.0442	0.4205	0.0301
5	0.0822	0.0411	0.3910	0.0280
6	0.0765	0.0382	0.3635	0.0260
7	0.0712	0.0356	0.3387	0.0242
8	0.0662	0.0331	0.3149	0.0225
9	0.0616	0.0308	0.2930	0.0206
10	0.0573	0.0286	0.2721	0.0195
11	0.0533	0.0265	0.2521	0.0181
12	0.0496	0.0248	0.2360	0.0169
13	0.0461	0.0231	0.2198	0.0157
14	0.0429	0.0215	0.2046	0.0146
15	0.0399	0.0200	0.1903	0.0136
16	0.0371	0.0186	0.1770	-

This design was carried out for Multiple Log Periodic Dipole Array (MLPDA) antennas of 16 dipole elements each as depicted in figure 3.9. The columns contain the Log Periodic Dipole Array (LPDA) antennas values for the dipole length (m), element length (m), dipole distance (m), and the element spacing (m).

From the Table, the length of the first and longest dipole – from the second column – was obtained to be 0.11m and the length of the last and shortest dipole – 16^{th} element – was 0.0371m. In the third column, the first half – dipole length was 0.055m and the length of the last half – dipole was 0.0186m.

The distance from the LPA antennas vertex to the longest dipole was 0.5233m and the distance from the LPA antennas vertex to the shortest dipole was 0.1770m. Finally, the element spacing between the first and the second elements was 0.0366m while the element spacing between the last two dipole elements – 15^{th} and 16^{th} elements – was 0.0136m

4.2 Discussion

For ease of comparison, the results discussed in this section were grouped into two main sets, namely:

i. Array Factor patterns for array antennas Of Equal Dimensions (Figures 4.1 and 4.2), SLPA Antennas (Figures 4.3 and 4.4) and MLPA Antennas (Figures 4.5 and 4.6).
ii. Electric and Magnetic fields generated by the First Radiating Element in MLPA antennas (Figure 4.7)
iii. SLPA and MLPA Antennas parameters. These parameters include: the Electric/Magnetic Fields of the SLPA (Figure 4.8) and MLPA Antennas (Figure 4.9); Average Poynting Vectors of SLPA (Figure 4.10) and MLPA Antennas (Figure 4.11); Radiated power of SLPA (Figure 4.12) and MLPA Antennas (Figures 4.13 and 4.14); the Directive Gain of SLPA (Figure 4.15) and MLPA Antennas (Figure 4.16); and the Radiation Intensity of a dipole antenna (Figure 4.17), SLPA (Figure 4.18) and MLPA Antennas (Figure 4.19).

These results were plotted at a design factor, τ, of 0.95 and phase angle, φ, of 45^0 in order to maximize the number of dipole elements required in the array. In the patterns generated from the SLPA and MLPA antennas, it was ensured that the second large interference lobe that was undesirable – which might appear within the visible range of the antenna pattern, were nullified from that pattern. However, the largest possible number of minor lobes were retained within the range of the array radiation angle, theta.

Care was taken in selecting the angle within which the signals were radiated to ensure that the generation of back lobes was possibly avoided. Back – lobes normally had adverse effect of subtracting from the total radiated power. Thus, as the angle of radiation was reduced (controlled), the directivity of the generated field patterns was increased. However, more side lobes were generated but with reduced magnitude.

a. From Figures 4.1 to 4.6, the patterns of the array antennas for Equal amplitude, SLPA, and MLPA antennas were presented. The array patterns for the Equal amplitude and Single LPA were similar except that the patterns for the SLPA antennas were more directive. This variation was attributed to the scaling factor (τ=0.95) used for the SLPA – this affected the dimensions of the LPA antennas. The main lobe for both SLPA and MLPA became more directive as the dipole elements increased along the arrays. The array pattern was most directive at the highest number of radiating elements (that is: for 20 dipoles) but has minimal directivity at the least number of dipole elements (that is: for 4 dipoles). When compared to the MLPA, the array patterns for the MLPA were not only very directive but spanned through a large band width. The biggest major lobe for the Multiple LPA antennas was generated for 8 sets of MLPA while the smallest size of the main lobe was generated for 2 sets of MLPA. This implies that the greater the number of LPA antennas in the array, the farer and wider the coverage area. The implication is that Array Factor for the MLPA antennas has much power concentrated per unit area compared to SLPA antennas. It ensures the farthest and widest signal coverage area. Hence, the greater the number of stacked LPA antennas in the array, the farer and wider the coverage area. This is appropriate for WASS applications.

b. From the Electric/Magnetic field patterns generated for the SLPA in Figures 4.8 and 4.9, it clearly indicated that the beam width became much narrower as the number of the dipole elements in the array increased (16 – dipoles). This was as compared with the Electric/Magnetic field patterns generated from a dipole antenna of Figure 4.7. Given that the narrower the beam width the more directive the field patterns of the antennas were, it then followed that the directivity of both SLPA and MLPA antennas increased with number of radiating elements. The side lobes were considerably reduced in size (not in number) as the number of dipole elements increased. Hence, this was a vital realization since side lobes needed to be curtailed in order to minimize the noise that could be received through the side lobes.

Consequently, the magnitude of the Electric and Magnetic field patterns of MLPA antennas (3,204 Newtons/coulomb and 8.5Tesla respectively) were much greater compared to that of the SLPA antennas (98.02Newtons/coulomb and 0.26Tesla respectively). The MLPA antennas had patterns whose beam widths were much directed/pointed and with a very large main lobe too. This attribute particularly attested to its appropriateness for application in wide area surveillance systems.

c. The Average Poynting Vector of the SLPA antennas was equivalent to 1.90Watt per square metre as read from the antenna pattern (Figure 4.10). The LPA antennas in view had sixteen (16) active elements. For the Multiple (3) LPA antennas of 16 active elements each, Average Poynting Vector was 193.75Watt per square metre. The implication was that the power density of 1.90Watts was focused within the preferred direction of interest from the SLPA antennas, while 193.75Watts from the MLPA antennas was directed to the area of

interest. Hence, much power is concentrated per unit area by the MLPA antennas as compared to the SLPA antennas.

d. From Figure 4.12, the power radiated by the SLPA antennas was 462W. Also, from figure 4.13, the power radiated by the Multiple (3) LPA antennas was 22.5kW. As compared in figure 4.14, power radiated by the Multiple (3) LPDA antennas had a very high magnitude compared to that of the single LPDA antennas. While in the receiving mode, it then means that the MLPA antennas had a higher power reception capability as well as higher power radiation capacity per unit solid angle compared to the SLPA antennas. The physical interpretation of this is that MLPA antennas patterns have wide area of coverage and could also travel far region compared to that of the SLPA antennas.

e. The directive gain of the SLPA antennas of 16 radiating elements was 13.8dB or 43.80dBm (24W) as indicated in figure 4.15. From figure 4.16, the directive gain of MLPA antennas had numeric value of 15.70dBor 45.68dBm (37W). This resulted to 35.4 percent gain advantage over SLPA antennas. MLPA antennas demonstrated close similarity with that of the SLPA antennas. The reason was that the directive gains of both antennas were generated from the product of the directivity of the array antennas and the square of the sine of the radiation angle, Ɵ. The MLPA antennas had a higher directive gain compared to SLPA antennas.

f. Figure 4.17 was the radiation intensity for a dipole antenna. The antenna pattern was oval and non – directive. Thus, the radiated signal dipole element does not travel far.

However, the radiation intensity generated by the normalized SLPA antennas of 16 – radiating elements was 1,170W/Sr (Figure 4.18). The pattern was very directive compared to the dipole element. For the Radiation Intensity of MLPA antennas (Figure 4.19), the generated pattern was 5,733W/sr. This value was obtained for the normalized Multiple (3) LPA of 16 – dipoles each. From the figures, the radiation intensity patterns was very directive for both antennas. However, the MLPA antennas had a higher magnitude compared to that of SLPA antennas. The physical interpretation of this was that 1.17kW of power was radiated from the Single LPA antennas per unit solid angle while 5.73kW of power was radiated from the MLPA antenna per unit solid angle.

In summary, the Array Factor for the MLPA antennas ensures better prediction of signal radiation for the farthest distance and widest area of signal coverage. The MLPA antennas patterns have a very large beam widths and much directed/pointed main lobe. Hence, much power is concentrated per unit area by the MLPA antennas compared to the SLPA antennas. While in the receiving mode, MLPA antennas have higher power radiation capacity per unit solid angle as well as higher power reception capability compared to the SLPA antennas. Consequently, the MLPA antennas had a higher directive gain compared to SLPA antennas. These attributes particularly attested to the appropriateness of the MLPA antennas in wide area surveillance systems applications.

CHAPTER FIVE

CONCLUSION AND RECOMMENDATIONS

5.1 Conclusion

This dissertation explored a novel Array Factor tailored for the characterization of Multiple Log-Periodic Array antennas, particularly in the context of Surveillance Systems. The analytical framework was built upon the Magnetic Vector Potential (MVP) model, providing a solid foundation for the study. Practical experimentation with Multiple Log-Periodic Dipole Array antennas was conducted, employing the novel Array Factor for analysis. The MLPA antennas demonstrated significant gains, measuring at 15.68dB or 45.68dBm, within the operational frequency range of 1.350GHz to 2.690GHz.

Numerical development and analysis of the Multiple Log-Periodic Array antenna parameters were executed in the far field of the array antenna using the developed array factor. The MatLab R2010a software suite played a pivotal role in simulating various parameters of the MLPA Antennas, including Electric/Magnetic fields, Array Antenna patterns, Average Poynting Vector, Radiation Intensity, Radiated Power, Directivity, and Directive Gain of the antennas.

While Log-Periodic Array antennas were designed to work across a wide range of frequencies; MLPA antennas expanded this function by ensuring enhanced radiation gain and expanded signal coverage. The collective patterns generated by the MLPA antennas aligned with theoretical expectations, drawing upon the corresponding field of single element. Consequently, the analyzed MLPA antennas demonstrated a substantial improvement in directive gain and signal coverage area. Notably, the MLPA antennas exhibited a 35.4% gain performance over their SLPA counterparts, as indicated by the generated antenna patterns.

This underscores the promising potential of MLPA antennas in the sphere of Surveillance Systems.

5.2 Recommendations

The outcome of this research is useful to both stakeholders in antenna system engineering and for surveillance applications. Thus, in order to further examine the performance of the Array Factor for MLPA antennas, the following are recommended.

i. The research on the characterization of MLPA antennas with the novel Array Factor could be repeated at varying phase angles by antenna designers. This is to ascertain the relationship that exist between the MLPA antennas behaviours and phase angle, φ. Hence, it will help to ascertain the optimum phase angle at which the MLPA antennas – of fixed number of radiating elements – operate in communication engineering applications.
ii. Antenna designers could also add varying numbers of the radiating elements to the MLPA antennas, at constant set of MLPA antennas – say 3 sets of MLPA antennas. Then, the array antennas patterns could be observed.

5.3 Contribution to Knowledge

i. Novel Array Factor for MLPA Antennas:

This study demonstrated a groundbreaking novel Array Factor developed to expedite the characterization of multiple array antenna parameters. By doing so, it effectively minimizes the bottleneck in computing antenna losses for MLPA antennas. This innovative approach not

only enhances the efficiency of the analysis but also contributes significantly to the understanding of MLPA antenna behavior, addressing the previously identified lack of an array-factor.

ii. **Improved Antenna Behavior Forecasting:**

Leveraging the developed Array Factor alongside deployed MLPA antennas, this research empowers system designers to forecast antenna behavior at the far field with ease. This capability proves instrumental in avoiding the costly and time-consuming process of prototype development and deployment. Additionally, the widened bandwidth of the designed MLPA antennas contributes to an enhanced coverage area for surveillance systems, thereby saving resources that would otherwise be spent on drive tests. This advancement directly addresses the challenges posed by the lack of an array-factor and aids in overcoming the forecasting difficulties outlined in the initial research gaps.

iii. **Enhanced Signal Transmission in Communication Industries:**

The novel Array Factor introduced in this work proves invaluable in communication industries by assisting system engineers in adjusting transmitted signal levels via radiated power density. This adjustment serves to check for mismatches between the transmitter and MLPA antennas, leading to enhanced effective radiated power and ensuring power economy. Such optimization directly addresses the technical problems identified in the AAA control systems, offering a potential solution to high costs and size constraints while maximizing signal efficiency in communication applications.

REFERENCES

Abdullahi Z. M., & Ahmad K. (2018). Design and Simulation of High Gain Log Periodic Dipole Array Antenna. *Bayero Journal of Engineering and Technology (Bjet),* 13(2), 28 – 36.

Abri, M., Bahloul, S. M., & Badaoui, H. A. (2012). Multi-Layered Ring Log Periodic Antennas Array Design for GPS Systems. *International Journal of Computer Networks and Communications* (ITCNC), 4(3).

Adekola, S. A. (2012). *Class work of EEE 654: Antenna and Electromagnetic Theory*, Federal University of Technology, Owerri. Unpublished.

Amiri, A. (2015). *Multi-Band And Dual-Polarised Ultra-Wide Band Horn Antenna For Landmine Detection Using Ground Penetrating Radar Technique.* A thesis submitted for the degree of Doctor of Philosophy of University College London.

Anagnostou, D. E. Papapolymerou, J., Tentzeris, M. M., & Christodoulou, C. G. (2008). A Printed Log Periodic Koch- Dipole Array (LPKDA). *IEEE Antennas and Wireless Propagation Letters,* Vol. 7.

Arpitha, S. & Kumar, M. S. (2015). Design Of and Analysis of Rectangular Patch Antenna and Arrays. *International Journal of Electronics and Communication Engineering (IJECE),* 4(5), 45-56.

Aziz – ul – Haq, M., Afzal, M. T., Rafique, U., Qamar – ud –Din, Khan, M.A., & Ahmed, M. M. (2012). Log Periodic Dipole Antenna Design Using Particle Swarm Optimization. *International Journal of Electromagnetics and Applications,* 65 – 68.

Balanis, C. A. (3rd Edition). (2005). *Antenna Theory Analysis and Design*. A John Wiley & sons Inc. Publication.

Biabanifard, M., Biabanifard, S., Javad, H. S. & Jahanshiri, A. (2018). Design and Comparison of Terahertz Graphene Antenna: Ordinary dipole, Fractal dipole, Spiral, Bow-tie and Log-periodic. *EngTechnol Open Acc*., 2(2), 49 – 54.

Bolli, P; Mezzadrelli, L; Monari, J; Perini, F; Tibaldi, A; Virone, G; Bercigli, M; Ciorba, L; Ninni, P. D.; Labate, M. G.; Loi, V. G.; Mattana, A; Paonessa, F; Rusticelli,

S. & Schiaffino, M. (2020), Test-Driven Design of an Active Dual-Polarized Log-Periodic Antenna for the Square Kilometre Array. *IEEE Open Journal of Antennas and Propagation*, 1(1), 253-263, doi: 10.1109/OJAP.2020.2999109.

Bontempo, M. M., Marques, P. S., Marins, C. N. M. & Arismar, C. S. (2015). A printed log-periodic antenna based on fractal tree elements. *2015 SBMO/IEEE MTT-S International Microwave and Optoelectronics Conference (IMOC)*, Porto de Galinhas, 2015, 1-5.

Carrel, R. (1961). The Design of Log-Periodic Dipole Antennas. *Electrical Engineering Research Laboratory University of Illinois Urbana, Illinois.*

Casula, G. A., Maxia, P., Mazzarella, G., & Montisci, G. (2013). Design of a Printed Log Periodic Dipole Array for Ultra-Wideband Applications. *Progress In Electromagnetics Research C*, 38(1), 15- 26.

Chen, Z., & Otto, S. A. (2016). *Tapper Optimization for pattern Synthesis of Microstrip Series-Fed Patch Array Antennas.*

CISCO Systems (2016). *Antenna Patterns and their meaning*. White Paper, 1- 17. Accessed: April, 2016.

Collin, R. E. (1985). *Antennas and Radiowave Propagation*. International student ed. New York: McGraw-Hill.

Collin, R. E. (2001). *Foundations for Microwave Engineering.* A john wiley and sons, inc publication. 2nd edition. New York: McGraw-Hill.

Daasari & Thallapelli (2012). Analysis of Radiation Patterns of Log-Periodic Dipole Array Using Transmission Line Matrix Model. *International Journal of Innovative Research in Science, Engineering and Technology*, 1(2), 197 – 205.

Daniel, F. (2008). *A student's Guide to Maxwell's Equations.* Cambridge University Press.

Dhande, P. (2009). *Antennas and its Applications.* DRDO Science Spectrum, 66-78.

Eberhart, R. & Kennedy, J. (1995). A new optimizer using Particle Swarm Theory. *Proceedings of the 6th International Symposium on Microwave Machine and Human Science*, 39 – 43.

Elliot, R.S. (1981). *Antenna Theory and Design.* Eaglewood Cliffs, Prentice-Hall.

Elprocus (2023). What is Helical Antenna : Working & Its Applications [White paper]. https://www.elprocus.com/helical-antenna/

Engargiola, G. (2016). *Non-Planar Log Periodic antenna feed for integration with a cryogenic microwave amplifier.* University of California, *Radio Astronomy Lab, Berkeley*.

Felici-Castell, S., Navarro, E A., Pérez-Solano,J. J., Segura-García, J. & García-Pineda, M. (2017). Practical Considerations in the Implementation of Collaborative Beamforming on Wireless Sensor Networks. *Multidisciplinary Digital Publishing Institute (MDPI) (Sensors (Basel)),* 17 (2), 237.

Fiorini, F., Morbidel, L., & Caso, P. C. (2017). A New Approach to Frequency Independent Radiating Systems: Conformal Edge Antennas. *Departamento de IngenieríaenTelecomunicaciones and InstitutoBalseiro, Centro AtómicoBariloche, Av. Ezequiel Bustillo 9500, CP8400, S.C. de Bariloche, Río Negro,* Argentina, 1 – 12.

Florence, P. V., & Raju, G. S. N. (2014). Optimization of Linear Dipole Antenna Array for Sidelobe Reduction and Improved Directivity using AAPSO algorithm". *IOSR Journal of Electronics and Communication Engineering*. Vol. 9, Issue 6, pp 17 – 27. www.iosrjournals.org

Gao, J., Zhang, Y., Sun, Y. & Wu, Q (2019). Ultra-Wide Band and Multifunctional Polarization Converter Based on Dielectric Metamaterial. *Materials (Basel)*; 12(23), p 3857.

Gruber, B., Froeling, M., Leiner, T., & Klomp, D. (2018). RF coils: A practical guide for nonphysicists. *Journal of magnetic resonance imaging: JMRI*, *48*(3), 590–604. Advance online publication. https://doi.org/10.1002/jmri.26187

Halder, A., & Pradhan, S. K. (2013). *Design of Microstrip log Periodic Antenna for Wireless Applications.* Department of Electronics and Communication Engineering, National Institute of Technology Rourkela, India, pp 1-36.

Hamadameen, J. A. (2008). Analysis, design, and simulation of a Log Periodic Antenna for Mobile Communication bands. *Electrical Engineering Department, Engineering CollegeSalahaddin University-Hawler Erbil Iraq,* vol 7, Isssue 5, pp 399 – 402.

Hasan, M. Z. & Al-Rizzo, H. (2020). *Beamforming Optimization in Internet of Things Applications Using Robust Swarm Algorithm in Conjunction with Connectable and Collaborative Sensors*. Sensors, pp 1 – 29.

Henry, R. (2016). Antenna Types and their differences: How do the different antenna designs perform and what are their strengths and differences. *Explorer Product Range*, pp 1 – 2.

Huong, N. T. (2020). Beamforming Phased Array Antenna toward Indoor Positioning Applications, *IntechOpen*, DOI: 10.5772/intechopen.93133. Available from: https://www.intechopen.com/online-first/beamforming-phased-array-antenna-toward-indoor-positioning-applications

Hui, H. T. (2016). *Antenna Arrays.* NUS/ECE: EE 6832. https://www.ece.nus.edu.sg/stfpage/elehht/Teaching/EE4101/Lecture%20Notes/Antenna%20Arrays.pdf. Pp 1 – 42.

International Christian Concern (2021). *1,470 Christians Killed in Nigeria Within Four Months.* https://www.persecution.org/2021/05/14/1470-christians-killed-nigeria-within-four-months/

Jackson, D. R. (2022). *ECE 3317 Applied Electromagnetic Waves.* https://courses.egr.uh.edu/ECE/ECE3317/SectionJackson/Class%20Notes/Notes%2021%203317%20Introduction%20to%20Antennas.pdf

Jeong, S., Ha, D., & Chappell, W. J. (2009). *A planar Plastic Array Antenna for Tunable Radiation pattern.* Department of Electrical and Computer Engineering Faculty publications, Purdue University.

Jha, K.R. & Singh, G. (2010). Dual-band rectangular microstrip patch antenna at terahertz frequency for surveillance system. *J Comput Electron* 9, pp31–41. https://doi.org/10.1007/s10825-009-0297-8

Kibona, L. (2013). Gain and Directiviy Analysis of the log Periodic Antenna. *International Journal of Scientific Engineering and Research*: Volume 1, Issue 3, pp 14 – 18.

kim, J. (1999). *Log-Periodic Loop Antennas.* Electrical Engineering Department Virginia Polytechnic Institute and State University.

Kraus, J. D. (2nd Edition). (1997). *Antennas for all Applications*. Tata McGraw-Hill publishing company Ltd, New Delhi.

Kraus, J. D., & Marhefka, R. J. (3rd Edition). (2001). *Antennas for all Applications.*

Lakshmi, V. R., & Raju, G. S. N. (2012). A novel Miniaturized Log Periodic Antenna. *International Journal of Scientific and Engineering Research*, Vol. 3, issue 2.

Lazadiris, P. I., Zaharis, Z. D., Xenos, T., Tziris, E., & Gallion, P. (2016). *Optimal design of UHF TV band log-periodic antenna using invasive weed optimization.*

Lema, G. G., & Hailu, D. H. (2019). Feasibility study of antenna synthesis using hyper beamforming. *Heliyon*, *5*(2): e01230.

Li, M., & Liang, H. (2012). *Analysis software for the preparation of the antenna characteristics in the wireless system.*

Madikwane, O. I. (2006). *Investigation, Design, Construction and Testing Broadband Antenna for Radio Telescope Array Receiver.* University of Capetown.

Maharimi, S. F., Abdul Malek, M. F., Jamlos, M. F., Neoh, S. C. & Jusoh, M. (2012). Impact of Spacing and Number of Elements on Array Factor. *Progress in Electromagnetics Research Symposium Proceedings*, KL, Malaysia, pp1550 – 1553.

Neelakanta, S.P., & Chatterjee, R. (2003). *Antennas for Information Super Skyways: An Exposition on Outdoor and Indoor Wireless Antennas.* Research Studies Press Ltd, England.

Nikolova (2014). *Lecture 13: Linear Array Theory – part I (linear arrays: the two-element array. N-element array with uniform amplitude and spacing. Broad-side array. End-fire array. Phased array.* pp1-21

Nugroho, R., Ruliyanta, & Nugroho, E. R. (2023). Directional Flat Panel Antenna Design for Analog to Digital TV Broadcast Transition in Indonesia. *International Journal of Intelligent Systems and Applications in Engineering, 11*(1), 63–69. Retrieved from https://ijisae.org/index.php/IJISAE/article/view/2444

Okoye, A. C. (2014). Analysis and Simulation of a Standard and Compact Array-Factor of Log-Periodic Antennas for Wireless Communications. *Unpublished MSc Thesis.* Federal University of Technology Owerri, Imo State.

Okoye, A. C., Ndinechi, M.C., Mbaocha, C. C. & Agubor, C. K. (2017). Derivation of Standard Array Factor for Log-Periodic Circular-Loop Antennas Using Magnetic Vector Potential Approach. *2017 IEEE 3rd International Conference on Electro-Technology for National Development (NIGERCON).* pp 276 – 279.

Ovsenik, Lubos & Kolesárová, Anna & Turán, Ján. (2010). Video Surveillance Systems. Acta Electrotechnica et Informatica. 10. 46-53.

Özgönül, M. C. & Seçmen, M. (2017). Size-reduced printed log periodic dipole antenna with single first order semi-circle iteration and feed point patches. *2017 10th International Conference on Electrical and Electronics Engineering (ELECO), Bursa*, 2017, pp. 995-999.

Pulse Electronics/Larsen Antennas (Accessed April, 2016). *Antenna Basic Concepts*. www.pulseelectronics.com/product/antennas.

Qing X. & Chen Z.N. (2015). *Omnidirectional Antennas*. In: Chen Z. (eds) Handbook of Antenna Technologies. Springer, Singapore. pp 1 – 53. https://doi.org/10.1007/978-981-4560-75-7_52-1

Reeve, W. D. (2016). *Modelling and Measuring the Creative Design CLP5130-2N Log Periodic Antenna.* Pp 1-14.

Rodrigo, R. (2010). *Fundamental Parameters of Antennas Basic Properties and Design*. Pp–19. http://www.aast.edu/pheed/staffadminview/pdf_retreive.php?url=66_10285_EC442_2015_1__1_1_antenna%20parameters.pdf&stafftype=staffcourses

Rodriguez (2011). *On the Radiation patterns of Common EMC Antennas.* EMC Directory and Design Guide, pp 34 – 40.

Rohde & Schwar (2015). *Antenna Basics.* http://cdn.rohde-schwarz.com/pws/dl_downloads/dl_application/application_notes/8ge01/Antenna_Basics_8GE01_1e.pdf. Pp 1-32.

Rohner, C., Demmel, F., Stark, A., & Stecher, M. (2006). *Antenna Basics.*

Saunders, S. R. & Zovala, A. A. (Second Edition). (2007). *Antennas and Propagation for Wireless Communication Systems*. John wiley and sons ltd.

Safar, M. A. & Al-Zayed, A. S. (2016). A Novel Three-Dimensional Beamforming Antenna Array for Wireless Power Focusing. *Hindawi Publishing Corporation Mathematical Problems in Engineering, Vol. 2016,* Article ID 7426429, 8 pages

Scholz, D. I. P. (2016). *Basic Antenna Principles for Mobile Communications.* Kathrein: Antennen. Electronic. Pp 1 – 18.

Singh, S. K., Solanki, P. & Solanki, R. (2014). Introduction to Antenna, their Types and their Application. *International Journal of Innovative Research in Technology*: volume 1, Issue 6, pp 1574 – 1577.

Smith, J. (2016). *Antenna Tutorial*. Aerocomm, Inc. 13256W. 98th Street, Lenaxa, KS 66216.

Srivastava, A. K., Pandey, N. & Singh, K. N. (2014). Comparative Study of Radiation Pattern of Some Different Type Antennas. *International Journal of Physics and Applications*. Vol. 6, Number 2, pp. 109-114.

Tanyer, F. M. (2005). *Design of Log-Periodic Dipole Array Feed and Wide Band Reflector Antenna System*. Middle East Technical University.

This Day (2016). *A Dialogue in Dispute.* *http://www.thisdaylive.com/index.php/2016/07/25/a-dialogue-in-dispute/*

TwahirKazema & Kisangiri Michael | Kun Chen (Reviewing Editor) (2016). Investigation and analysis of the effects of geometry orientation of array antenna on directivity for wireless communication, *Cogent Engineering*, 3:1, DOI: 10.1080/23311916.2016.1232330

Typical Antenna Pattern.jpg. (2021, June 23). *Wikimedia Commons*. Retrieved 23:25, December 2, 2023 from https://commons.wikimedia.org/w/index.php?title=File:Typical_Antenna_Pattern.jpg&oldid=570875530.

Uchendu, I. & Kelly, J. (2016). Survey of Beam Steering Techniques Available for Millimeter Wave Applications. *Progress In Electromagnetics Research B*, Vol. 68, pp 35–54.

Uchida, N., Ito, K., Hirakawa, G. & Shibata, Y. (2016). Adaptive Array Antenna Control Methods on Delay Tolerant Networks for Road Surveillance Systems. *2016*

10th International Conference on Innovative Mobile and Internet Services in Ubiquitous Computing (IMIS), 2016, pp. 209-214, doi: 10.1109/IMIS.2016.104.

United States Marine Corps (2016). *Antenna Hand – Book*. Department of the Navy Headquarters Washington, D.C. 20380-1775.

Vaughan, R. & Andersen J. B. (2003). *Channels, Propagation and Antennas for mobile Communication.* London, UK Institute of Electrical Engineers.

Wang, W. (2016). Moving-Target Tracking by Cognitive RF Stealth Radar Using Frequency Diverse Array Antenna. *IEEE Transactions on Geoscience and Remote Sensing*, vol. 54, no. 7, pp. 3764-3773, doi: 10.1109/TGRS.2016.2527057.

Wankhade, P., & Nema, R. (2013). Review Paper on Ultra Wideband Log- periodic Antenna for Wireless Communication. *International Journal of Engineering Research and Applications (IJERA):* vol. 3, issue 1, pp. 274 - 278.

Wiesbeck, W. & Sturm, C. (2009). Principles of UWB Antennas. *Proceedings of the IEEE:* Vol. 97, No. 2, pp 372 - 385. http://www.ee.oulu.fi/~kk/dtsp/tutoriaalit/Wiesbeck.pdf.

Yalew, A. T., & *Getu*, N.B. (2010). A direct Derivation Technique for the near fields of Dipole Antennas. *IEEE Antennas and Propagation Magazine,* Vol. 52, No.3.

Yeo, J. & Lee, J. (2012). Miniaturized LPDA Antenna for Portable Direction Finding Applications. *ETRI Journal*: Vol. 34, No. 1, pp 118 – 121.

Yuang, Y., & Boyle K. (2008). *Antennas from Theory to Practice.* John Wiley & Sons, Ltd.

Yu-Jiun, R. & Chieh-Ping, L. (2010). *Wideband Antennas for Modern Radar Systems.* Radar Technology, Guy Kouemou, IntechOpen, DOI: 10.5772/7187. Available from: https://www.intechopen.com/books/radar-technology/wideband-antennas-for-modern-radar-systems

Zabri, A., Kamal, M, Rahim, A. ,Zubir, F., Nadzir, N. M. & Majid, H. A. (2017). Video Monitoring Application Using Wireless Sensor Node with Various External

Antenna. *Indonesian Journal of Electrical Engineering and Computer Science* Vol. 6, No. 1, pp. 148 - 154 DOI: 10.11591/ijeecs.v6.i1.pp148-154.

Zhang, J., Cui, X., Xu,H. & Lu, M. (2019). A Two-Stage Interference Suppression Scheme Based on Antenna Array for GNSS Jamming and Spoofing. *Sensors (Basel);* 19(18): 3870.

Zhong, C., Jiang, X., Qu, F. & Zhang, Z. (2017). Multi-Antenna Wireless Legitimate Surveillance Systems: Design and Performance Analysis. *IEEE Transactions on Wireless Communications*, vol. 16, no. 7, pp. 4585-4599. doi:10.1109/TWC.2017.2700379.

Appendix A

A MatLab program for Electric and Magnetic fields of a dipole element

```
%  An electric and magnetic fields of a dipole antenna
 tau=1;% the design factor
k=1;% k=wave number
d=2;% d=distance between dipoles
l=1.5;% l=length of first dipole
r=5;% r=distance from far field
curr=5;% curr=current through the dipole
imp=377;% imp=intrinsic impedance
pi=3.142;% pi=22/7
% enter the number of dipoles for each lpda
N1=input('Enter number of lpda dipoles:');

M1=N1;

    summ1=zeros(1,300);
    summ2=zeros(1,300);

     elem=zeros(1,300);
     elem2=zeros(1,300);
     efield=zeros(1,300);
     hfield=zeros(1,300);

    b=zeros(1,300);
  angle1=0.01:0.01:0.01*size(b,2);
 for sn1=1:1:300;
    b(sn1)=(1i*k*d.*cos(angle1(sn1)));
            summ1(sn1)=1;
            sumd1=1;
```

```
for n=1:1:M1;
   hd1=tau^((2*n)-2);
   sumd1=sumd1+hd1;
        sumh1=0;
     for i=1:1:n;
        h1=tau^(i-1);
        sumh1=sumh1+h1;
     end;

fx1=exp(sumh1.*b(sn1));

 summ1(sn1)=summ1(sn1)+fx1;

 elem=(((1i)*imp*(k^2)*curr*(l*sumd1)*exp(-
(1i)*k*r))./(16*pi*r)).*sin(angle1(sn1));
 efield(sn1)=elem.*summ1(sn1);
 end;

   summ2(sn1)=1;
   sumd2=1;

for n=1:1:M1;
   hd2=tau^((2*n)-2);
   sumd2=sumd2+hd2;
        sumh2=0;
     for i=1:1:n;
        h2=tau^(i-1);
        sumh2=sumh2+h2;
     end;
```

```
        fx2=exp(sumh2.*b(sn1));

         summ2(sn1)=summ2(sn1)+fx2;

         elem2=(((1i)*(k^2)*curr*(l*sumd2)*exp(-(1i)*k*r))./(16*pi*r)).*sin(angle1(sn1));
         hfield(sn1)=elem2.*summ2(sn1);
         end;
 end;

subplot (1,2,1); polar(angle1,abs(efield/N1));
 xlabel('Electric Field');
subplot (1,2,2); polar(angle1,abs(hfield/N1));
 xlabel('Magnetic Field');
```

Appendix B

A MatLab program of Array Factor for equal amplitude array elements

```
%  A matlab program for array factors for equal dipole elements
k=1; % k=wave number
d=2; % d=distance between dipoles

% enter the number of dipoles
N1=input('Enter number of dipoles in the equal amplitude array:');
N2=input('Enter number of dipoles in the equal amplitude array:');
N3=input('Enter number of dipoles in the equal amplitude array:');
N4=input('Enter number of dipoles in the equal amplitude array:');
M1=N1-1;
M2=N2-1;
M3=N3-1;
M4=N4-1;
    sum1=zeros(1,300);
    sum2=zeros(1,300);
    sum3=zeros(1,300);
    sum4=zeros(1,300);
    p=zeros(1,300);

    theta=0.01:0.01:0.01*size(p,2);
 for s=1:1:300;
    p(s)=(1i*k*d.*cos(theta(s)));

              sum1(s)=1;
          for n=1:1:M1;
                sumh1=0;
              for i=1:1:n;
```

```
        sumh1=sumh1+1;
    end;

    af1=exp(sumh1.*p(s));
    sum1(s)=sum1(s)+af1;

 end;
   sum2(s)=1;

for n=1:1:M2;

        sumh2=0;
    for i=1:1:n;

        sumh2=sumh2+1;
    end;

    af2=exp(sumh2.*p(s));

    sum2(s)=sum2(s)+af2;

end;
   sum3(s)=1;

for n=1:1:M3;

        sumh3=0;
    for i=1:1:n;

        sumh3=sumh3+1;
```

```
            end;

            af3=exp(sumh3.*p(s));

            sum3(s)=sum3(s)+af3;

        end;
          sum4(s)=1;
        for n=1:1:M4;
              sumh=0;
              sumh4=0;
            for i=1:1:n;

              sumh4=sumh4+1;
            end;
           af4=exp(sumh4.*p(s));

            sum4(s)=sum4(s)+af4;

        end;
end;
subplot (2,2,1);   plot (theta,abs(sum1/N1),'r');
legend ('N=4');
xlabel('Angle (radians)'),ylabel('array-factor');
subplot (2,2,2);   plot(theta,abs(sum2/N2),'k');
legend ('N=6');
xlabel('Angle (radians)'),ylabel('array-factor');
subplot (2,2,3);   plot(theta,abs(sum3/N3),'m');
legend ('N=8');
xlabel('Angle (radians)'),ylabel('array-factor');
```

```
subplot (2,2,4);   plot(theta,abs(sum4/N4),'b');
legend ('N=10');
xlabel('Angle (radians)'),ylabel('array-factor');
```

Appendix C

A MatLab program of Array Factor for equal dipole elements (combined)

```
k=1; % k=wave number
d=2; % d=distance between dipoles

% enter the number of dipoles
N1=input('Enter number of dipoles in the equal amplitude array:');
N2=input('Enter number of dipoles in the equal amplitude array:');
N3=input('Enter number of dipoles in the equal amplitude array:');
N4=input('Enter number of dipoles in the equal amplitude array:');

M1=N1-1;
M2=N2-1;
M3=N3-1;
M4=N4-1;

  sum1=zeros(1,300);
   sum2=zeros(1,300);
   sum3=zeros(1,300);
   sum4=zeros(1,300);
   p=zeros(1,300);

   theta=0.01:0.01:0.01*size(p,2);

for s=1:1:300;
   p(s)=(1i*k*d.*cos(theta(s)));

            sum1(s)=1;
        for n=1:1:M1;
              sumh1=0;
```

```
      for i=1:1:n;

         sumh1=sumh1+1;
      end;

      af1=exp(sumh1.*p(s));
      sum1(s)=sum1(s)+af1;

 end;
   sum2(s)=1;

for n=1:1:M2;

         sumh2=0;
      for i=1:1:n;

         sumh2=sumh2+1;
      end;

      af2=exp(sumh2.*p(s));

      sum2(s)=sum2(s)+af2;

end;
   sum3(s)=1;

for n=1:1:M3;

         sumh3=0;
      for i=1:1:n;
```

```
            sumh3=sumh3+1;
        end;

        af3=exp(sumh3.*p(s));

        sum3(s)=sum3(s)+af3;

    end;
      sum4(s)=1;
    for n=1:1:M4;
            sumh=0;
            sumh4=0;
        for i=1:1:n;

            sumh4=sumh4+1;
        end;

        af4=exp(sumh4.*p(s));

        sum4(s)=sum4(s)+af4;
    end;
end;
plot (theta, abs(sum1/N1),'r');

xlabel('Angle (radians)'),ylabel('array-factor');
hold on,

plot(theta,abs(sum2/N2),'k');
```

```
xlabel('Angle (radians)'),ylabel('array-factor');
hold on,

plot(theta,abs(sum3/N3),'m');

xlabel('Angle (radians)'),ylabel('array-factor');
 hold on,

plot(theta,abs(sum4/N4),'b');

xlabel('Angle (radians)'),ylabel('array-factor');
 hold off,

legend ('N=4 dipoles','N=6 dipoles','N=8 dipoles','N=10 dipoles');
title('Array factor for equal dimension antennas');
```

Appendix D

A matlab program for Array Factors of SLPA Antennas plotted seperately

```
 tau=0.95;% the design factor
k=1;% k=wave number
d=2;% d=distance between dipoles

% enter the number of dipoles for each lpda
N1=input('Enter number of lpda dipoles:');
N2=input('Enter number of lpda dipoles:');
N3=input('Enter number of lpda dipoles:');
N4=input('Enter number of lpda dipoles:');
M1=N1-1;
M2=N2-1;
M3=N3-1;
M4=N4-1;
    sum1=zeros(1,300);
    sum2=zeros(1,300);
    sum3=zeros(1,300);
    sum4=zeros(1,300);
    q=zeros(1,300);

    theta=0.01:0.01:0.01*size(q,2);
 for s1=1:1:300;
    q(s1)=(1i*k*d.*cos(theta(s1)));
            sum1(s1)=1;

         for n=1:1:M1;
                sumh1=0;
              for i=1:1:n;
                h1=tau^(i-1);
```

```
        sumh1=sumh1+h1;
    end;

    fx1=exp(sumh1.*q(s1));

    sum1(s1)=sum1(s1)+fx1;

end;
  sum2(s1)=1;

for n=1:1:M2;

        sumh2=0;
    for i=1:1:n;

        h2=tau^(i-1);

        sumh2=sumh2+h2;
    end;

    fx2=exp(sumh2.*q(s1));
   sum2(s1)=sum2(s1)+fx2;
end;
  sum3(s1)=1;

for n=1:1:M3;
       sumh3=0;
    for i=1:1:n;

        h3=tau^(i-1);
```

```
            sumh3=sumh3+h3;
        end;

        fx3=exp(sumh3.*q(s1));
        sum3(s1)=sum3(s1)+fx3;
    end;

      sum4(s1)=1;

    for n=1:1:M4;
            sumh=0;
            sumh4=0;
        for i=1:1:n;
         h4=tau^(i-1);

            sumh4=sumh4+h4;
        end;
       fx4=exp(sumh4.*q(s1));

        sum4(s1)=sum4(s1)+fx4;
    end;
end;
 subplot(2,2,1), plot (theta,abs(sum1/N1),'r');
legend ('N=4 dipoles');
xlabel('Angle (radians)'),ylabel('array-factor');
 subplot(2,2,2); plot(theta,abs(sum2/N2),'k');

 legend ('N=7 dipoles');
 xlabel('Angle (radians)'),ylabel('array-factor');
```

```
subplot(2,2,3); plot(theta,abs(sum3/N3),'m');

 legend ('N=10 dipoles');
 xlabel('Angle (radians)'),ylabel('array-factor');
 subplot(2,2,4); plot(theta,abs(sum4/N4),'b');
 legend ('N=20');
 xlabel('Angle (radians)'),ylabel('array-factor');
```

Appendix E

A MatLab program for Array Factor of SLPA Antennas (Plotted together)

```
%  A matlab program for array factors of log periodic dipole antennas
tau=0.95;% the design factor
k=1;% k=wave number
d=2;% d=distance between dipoles

% enter the number of dipoles for each lpda
N1=input('Enter number of dipoles:');
N2=input('Enter number of dipoles:');
N3=input('Enter number of dipoles:');
N4=input('Enter number of dipoles:');
M1=N1-1;
M2=N2-1;
M3=N3-1;
M4=N4-1;
    sum1=zeros(1,300);
    sum2=zeros(1,300);
    sum3=zeros(1,300);
    sum4=zeros(1,300);
    q=zeros(1,300);

    theta=0.01:0.01:0.01*size(q,2);
 for s1=1:1:300;
    q(s1)=(1i*k*d.*cos(theta(s1)));
            sum1(s1)=1;

         for n=1:1:M1;
                 sumh1=0;
              for i=1:1:n;
```

```
        h1=tau^(i-1);
        sumh1=sumh1+h1;
      end;
      fx1=exp(sumh1.*q(s1));
      sum1(s1)=sum1(s1)+fx1;

end;
   sum2(s1)=1;
for n=1:1:M2;
        sumh2=0;
      for i=1:1:n;
        h2=tau^(i-1);
        sumh2=sumh2+h2;
      end;
      fx2=exp(sumh2.*q(s1));
     sum2(s1)=sum2(s1)+fx2;

end;
   sum3(s1)=1;
for n=1:1:M3;
        sumh3=0;
      for i=1:1:n;
        h3=tau^(i-1);
        sumh3=sumh3+h3;
      end;
      fx3=exp(sumh3.*q(s1));
      sum3(s1)=sum3(s1)+fx3;

end;
```

```
            sum4(s1)=1;

        for n=1:1:M4;
                sumh=0;
                sumh4=0;
            for i=1:1:n;

                h4=tau^(i-1);
                sumh4=sumh4+h4;
            end;
           fx4=exp(sumh4.*q(s1));

            sum4(s1)=sum4(s1)+fx4;

        end;
end;
plot (theta,abs(sum1/N1),'r');
hold on
plot(theta,abs(sum2/N2)),'k';
hold on
plot(theta,abs(sum3/N3),'m');
hold on
 plot(theta,abs(sum4/N4),'b');
  hold off
  legend ('N=4','N=7','N=10','N=20');
 title('Array factor for lpda antennas');
 xlabel('Angle (radians)'),ylabel('array-factor');
```

Appendix F

A MatLab program for array factors of Multiple Log Periodic Array Antennas

```
% A matlab program for array factors of multiple log periodic dipole antennas
tau=0.95;% the design factor
k=1;% k=wave number
d=2;% d=distance between dipoles
s2=90;
% enter the number of dipoles for the lpda
N1=input('Enter number of dipoles:');
% enter the number of lpda in the multiple array
e1=input('Enter number of lpda in the mlpda array:');
% enter the number of dipoles for each lpda
N2=input('Enter number of dipoles:');
% enter the number of lpda in the multiple array
e2=input('Enter number of lpda in the mlpda array:');
% enter the number of dipoles for each lpda
N3=input('Enter number of dipoles:');
% enter the number of lpda in the multiple array
e3=input('Enter number of lpda in the mlpda array:');
% enter the number of dipoles for each lpda
N4=input('Enter number of dipoles:');
% enter the number of lpda in the multiple array
e4=input('Enter number of lpda in the mlpda array:');
M1=N1-1;
M2=N2-1;
M3=N3-1;
M4=N4-1;
    sum1=zeros(1,300);
    sum2=zeros(1,300);
    sum3=zeros(1,300);
```

```
   sum4=zeros(1,300);
   q=zeros(1,300);
   afmlpa1=zeros(1,300);
   afmlpa2=zeros(1,300);
   afmlpa3=zeros(1,300);
   afmlpa4=zeros(1,300);
    sn2=zeros(1,300);
   theta1=0.01:0.01:0.01*size(q,2);

    equa1=(sin(e1*(k*d*sin(theta1(s2))))/2)/(0.5*k*d*sin(theta1(s2)));
   equa12=(sin(e2*(k*d*sin(theta1(s2))))/2)/(0.5*k*d*sin(theta1(s2)));
   equa13=(sin(e3*(k*d*sin(theta1(s2))))/2)/(0.5*k*d*sin(theta1(s2)));
   equa14=(sin(e4*(k*d*sin(theta1(s2))))/2)/(0.5*k*d*sin(theta1(s2)));
for s1=1:1:300;
   q(s1)=(1i*k*d.*cos(theta1(s1)));

          sum1(s1)=1;

       for n=1:1:M1;
             sumh1=0;
          for i=1:1:n;
             h1=tau^(i-1);
             sumh1=sumh1+h1;
          end;
          fx1=exp(sumh1.*q(s1));
          sum1(s1)=sum1(s1)+fx1;
       end;
  afmlpa1(s1)=sum1(s1).*equa1;

          sum2(s1)=1;
```

```
    for n=1:1:M2;
            sumh2=0;
        for i=1:1:n;
            h2=tau^(i-1);
            sumh2=sumh2+h2;
        end;

        fx2=exp(sumh2.*q(s1));

        sum2(s1)=sum2(s1)+fx2;
    end;
afmlpa2(s1)=sum2(s1).*equa12;

       sum3(s1)=1;

    for n=1:1:M3;
            sumh3=0;
        for i=1:1:n;
            h3=tau^(i-1);
            sumh3=sumh3+h3;
        end;

        fx3=exp(sumh3.*q(s1));

        sum3(s1)=sum3(s1)+fx3;
    end;
afmlpa3(s1)=sum3(s1).*equa13;

       sum4(s1)=1;
```

```
        for n=1:1:M4;
            sumh4=0;
           for i=1:1:n;
            h4=tau^(i-1);
            sumh4=sumh4+h4;
           end;

           fx4=exp(sumh4.*q(s1));

           sum4(s1)=sum4(s1)+fx4;
        end;
   afmlpa4(s1)=sum4(s1).*equa14;
 end;
  disp(afmlpa1)
  disp(afmlpa2)
  disp(afmlpa3)
  disp(afmlpa4)
  disp(equal)
  disp(equal2)
disp(equal3)
  disp(equal4)

subplot(2,2,1);polar(theta1,abs(afmlpa1),'r');
legend ('2 mlpa,16 dipoles each');
xlabel('Angle (radians)'),
subplot(2,2,2);polar(theta1,abs(afmlpa2),'k');
legend ('4 mlpa,16 dipoles each');
xlabel('Angle (radians)'),
subplot(2,2,3);polar(theta1,abs(afmlpa3),'m');
```

```
legend ('6 mlpa,16 dipoles each');
xlabel('Angle (radians)'),
subplot(2,2,4);polar(theta1,abs(afmlpa4),'b');
legend ('8 mlpa,16 dipoles each');
xlabel('Angle (radians)'),
 title('Array factor for mlpda antennas');
 xlabel('Angle (radians)'),ylabel('array-factor');
```

Appendix G

A matlab program for array factors of MLPA Antennas

```
% tau=0.95; the design factor
k=1;% k=wave number
d=2;% d=distance between dipoles
s2=90;

% enter the number of dipoles for the lpda
N1=input('Enter number of dipoles:');

% enter the number of lpda in the multiple array
e1=input('Enter number of lpda in the mlpda array:');

% enter the number of dipoles for each lpda
N2=input('Enter number of dipoles:');

% enter the number of lpda in the multiple array
e2=input('Enter number of lpda in the mlpda array:');

% enter the number of dipoles for each lpda
N3=input('Enter number of dipoles:');

% enter the number of lpda in the multiple array
e3=input('Enter number of lpda in the mlpda array:');

% enter the number of dipoles for each lpda
N4=input('Enter number of dipoles:');

% enter the number of lpda in the multiple array
e4=input('Enter number of lpda in the mlpda array:');
```

```
M1=N1-1;
M2=N2-1;
M3=N3-1;
M4=N4-1;
    sum1=zeros(1,300);
    sum2=zeros(1,300);
    sum3=zeros(1,300);
    sum4=zeros(1,300);
    q=zeros(1,300);

    afmlpa1=zeros(1,300);
    afmlpa2=zeros(1,300);
    afmlpa3=zeros(1,300);
    afmlpa4=zeros(1,300);
     sn2=zeros(1,300);
    theta1=0.01:0.01:0.01*size(q,2);

     equa1=(sin(e1*(k*d*sin(theta1(s2))))/2)/(0.5*k*d*sin(theta1(s2)));
    equa12=(sin(e2*(k*d*sin(theta1(s2))))/2)/(0.5*k*d*sin(theta1(s2)));
    equa13=(sin(e3*(k*d*sin(theta1(s2))))/2)/(0.5*k*d*sin(theta1(s2)));
    equa14=(sin(e4*(k*d*sin(theta1(s2))))/2)/(0.5*k*d*sin(theta1(s2)));

 for s1=1:1:300;
    q(s1)=(1i*k*d.*cos(theta1(s1)));


            sum1(s1)=1;
```

```
    for n=1:1:M1;
            sumh1=0;

         for i=1:1:n;
            h1=tau^(i-1);
            sumh1=sumh1+h1;
          end;
          fx1=exp(sumh1.*q(s1));
          sum1(s1)=sum1(s1)+fx1;
    end;
afmlpa1(s1)=sum1(s1).*equa1;

        sum2(s1)=1;

    for n=1:1:M2;
            sumh2=0;
          for i=1:1:n;
            h2=tau^(i-1);
            sumh2=sumh2+h2;
          end;

          fx2=exp(sumh2.*q(s1));

          sum2(s1)=sum2(s1)+fx2;
    end;
afmlpa2(s1)=sum2(s1).*equa12;

        sum3(s1)=1;

    for n=1:1:M3;
```

```
            sumh3=0;
          for i=1:1:n;
            h3=tau^(i-1);
            sumh3=sumh3+h3;
          end;

          fx3=exp(sumh3.*q(s1));

          sum3(s1)=sum3(s1)+fx3;
      end;
  afmlpa3(s1)=sum3(s1).*equa13;

        sum4(s1)=1;

      for n=1:1:M4;
            sumh4=0;
          for i=1:1:n;
            h4=tau^(i-1);
            sumh4=sumh4+h4;
          end;

          fx4=exp(sumh4.*q(s1));

          sum4(s1)=sum4(s1)+fx4;
      end;
  afmlpa4(s1)=sum4(s1).*equa14;
end;
disp(afmlpa1)
disp(afmlpa2)
disp(afmlpa3)
```

```
 disp(afmlpa4)

 polar (theta1,abs(afmlpa1),'r');
hold on

polar (theta1,abs(afmlpa2),'k');
hold on

polar (theta1,abs(afmlpa3),'m');
hold on

polar (theta1,abs(afmlpa4),'b');
hold off

legend ('2 mlpa,16 dipoles each','4 mlpa,16 dipoles each','6 mlpa,16 dipoles each','8 mlpa,16
dipoles each');
title('Array Factors for mlpda antennas');
xlabel('Angle (radians)'),
% ylabel('array-factor');
```

Appendix H

An Electric and Magnetic Fields of SLPA Antennas respectively for N equals 16

```
tau=0.95;% the design factor
k=1;% k=wave number
d=2;% d=distance between dipoles
l=1.5;% l=length of first dipole
r=5;% r=distance from far field
curr=5;% curr=current through the dipole
imp=377;% imp=intrinsic impedance
pi=3.142;% pi=22/7
% enter the number of dipoles for each lpda
N1=input('Enter number of lpda dipoles:');

M1=N1-1;

    summ1=zeros(1,300);
    summ2=zeros(1,300);

     elem=zeros(1,300);
     elem2=zeros(1,300);
     efield=zeros(1,300);
     hfield=zeros(1,300);

    b=zeros(1,300);
  angle1=0.01:0.01:0.01*size(b,2);
 for sn1=1:1:300;
    b(sn1)=(1i*k*d.*cos(angle1(sn1)));
            summ1(sn1)=1;
            sumd1=1;
```

```
for n=1:1:M1;
   hd1=tau^((2*n)-2);
   sumd1=sumd1+hd1;
       sumh1=0;
     for i=1:1:n;
       h1=tau^(i-1);
       sumh1=sumh1+h1;
     end;

fx1=exp(sumh1.*b(sn1));

 summ1(sn1)=summ1(sn1)+fx1;

 elem=(((1i)*imp*(k^2)*curr*(l*sumd1)*exp(-
(1i)*k*r))./(16*pi*r)).*sin(angle1(sn1));
 efield(sn1)=elem.*summ1(sn1);
 end;

   summ2(sn1)=1;
   sumd2=1;
for n=1:1:M1;
   hd2=tau^((2*n)-2);
   sumd2=sumd2+hd2;
       sumh2=0;
     for i=1:1:n;
       h2=tau^(i-1);
       sumh2=sumh2+h2;
     end;
```

```
        fx2=exp(sumh2.*b(sn1));

         summ2(sn1)=summ2(sn1)+fx2;

         elem2=(((1i)*(k^2)*curr*(l*sumd2)*exp(-(1i)*k*r))./(16*pi*r)).*sin(angle1(sn1));
         hfield(sn1)=elem2.*summ2(sn1);
         end;
end;

subplot (1,2,1); polar(angle1,abs(efield/N1),'b');
 xlabel('Electric Field');
subplot (1,2,2); polar(angle1,abs(hfield/N1),'r');
 xlabel('Magnetic Field');
```

Appendix I

An Electric and Magnetic fields of MLPA antennas

```
%  respectively for N equals 10

tau=0.95;% the design factor
k=1;% k=wave number
d=2;% d=distance between dipoles
l=1.5;% l=length of first dipole
r=5;% r=distance from far field
s2=90;
curr=5;% curr=current through the dipole
imp=377;% imp=intrinsic impedance
pi=3.142;% pi=22/7
sn2=45;



% enter the number of dipoles for the lpda
N1=input('Enter number of dipoles in each lpda:');

% enter the number of lpda in the multiple array
e1=input('Enter number of lpda in the mlpda array:');

M1=N1-1;

    equa1=zeros(1,300);
    summ1=zeros(1,300);
    summ2=zeros(1,300);

     elem=zeros(1,300);
```

```
elem2=zeros(1,300);
efieldlpda=zeros(1,300);
hfieldlpda=zeros(1,300);
efieldmlpda=zeros(1,300);
hfieldmlpda=zeros(1,300);
b=zeros(1,300);

angle1=0.01:0.01:0.01*size(b,2);

for sn1=1:1:300;
b(sn1)=(1i*k*d.*cos(angle1(sn1)));
summ1(sn1)=1;
sumd1=1;

for n=1:1:M1;
hd1=tau^((2*n)-2);
sumd1=sumd1+hd1;
sumh1=0;

for i=1:1:n;
h1=tau^(i-1);
sumh1=sumh1+h1;
end;

fx1=exp(sumh1.*b(sn1));
summ1(sn1)=summ1(sn1)+fx1;

elem=(((1i)*imp*(k^2)*curr*(l*sumd1)*exp(-
(1i)*k*r))./(16*pi*r)).*sin(angle1(sn1));
```

```
 equa1=sin(e1/2)*k*d*sin(angle1(s2))/(1/2*k*d*sin(angle1(s2)));

 efieldlpda(sn1)=elem.*summ1(sn1);
end;

  efieldmlpda(sn1)=efieldlpda(sn1).*equa1;
   summ2(sn1)=1;
   sumd2=1;

for n=1:1:M1;
   hd2=tau^((2*n)-2);
   sumd2=sumd2+hd2;
        sumh2=0;

      for i=1:1:n;
        h2=tau^(i-1);
        sumh2=sumh2+h2;
      end;

fx2=exp(sumh2.*b(sn1));

 summ2(sn1)=summ2(sn1)+fx2;

 elem2=(((1i)*(k^2)*curr*(l*sumd2)*exp(-(1i)*k*r))./(16*pi*r)).*sin(angle1(sn1));

 equa1=sin(e1/2)*k*d*sin(angle1(sn2))/(1/2*k*d*sin(angle1(sn2)));

 hfieldlpda(sn1)=elem2.*summ2(sn1);
end;
```

```
 hfieldmlpda(sn1)=hfieldlpda(sn1).*equa1;
 end;
size (efieldmlpda)
subplot (1,2,1); polar(angle1,abs(efieldmlpda),'b');
 xlabel('MLPA Electric Field');

subplot (1,2,2); polar(angle1,abs(hfieldmlpda),'r');
 xlabel('MLPA Magnetic Field');
```

Appendix J

A matlab program for an Average Poynting Vector of SLPA antennas for N equals 16

```
tau=0.95;% the design factor
k=1;% k=wave number
d=2;% d=distance between dipoles
l=1.5;% l=length of first dipole
r=5;% r=distance from far field
curr=5;% curr=current through the dipole
imp=377;% imp=intrinsic impedance
pi=3.142;% pi=22/7
% enter the number of dipoles for each lpda
N1=input('Enter number of lpda dipoles:');

M1=N1-1;

    summ1=zeros(1,300);

     elem=zeros(1,300);
     apv=zeros(1,300);

    b=zeros(1,300);

    angle1=0.01:0.01:0.01*size(b,2);
 for sn1=1:1:300;
            summ1(sn1)=1;
            sumd1=1;

          for n=1:1:M1;
            hd1=tau^((4*n)-4);
```

```
            sumd1=sumd1+hd1;
                sumh1=0;
              for i=1:1:n;
                h1=tau^(i-1);
                sumh1=sumh1+h1;
              end;

          pv=1+2*cos(sumh1.*sin(angle(sn1)));

           summ1(sn1)=summ1(sn1)+pv;

           elem=(imp*(k^4)*(curr^2)*((l^4)*sumd1)*exp(-
(1i)*k*r))./((16^2*pi^2*r^2)).*(sin(angle1(sn1))^2);
           apv(sn1)=(elem.*summ1(sn1))/2;
           end;
end;
 polar(angle1,real(apv/N1));
 xlabel('LPDA Average Poynting Vector');
 title('Average poynting vector for N equals 16');
```

Appendix K

A Matlab Program for an Average Pointing Vector of MLPA Antennas for N Equals 10; Antenna Set Equals 3

```
tau=0.95;% the design factor
k=1;% k=wave number
d=2;% d=distance between dipoles
l=1.5;% l=length of first dipole
r=5;% r=distance from far field
curr=5;% curr=current through the dipole
imp=377;% imp=intrinsic impedance
pi=3.142;% pi=22/7
sn2=45;
% enter the number of dipoles for each lpda
N1=input('Enter number of lpda dipoles:');
e1=input('Enter number of lpda in the mlpda array:');
M1=N1-1;

    summ1=zeros(1,300);

     elem=zeros(1,300);
     apv=zeros(1,300);
     equa=zeros(1,300);
    b=zeros(1,300);

    angle1=0.01:0.01:0.01*size(b,2);
 for sn1=1:1:300;
              summa1=1;
             sumd1=1;
```

```
for n=1:1:M1;
   hd1=tau^((4*n)-4);
   sumd1=sumd1+hd1;
       sumh1=0;
     for i=1:1:n;
       h1=tau^(i-1);
       sumh1=sumh1+h1;
     end;

pv=1+2*cos(sumh1.*sin(angle(sn1)));
equa=(sin((e1*k*d*sin(angle1(sn2))/2)./((sin (k*d*sin(angle1(sn2))))/2))^2;
summa1=summa1+pv;

end;
 elem=(imp*(k^4)*(curr^2)*((l^4)*sumd1)*exp(-
(1i)*k*r))./((16^2*pi^2*r^2)).*(sin(angle1(sn1))^2);
 apv(sn1)=(elem.*equa.*summa1)./2;
end;
polar(angle1,real(apv));

xlabel('MLPDA Average Poynting Vector');
 title('Average poynting vector for N equals 16');
```

Appendix L

Radiated Power of SLPA Antennas For N Equals 16

```
tau=0.95;% the design factor
k=1;% k=wave number
d=2;% d=distance between dipoles
l=1.5;% l=length of first dipole
r=5;% r=distance from far field
curr=0.25;% curr=current through the dipole
imp=377;% imp=intrinsic impedance
pi=3.142;% pi=22/7
lamda=0.25;% wavelength
% enter the number of dipoles for each lpda
N1=input('Enter number of lpda dipoles:');

M1=N1-1;

    summ1=zeros(1,300);

     elempow=zeros(1,300);

     radpowlpda=zeros(1,300);

    b=zeros(1,300);
    angle1=0.01:0.01:0.01*size(b,2);
 for sn1=1:1:300;
    b(sn1)=(1i*k*d.*cos(angle1(sn1)));
            summ1(sn1)=1;
            sumd1=1;

          for n=1:1:M1;
```

```
            hd1=tau^((2*n)-2);
            sumd1=sumd1+hd1;% variation in the dipole elements
                sumh1=0;
              for i=1:1:n;
                h1=tau^(i-1);
                sumh1=sumh1+h1;
              end;

           fx1=exp(sumh1.*b(sn1));% array exponentials

            summ1(sn1)=summ1(sn1)+fx1;

            elempow=((imp*(pi^3)*(curr^2))./12).*((((l*sumd1))./lamda^2))^2 ;
            radpowlpda(sn1)=elempow.*(summ1(sn1))^2;
            end;
end;
size(radpowlpda)
size(angle1)
polar(angle1,abs(radpowlpda/N1));
 xlabel('LPDA Radiated Power(W)');
```

Appendix M

Radiated Power of Multiple (3) LPA Antennas for N Equals 16

```
tau=0.95;% the design factor
k=1;% k=wave number
d=2;% d=distance between dipoles
% l=1.5;% l=length of first dipole
r=5;% r=distance from far field
curr=0.25;% curr=current through the dipole
imp=377;% imp=intrinsic impedance
pi=3.142;% pi=22/7
lamda=0.25;% wavelength
sn2=45;
% enter the number of dipoles for each lpda
N1=input('Enter number of lpda dipoles:');
M1=N1-1;
e1=input('Enter number of lpda in the mlpda array:');

    summ2=zeros(1,300);
    summ1=zeros(1,300);
    sumh1=zeros(1,300);
    elempow=zeros(1,300);
    radpowlpda=zeros(1,300);
    radpowmlpda=zeros(1,300);
    equa1=zeros(1,300);
    radpow=zeros(1,300);
    b=zeros(1,300);

    angle1=0.01:0.01:0.01*size(b,2);
 for sn1=1:1:300;
```

```
    b(sn1)=(1i*k*d.*cos(angle1(sn1)));
            summ1(sn1)=1;
            sumd1=1;
            summ2(sn1)=0;
          for n=1:1:M1;
            hd1=tau^((2*n)-2);
            sumd1=sumd1+hd1;% variation in the dipole elements
                sumh1=0;
              for i=1:1:n;
                h1=tau^(i-1);
                sumh1=sumh1+h1;
              end;

          fx1=exp(sumh1.*b(sn1));% array exponentials

           summ1(sn1)=summ1(sn1)+fx1;
           elempow=((imp*(pi^3)*(curr^2))./12).*((((l*sumd1))./lamda^2))^2 ;
           radpowlpda(sn1)=elempow.*(summ1(sn1))^2;



 end;
          equa1=(sin(e1/2*(k*d*sin(angle1(sn2))))/(0.5*k*d*sin(angle1(sn2))))^2;
           radpowmlpda(sn1)=radpowlpda(sn1).*equa1;
end;
size(radpowmlpda)
size(angle1)
 disp( radpowmlpda)
plot(angle1,abs(radpowlpda/N1),'r');
hold on,
plot(angle1,abs(radpowmlpda/N1),'b');
```

```
hold off,
  legend ('LPDA','MLPDA');
 Title('LPDA vs MLPDA Radiated Power(W)');
```

Appendix N

Radiation Intensity of SLPA Antennas for N Equals 7

```
tau=0.95;% the design factor
k=1;% k=wave number
d=2;% d=distance between dipoles
l=0.11;% l=length of first dipole
r=5;% r=distance from far field
curre=0.05;% curr=current through the dipole
imp=377;% imp=intrinsic impedance
pi=3.142;% pi=22/7
lamda=0.25;% wavelength
% enter the number of dipoles for each lpda
N1=input('Enter number of lpda dipoles:');
 M1=N1-1;
      summ1=zeros(1,300);
     elemradint=zeros(1,300);
      radintlpda=zeros(1,300);
    b=zeros(1,300);

    angle1=0.01:0.01:0.01*size(b,2);
 for sn1=1:1:300;
    b(sn1)=(1i*k*d.*cos(angle1(sn1)));
            summ1(sn1)=1;
            sumd1=1;
          for n=1:1:M1;
            hd1=tau^((2*n)-2);
            sumd1=sumd1+hd1;% variation in the dipole elements
                 sumh1=0;
              for i=1:1:n;
```

```
            h1=tau^(i-1);
            sumh1=sumh1+h1;
          end;
      fx1=exp(sumh1.*b(sn1));% array exponentials

       summ1(sn1)=summ1(sn1)+fx1;

elemradint(sn1)=((imp/32)*(pi^2)*(curre^2)).*((((l*sumd1))./lamda))^4*((sin(angle1(sn1)))^
2) ;
       radintlpda(sn1)=elemradint(sn1).*(summ1(sn1))^2;
       end;

end;
 disp(radintlpda)
polar(angle1,abs(radintlpda/N1));
 xlabel('LPDA Radiation Intensity');
```

Appendix O

Radiation Intensity of MLPA Antennas for N Equals 16

```
tau=0.95;% the design factor
k=1;% k=wave number
d=2;% d=distance between dipoles
l=1.5;% l=length of first dipole
r=5;% r=distance from far field
curre=0.05;% curr=current through the dipole
imp=377;% imp=intrinsic impedance
pi=3.142;% pi=22/7
lamda=0.25;% wavelength
 l=0.11; %antenna length
 sn2=45;

% enter the number of dipoles for each lpda
N1=input('Enter number of lpda dipoles:');
e1=input('Enter number of lpda in the mlpda array:');
M1=N1-1;

    summ1=zeros(1,300);
    sumh1=zeros(1,300);
    elemradint=zeros(1,300);
    radintlpda=zeros(1,300);
    radintmlpda=zeros(1,300);
    equa1=zeros(1,300);
     radint=zeros(1,300);
    b=zeros(1,300);
    angle1=0.01:0.01:0.01*size(b,2);
 for sn1=1:1:300;
```

```
    b(sn1)=(1i*k*d.*cos(angle1(sn1)));
            summ1(sn1)=1;
            sumd1=1;

          for n=1:1:M1;
            hd1=tau^((2*n)-2);
            sumd1=sumd1+hd1;% variation in the dipole elements
                sumh1=0;
              for i=1:1:n;
                h1=tau^(i-1);
                sumh1=sumh1+h1;
              end;

          fx1=exp(sumh1.*b(sn1));% array exponentials

           summ1(sn1)=summ1(sn1)+fx1;
           equa1(sn1)=((sin((e1/2)*(k*d*sin(angle1(sn1)))))/(1/2*k*d*sin(angle1(sn1))))^2;
            equa1(sn2)=(sin(e1/2*(k*d*sin(angle1(sn2))))/(0.5*k*d*sin(angle1(sn2))))^2;

elemradint(sn1)=((imp/32)*(pi^2)*(curre^2)).*((((l*sumd1))./lamda))^4*((sin(angle1(sn1)))^
2) ;
           radintlpda(sn1)=elemradint(sn1).*(summ1(sn1))^2;
          end;
           radintmlpda(sn1)=radintlpda(sn1).*equa1(sn2);
end;
size(radintmlpda)
disp(radintmlpda)
size(angle1)
 plot(angle1,abs(radintlpda));
 hold on,
```

```
 plot(angle1,abs(radintmlpda));
 hold off,
polar(angle1,abs(radintmlpda)/N1);
 xlabel('LPDA vs MLPDA Radiation Intensity');
```